REPORT DOCUMENTATION PAGE

Form Approved
OMB No. 0704-0188

1. REPORT DATE *(DD-MM-YYYY)*	2. REPORT TYPE	3. DATES COVERED *(From - To)*
30-01-2012	FINAL	Sept 2006 - Oct 2011

4. TITLE AND SUBTITLE

VERIFICATION OF ACCERELATED TESTING METHODOLOGY FOR LONG-TERM DURABILITY OF CFRP LAMINATES FOR MARINE USE

5a. CONTRACT NUMBER

5b. GRANT NUMBER

N00014-06-1-1139

5c. PROGRAM ELEMENT NUMBER

6. AUTHOR(S)

Miyano, Yasushi
Kimpara, Isao

5d. PROJECT NUMBER

5e. TASK NUMBER

5f. WORK UNIT NUMBER

7. PERFORMING ORGANIZATION NAME(S) AND ADDRESS(ES)

Kanazawa Institute of Technology
Materials System Research Laboratory
3-1 Yatsukaho, Hakusan, Ishikawa 924-0838, Japan

8. PERFORMING ORGANIZATION REPORT NUMBER

KIT-MSRL-12-01

9. SPONSORING/MONITORING AGENCY NAME(S) AND ADDRESS(ES)

Office of Naval Research, Boston Regional Office N62879
495 Summer Street
Boston, MA02210-2109

10. SPONSOR/MONITOR'S ACRONYM(S)

ONR

11. SPONSOR/MONITOR'S REPORT NUMBER(S)

12. DISTRIBUTION/AVAILABILITY STATEMENT

Approved for Public Release. Distribution is Unlimited.

13. SUPPLEMENTARY NOTES

14. ABSTRACT

The accelerated testing methodology (ATM) for the fatigue life prediction of CFRP laminates proposed and confirmed experimentally in the previous ONR project of Grant # N000140110949 was verified theoretically and refined quantitatively based on the viscoelasticity of matrix resin in this ONR project.

15. SUBJECT TERMS

CFRP, Durability, Fatigue, Accelerated testing methodology, Time-temperature superposition principle

16. SECURITY CLASSIFICATION OF:			17. LIMITATION OF ABSTRACT	18. NUMBER OF PAGES	19a. NAME OF RESPONSIBLE PERSON
a. REPORT	b. ABSTRACT	c. THIS PAGE			Toshiaki IZUMIYA
					19b. TELEPHONE NUMBER *(Include area code)*
U	U	U	UU	77	+81 76-248-9504

Standard Form 298 (Rev. 8/98)
Prescribed by ANSI Std. Z39.18

20120125188

F12-04-0216

VERIFICATION OF ACCERELATED TESTING METHODOLOGY FOR LONG-TERM DURABILITY OF CFRP LAMINATES FOR MARINE USE

Principal Investigator
Yasushi Miyano
Co-principal Investigator
Isao Kimpara
Materials System Research Laboratory
Kanazawa Institute of Technology
3-1 Yatsukaho Hakusan Ishikawa 924-0838, Japan
miyano@neptune.kanazawa-it.ac.jp

ONR Award Number: N00014-06-1-1139
Period: September 20, 2006 – October 31, 2011

SUMMARY

The accelerated testing methodology (ATM) for the fatigue life prediction of CFRP laminates proposed and confirmed experimentally in the previous ONR project of Grant # N000140110949 was verified theoretically and refined quantitatively based on the viscoelasticity of matrix resin in this ONR project.

1. The advanced accelerated testing methodology (ATM-2) in which the role of viscoelastic behavior of matrix resin on the long-term fatigue life of CFRP laminates was cleared statistically and quantitatively was proposed and the formulation of long-term fatigue life of CFRP laminates under an actual loading was constructed based on ATM-2.

2. The formulation by ATM-2 was applied to the flexural fatigue strengths of three kinds of CFRP laminates for marine use and the parameters in the formulations were determined.

3. The flexural fatigue strengths of quasi-isotropic CFRP laminates exposed to general loading in which the stress and temperature are changed with time were predicted by the formulation by ATM-2 and measured experimentally. The validity of ATM-2 was confirmed by comparing of the predicted ones and the measured data.

4. ATM-2 for the fatigue life prediction of CFRP laminates was expanded to MMF/ATM method for the fatigue life prediction of the structures made of CFRP laminates.

5. Damage evolution under post-impact fatigue of CFRP laminates for marine use were discussed in this project.

NAVY RELEVANCE

The proposed accelerated testing methodology (ATM-2) has effectively combined the effects of time, temperature and water absorption on the strength and life of composite materials. It was confirmed that the methodology is applicable to the innovative CFRP laminates for marine use exposed to active loading of variable stress and temperature history.

MAJOR ACCMPLISHMENTS

The major accomplishments of this ONR project were reported at ONR Review Meetings for Solid Mechanics Program held in September of every year at The Inn and Conference Center, University of Maryland University College, Adelphi, MD. The following reports are the extended abstracts of this project published on the proceedings of ONR Solid Mechanics Programs.

PART 1

2007 ONR Solid Mechanics Program

Verification of Accelerated Testing Methodology for Long-Term CSR Strengths on Three Directions of Unidirectional CFRP

Yasushi Miyano and Masayuki Nakada
Materials System Research Laboratory, Kanazawa Institute of Technology
3-1 Yatsukaho, Hakusan, Ishikawa 924-0838, Japan

OBJECTIVE

As the coupon–level constant strain rate (CSR) strength of CFRP laminates is matrix-dominated and the initial failure controls the ultimate fracture, it is shown to be valid that the failure process is unchanged due to the accelerated loading history under elevated temperature and that the same time-temperature superposition principle (TTSP) for the viscoelastic behavior of matrix resin holds for the CSR strength of CFRP laminates.

APPROACH

Time and temperature dependent CSR strengths for three directions of unidirectional CFRP laminates, which are the tensile and compressive CSR strengths for the longitudinal direction and the tensile strength for the transverse direction, were measured at various strain rates and temperatures in our previous paper. By using these measured data, the master curves of these CSR strengths are constructed based on the time-temperature superposition principle to be held for the creep compliance of matrix resin. And the relationships between the viscoelastic behavior of matrix resin and these CSR strengths are evaluated on the viewpoints of failure mechanism.

RECENT ACHIEVEMENTS

The same time-temperature superposition for the viscoelastic behavior of matrix resin holds for each of CSR strengths for typical three kinds of direction for unidirectional CFRP laminates because the smooth master curves of three kinds of CSR strength are obtained by using the time-temperature shift factor for the viscoelastic behavior of matrix resin. The relationship between the viscoelastic behavior of matrix resin and each of three kinds of CSR strength is uniquely determined on the viewpoints of failure mechanism. As results, the long-term CSR strengths of CFRP laminates can be predicted by using the short-term CSR strengths measured based on TTSP for the viscoelastic behavior of matrix resin and the accelerated testing methodology (ATM) can be applied to predict the long-term CSR strength of CFRP laminates.

1. Introduction

The mechanical behavior of polymer resins exhibits time and temperature dependence, called viscoelastic behavior, not only above the glass-transition temperature T_g but also below T_g. Thus, it can be presumed that the mechanical behavior of CFRP using polymer resins as matrices also depends on time and temperature even below T_g which is within the normal operating-temperature range. The presumption is confirmed experimentally by Aboudi et al. [1], Sullivan [2], Gates [3], and Miyano et al. [4-7].

In our previous papers [8-10], the time-temperature dependence of the CSR, creep and fatigue strengths for various directions of CFRP laminates with various combinations of fiber and matrix were measured at various frequencies and temperatures. The master curves of these CSR, creep and fatigue strengths of CFRP laminates were constructed by using measured data based on the time-temperature superposition principle (TTSP) to be held for the creep compliance of matrix resin. As results, it was cleared experimentally that the long-term CSR, creep and fatigue strengths of CFRP laminates can be predicted by using the short-term strengths measured based on TTSP for the viscoelastic behavior of matrix resin. The accelerated testing methodology (ATM) to predict the long-term CSR, creep and fatigue strengths of CFRP laminates by measuring the short-term strengths based on TTSP for the viscoelastic behavior of matrix resin was proposed.

Time and temperature dependent CSR strengths for typical three directions of unidirectional CFRP laminates, which are the tensile and compressive CSR strengths for the longitudinal direction and the tensile strength for the transverse direction, were measured at various strain rates and temperatures in our previous paper [4]. By using these measured data, the master curves of these CSR strengths are constructed based on TTSP to be held for the creep compliance of matrix resin. Additionally, the relationships between the viscoelastic behavior of matrix resin and these CSR strengths are evaluated on the viewpoints of failure mechanism. The applicability of ATM for predicting the long-term CSR strengths on CFRP laminates is discussed experimentally and theoretically.

2. Experimental Procedure

2.1 Preparation of Specimen

The compositions and cure conditions for the epoxy resin used as the matrix and the unidirectional CFRP laminates are given in Table 1. The epoxy resin plates were made by the infusion technique and the unidirectional CFRP laminates plates were made by the filament winding technique. It was confirmed by microscopic observation that the plates of epoxy resin and CFRP laminates were void-free. Two types of epoxy resin specimens and three types of CFRP laminates specimens were machined from the plates of epoxy resin and CFRP laminates, respectively.

Table 1 Compositions and cure conditions for the epoxy resin and the unidirectional CFRP laminates

Composition	
Resin	CFRP
Epoxy : EPIKOTE 828 / 100*	Matrix : Epoxy resin
Hardener : Methyl himic anhydride / 104*	Carbon fiber : TORAYCA T300-3K
Cure accelerator : 2-ethyl-4-methylimidazol / 1*	Volume fraction of fiber : 53.4% - 58.0%
Curing condition	
70°C for 12h (5MPa), 150°C for 4h and 190°C for 2h	

* : Weight fraction

2.2 Test Procedures

The bending creep tests for the epoxy resin were carried out for getting the creep compliance and the tension CSR tests for the epoxy resin were carried out for getting tensile CSR strength.

The tension CSR tests for the longitudinal direction, the bending CSR tests for the longitudinal direction and the bending CSR tests for the transverse direction of unidirectional CFRP laminates were carried for getting the tensile and flexural CSR strengths for the longitudinal direction and the transverse direction of unidirectional CFRP laminates. These testing methods and conditions are shown in Fig. 1 and Table 2, respectively.

The flexural strengths for the longitudinal and transverse directions of unidirectional CFRP laminates can be considered to be the compressive and tensile strength, respectively, because the failure mode in the bending tests for the longitudinal direction is compressive and that for the transverse direction is tensile in all ranges of deflection rate and temperature.

These CSR strengths for three directions of unidirectional CFRP laminates were measured in our previous paper [4]. The details of testing methods and data are published in this paper.

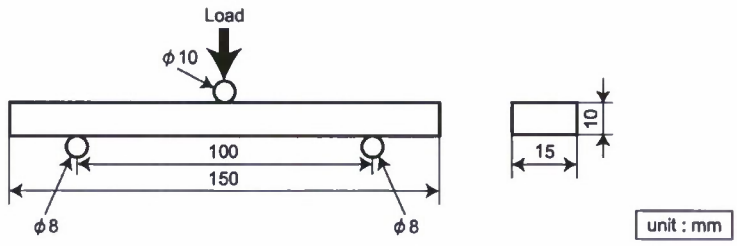

(a) Bending creep test for epoxy resin

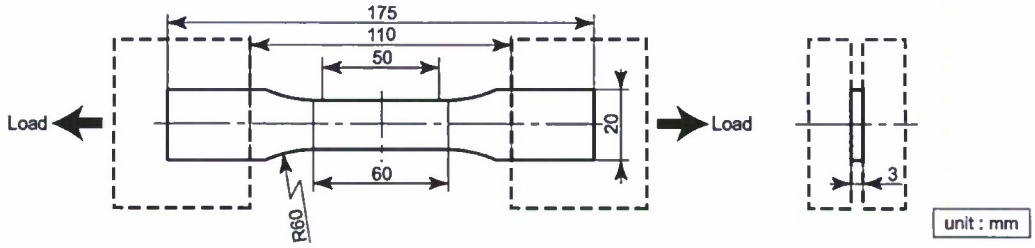

(b) Tension CSR test for epoxy resin

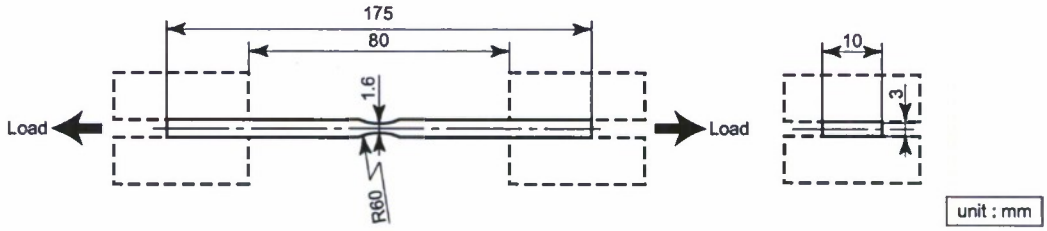

(c) Longitudinal tension CSR test for unidirectional CFRP laminates

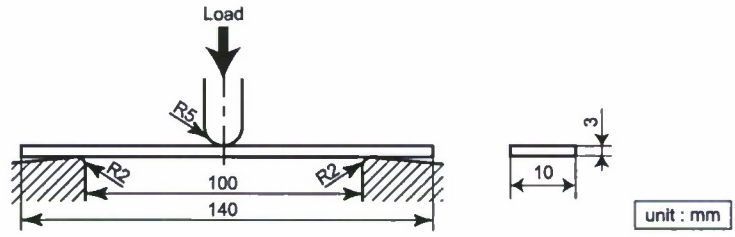

(d) Longitudinal bending CSR test for unidirectional CFRP laminates

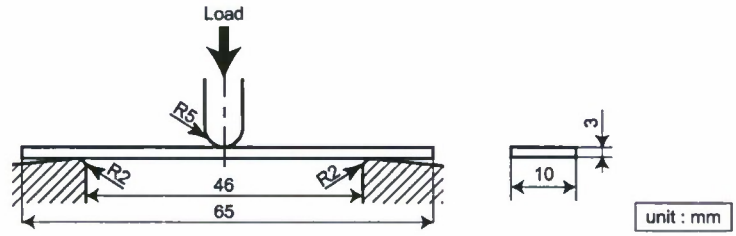

(e) Transverse bending CSR test for unidirectional CFRP laminates

Fig.1 Configurations of specimen and testing methods

Table 2 Testing conditions

	Displacement or deflection rate [mm/min]	Temperature [°C]
Bending creep test for neat epoxy resin	-	40, 60, 70, 80, 90, 100, 110, 120, 130, 140, 150, 160, 180
Tension CSR test for neat epoxy resin	0.05, 0.5, 5, 50	60, 80, 100, 120, 140, 160, 180
Longitudinal tension CSR test for CFRP	0.5, 5, 50	
Longitudinal bending CSR test for CFRP	0.05, 0.5, 5, 50	
Transverse bending CSR test for CFRP	0.01, 0.1, 1, 10	

3. Results and Discussion

3.1 Time-Temperature Shift Factor for Creep Compliance of Matrix Resin

The left side of Fig.2 shows the creep compliance D_M versus loading time t at various temperatures T for the epoxy resin. The master curves of D_M versus the reduced loading time t' were constructed by shifting D_M at various constant temperatures along the log scale of time. Since the smooth master curve of D_M can be obtained as shown in the right side graph, the TTSP is applicable for D_M.

The time-temperature shift factor $a_{T_0}(T)$ at a reference temperature T_0 plotted in Fig.3, which is the horizontal shift amount, is defined by

$$\log a_{T_0}(T) = \log t - \log t' \tag{1}$$

The $a_{T_0}(T)$ are described by two Arrhenius' equations shown in Eq.(2) with different activation energies ΔH.

$$\log a_{T_0}(T) = \frac{\Delta H}{2.303G}\left(\frac{1}{T} - \frac{1}{T_0}\right) \tag{2}$$

where G is the gas constant, 8.314×10^{-3} [kJ/(K mol)].

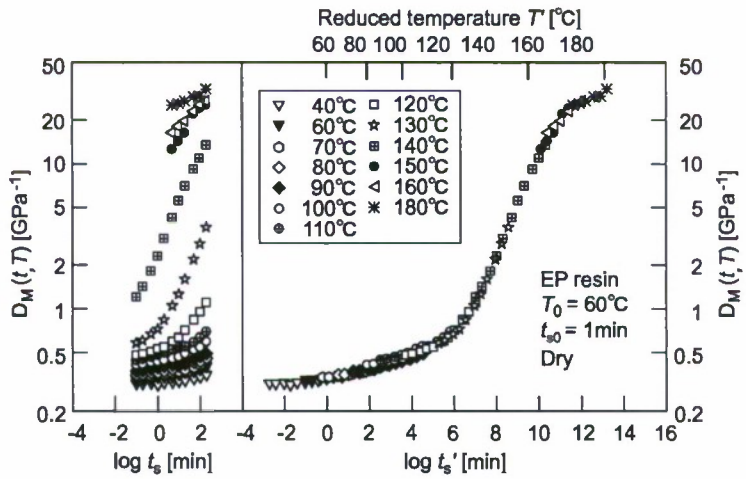

Fig.2 Master curve of creep compliance for epoxy resin

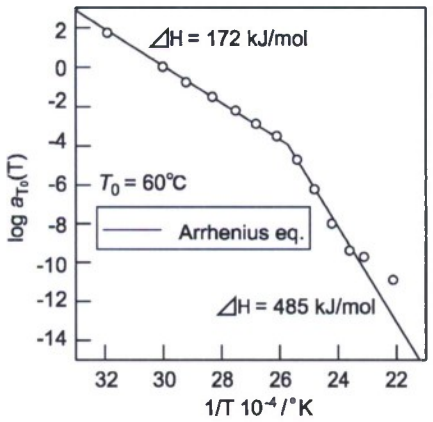

Fig.3 Time-temperature shift factor of creep compliance for epoxy resin

3.2 Master Curve of Tensile CSR Strength of Matrix Resin

The left side of Fig.4 shows the tensile CSR strength σ_M versus time to failure t_s at various temperatures T for epoxy resin, where t_s is the time period from initial load to maximum load during testing. The master curve of σ_M versus the reduced time to failure t_s' were constructed by shifting σ_M at various constant temperatures along the log scale of t_s using the same time-temperature shift factors for D_M shown in Fig.3. Since the smooth master curve of σ_M can be obtained as shown in the right side graph, the TTSP for D_M of epoxy resin is also applicable for the σ_M of epoxy resin.

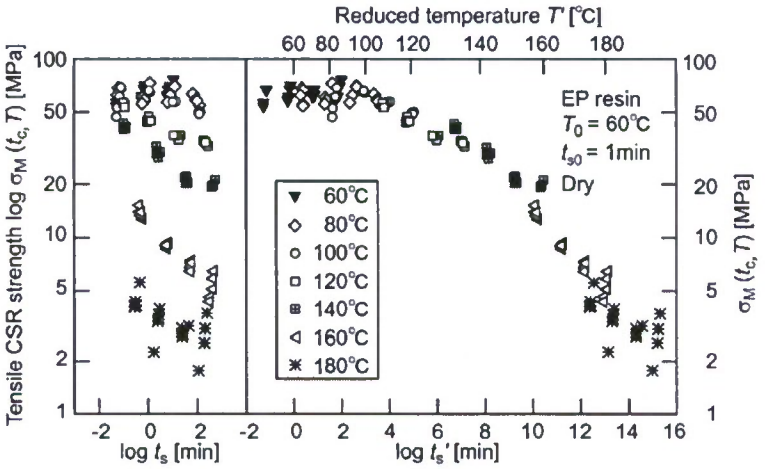

Fig.4 Master curve of tensile CSR strength for epoxy resin

3.3 Master Curves of Various CSR strengths of Unidirectional CFRP

The left side of each graph in Figs.5-7 shows the tensile and flexural CSR strengths, σ_{LT} and σ_{LB}, for the longitudinal direction and the flexural CSR strength, σ_{TB}, for the transverse direction of unidirectional CFRP laminates, which are plotted against time to failure t_s at various temperatures T, where t_s is the time period from initial load to maximum load during testing. The master curve for each strength versus the reduced time to failure t_s' was constructed by shifting each strength at various constant temperatures along the log scale of t_s using the same time-temperature shift factors for D_c of epoxy resin shown in Fig.3. Since the smooth master curve for each strength can be obtained as shown in the right side of each graph, the TTSP for D_c of epoxy resin is also applicable for each strength.

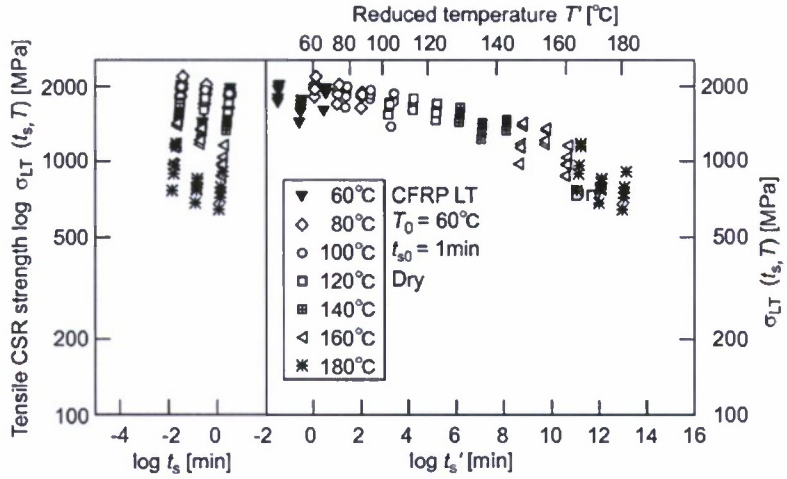

Fig.5 Master curve of tensile CSR strength for the longitudinal direction of unidirectional CFRP

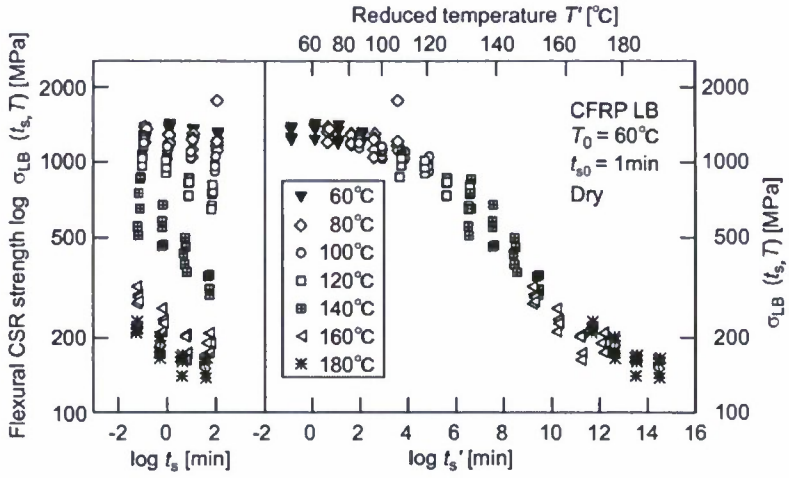

Fig.6 Master curve of flexural CSR strength for the longitudinal direction of unidirectional CFRP

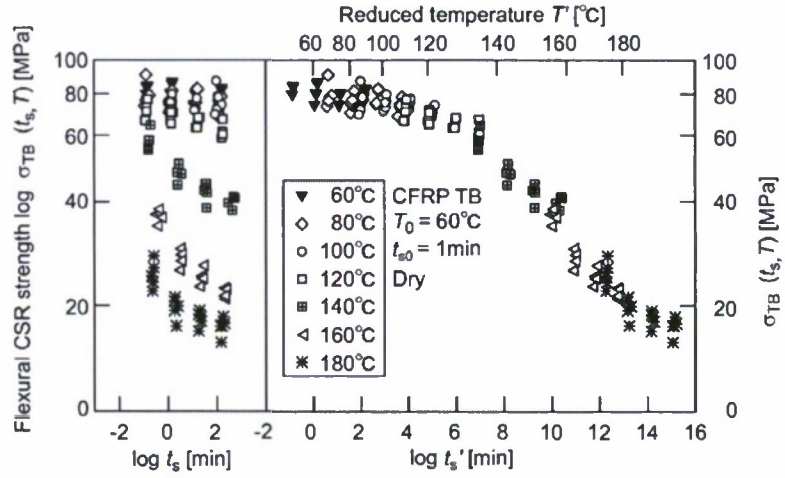

Fig.7 Master curve of flexural CSR strength for the transverse direction of unidirectional CFRP

3.4 Relationships between CSR strengths of Unidirectional CFRP and Creep Compliance of Matrix Resin

Figs.8-10 show the graphs that the tensile and flexural CSR strengths of the longitudinal direction and the flexural CSR strength of the transverse direction of unidirectional CFRP laminates are plotted against the inverse of creep compliance for epoxy resin at the same conditions of time and temperature. The relationship of each CSR strength of CFRP laminates versus the inverse creep compliance of epoxy resin makes smooth curve, respectively. Therefore, each of three kinds of CSR strength of CFRP laminates is uniquely determined by the creep compliance of matrix resin. Therefore, it is cleared experimentally that these CSR strengths are controlled by the viscoelastic behavior of matrix resin.

The tensile CSR strength for the longitudinal direction of unidirectional CFRP laminates, σ_{LT}, can be shown by the following equation based on Rosen's shear lag model [11].

$$\frac{\sigma_{LT}(t_s,T)}{\sigma_{LTg}} = \left[\frac{G_m(t,T)}{G_{mg}}\right]^{1/(2m)} \tag{3}$$

where σ_{LT} and σ_{LTg} is the tensile CSR strength at time to failure and temperature and its glassy value, $G_m(t,T)$ and G_{mg} are the shear relaxation modulus of matrix resin at relaxation time and temperature and its glassy value, and m is Weibull shape parameter of tensile strength of carbon fiber (T300, m=8.2). G_m/G_{mg} is nearly equal to E_m/E_{mg}, where E_m and E_{mg} are the relaxation modulus of matrix resin at relaxation time and temperature and its glassy value. In Fig. 8, the straight line with slope of 1/2m = 1/16.4 capture the test data approximately, therefore, it is also cleared in the view point of failure mechanism that the time-temperature dependent tensile CSR strength for the longitudinal direction of unidirectional CFRP laminates is controlled by the viscoelastic behavior of matrix resin.

The flexural fracture in the longitudinal direction of unidirectional CFRP laminates is the microbuckling of carbon fibers in the compression side of specimen. In this case, the flexural CSR strength for the longitudinal direction of unidirectional CFRP laminates, σ_{LB}, can be shown by the following equation based on Dow's microbuckling theory [12].

$$\frac{\sigma_{LB}(t_s,T)}{\sigma_{LBg}} = \left[\frac{E_m(t,T)}{E_{mg}}\right]^{1/2} \tag{4}$$

where σ_{LB} and σ_{LBg} is the flexural CSR strength at time to failure and temperature and its glassy value, $E_m(t,T)$ and E_{mg} are the relaxation modulus of matrix resin at relaxation time and temperature and its glassy value. In Fig.9, the straight line with slope of 1/2 capture the test data adequately, therefore, it is also cleared in the view point of failure mechanism that the time-temperature dependent flexural CSR strength for the longitudinal direction of unidirectional CFRP laminates is controlled by the viscoelastic behavior of matrix resin.

The flexural CSR fracture for the transverse direction of unidirectional CFRP laminates is triggered by the tensile fracture of matrix resin in the tension side of specimen. It can be theoretically presumed that this CSR strength of CFRP laminates is uniquely determined by the creep compliance of matrix resin, because the same TTSP for the creep compliance of matrix resin holds for the tensile strength of epoxy resin. Fig. 10 shows that this presumption is also experimentally true.

4. Conclusion

Time and temperature dependent CSR strengths for typical three directions of unidirectional CFRP laminates, which are the tensile and compressive CSR strengths for the longitudinal direction and the tensile strength for the transverse direction, are measured at various strain rates and temperatures. The master curves of these CSR strengths are constructed by using measured data based on TTSP to be held for the creep compliance of matrix resin. Additionally, the relationships between the viscoelastic behavior of matrix resin and these CSR strengths are evaluated on the

viewpoints of failure mechanism. The applicability of ATM for predicting the long-term CSR strengths of CFRP laminates is confirmed experimentally and theoretically.

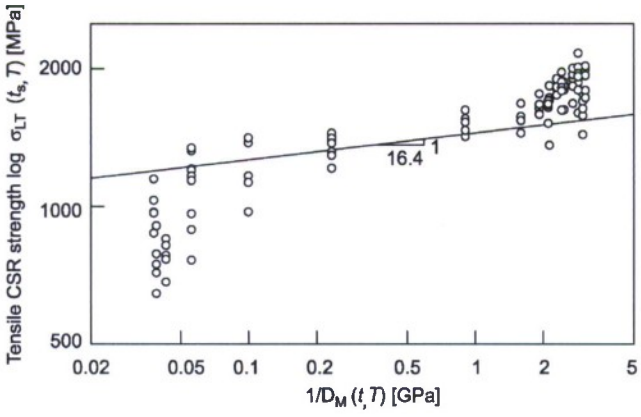

Fig.8 Tensile CSR strength for the longitudinal direction for unidirectional CFRP versus inverse of creep compliance of matrix resin

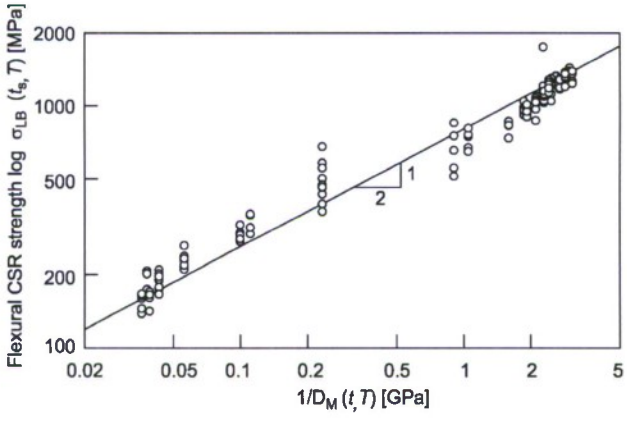

Fig.9 Flexural CSR strength for the longitudinal direction for unidirectional CFRP versus inverse creep compliance of matrix resin

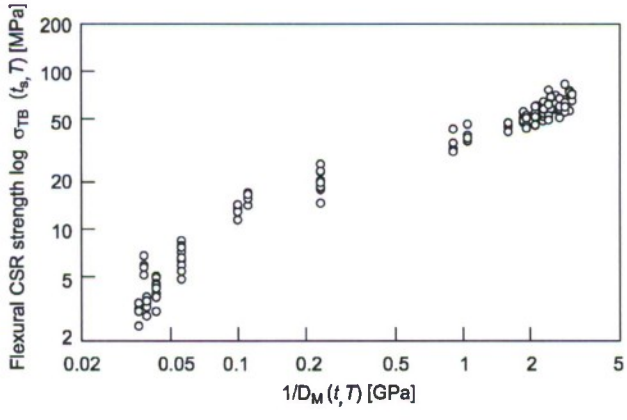

Fig.10 Flexural CSR strength for the transverse direction for unidirectional CFRP versus inverse creep compliance of matrix resin

NAVY RELEVANCE

The proposed accelerated testing methodology has effectively combined the effects of time, temperature and water absorption on the strength and life of composite materials. It can be confirmed experimentally and theoretically that the methodology is applicable to the innovative CFRP laminates for marine use.

ACKNOWLEDGEMENTS

The authors thank the Office of Naval Research for supporting this work through an ONR award (N000140110949) with Dr. Yapa Rajapakse as the program manager of solid mechanics. The authors thank Professor Richard Christensen at Stanford University as the consultant of this project and Toray Industries, Inc. as the supplier of CFRP laminates.

REFERENCES

1. Aboudi, J. and G. Cederbaum, "Analysis of Viscoelastic Laminated Composite Plates", Composite Structures, 12 (1989), 243-256.
2. Sullivan, J., "Creep and Physical Aging of Composites", Composite Science and Technology, 39 (1990), 207-232.
3. Gates, T., "Experimental Characterization of Nonlinear, Rate Dependent Behavior in Advanced Polymer Matrix Composites", Experimental Mechanics, 32 (1992), 68-73.
4. Miyano, Y., M. Kanemitsu, T. Kunio and H. Kuhn, "Role of Matrix Resin on Fracture Strengths of Unidirectional CFRP", Journal of Composite Materials, 20 (1986), 520-538.
5. Enyama, J., M. K. McMurray, M. Nakada and Y. Miyano, "Effects of Stress Ratio on Flexural Fatigue Behavior of a Satin Woven CFRP Laminate", Proceedings of 3rd Japan SAMPE, Vol. 2: (1993), 2418-2421.
6. McMurray, M. K., J. Enyama, M. Nakada and Y. Miyano, "Loading Rate and Temperature Dependence on Flexural Fatigue Behavior of a Satin Woven CFRP Laminate", Proceedings of 38th SAMPE, No. 2 (1993), 1944-1956.
7. Miyano, Y., M. K. McMurray, J. Enyama and M. Nakada, "Loading Rate and Temperature Dependence on Flexural Fatigue Behavior of a Satin Woven CFRP laminate", Journal of Composite Materials, 28 (1994), 1250-1260.
8. Miyano, Y., M. Nakada, M. K. McMurray and R. Muki, "Prediction of Flexural Fatigue Strength of CFRP Composites under Arbitrary Frequency, Stress Ratio and Temperature", Journal of Composite Materials, 31 (1997), 619-638.
9. Miyano, Y., Nakada, M., Kudoh, H. and Muki, R., "Prediction of tensile fatigue life under temperature environment for unidirectional CFRP", Advanced Composite Materials, **8**, 235-246 (1999).
10. Miyano, Y., Nakada, M. and Muki, R., "Applicability of Fatigue Life Prediction Method to Polymer Composites", Mechanics of Time-Dependent Materials, **3**, 141-157 (1999).
11. Nakada, M., Miyano, Y., Kinoshita, M., Koga, R., Okuya, T. and Muki, R., "Time-Temperature Dependence of Tensile Strength of Unidirectional CFRP", Journal of Composite Materials, **36**, 2567-2581 (2002).
12. Dow, F., Gruntfest, I. J., "Determination of Most-needed, potentially possible Improvements in Materials for Ballistic and Space Vehicles", Space Sciences Laboratory Structures and Dynamics Operation, T.I.S.R60SD389 (1960).

PUBLICATIONS (ONR supported)

Papers in refereed journals

1. Y. Miyano, M. Nakada and N. Sekine, "Accelerated Testing for Long-Term Durability of GFRP Laminates for Marine Use", Composites Part B, 35 (2004), pp497-502.
2. Y. Miyano, M. Nakada and N. Sekine, "Accelerated Testing for Long-Term Durability of FRP Laminates for Marine Use", Journal of Composite Materials, Vol.39 (2005), pp5-20.
3. Y. Miyano and M. Nakada, "Long-Term Durability and Damage Tolerance of Innovative Marine

Composites (NICOP), Part I: Accelerated Testing for Long-Term Durability of Various FRP Laminates for Marine Use", Materials System, Vol.25 (2007), pp.71-82.
4. I. Kimpara and H. Saito, "Long-Term Durability and Damage Tolerance of Innovative Marine Composites (NICOP), Part II: Post-Impact Fatigue Behavior of Woven and Knitted Fabric CFRP Laminates for Marine Use", Materials System, Vol.25 (2007), pp.83-94.

Data base

1. Data Base on the ONR Project "Long-Term Durability and Damage Tolerance of Innovative Marine Composites (NICOP)", Materials System, Vol.25 (2007), pp.95-147.

Conference proceedings

1. Y. Miyano, N. Sekine, J. Ichimura and M. Nakada, "Time-Temperature-Water Absorption Dependence of Flexural Fatigue Strength of Plain Woven CFRP Laminates", 6th International Conference on Durability Analysis of Composite Systems, (Riga, May 2004).
2. Y. Miyano, J. Ichimura, N. Sekine and M. Nakada, "Accelerated Testing for Long-Term Durability of Advanced CFRP Laminates for Marine Use", 11th Japan-United States Conference on Composite Materials, (Yonezawa, Sept. 2004).
3. M. Nakada, J. Ichimura, N. Sekine and Y. Miyano, "Time-Temperature-Water Absorption Dependent Fatigue Strength of Plain Woven CFRP Laminates", 11th Japan-United States Conference on Composite Materials, (Yonezawa, Sept. 2004).
4. M. Nakada, J. Ichimura and Y. Miyano, "Long-Term Durability of Plain-Woven CFRP Laminates under Water Conditions", 2nd JSME/ASME International Conference on Materials and Processing 2005 (Seattle, June 2005).
5. E. Hayakawa, J. Ichimura, M. Nakada, Y. Miyano, "Influence of Water Absorption on the Time-Temperature Dependent Flexural Strength of Plain Woven CFRP", 2nd JSME/ASME International Conference on Materials and Processing 2005 (Seattle, June 2005).
6. Y. Miyano, J. Ichimura and M. Nakada," Accelerated Testing for Long-Term Durability of Advanced CFRP Laminates for Marine Use", 15th International Conference on Composite Materials, (Durban, June 2005)
7. M. Nakada, J. Ichimura, J. Noda and Y. Miyano, "Time-Temperature-Water Absorption Dependent Flexural Strength of CFRP Laminates for Marine Use", 5th International Conference on Mechanics of Time Dependent Materials, (Karuizawa, October 2005).
8. M. Nakada, E. Hayakawa, J. Noda and Y. Miyano, "Influence of Water Absorption on Time-Temperature Dependent Fatigue Strength of Plain Woven FRP Laminates", 12th US-Japan Conference on Composite Materials, (Dearborn, September 2006).
9. M. Nakada and Y. Miyano, "Accelerated Testing for Long-term Durability of Various FRP Laminates for Marine Use", 16th International Conference on Composite Materials, (Kyoto, July 2007).
10. J. Noda, M. Nakada, and Y. Miyano, "Formulation of Time-temperature Dependent Long-term Fatigue Strength of CFRP Laminates", 16th International Conference on Composite Materials, (Kyoto, July 2007).

Part 2
2007 ONR Solid Mechanics Program

Damage Evolution under Post-Impact Fatigue of CFRP Laminates for Marine Use

Isao Kimpara and Hiroshi Saito
Materials System Research Laboratory, Kanazawa Institute of Technology
3-1 Yatsukaho, Hakusan, Ishikawa 924-0838, Japan

OBJECTIVE

The damage tolerance performance of CFRP laminates for marine use was evaluated based on the clarification of impact damage and its evolution behavior. The damages within CFRP laminates were clarified with non-destructive methods and the direct observation of cross-section three-dimensionally.

APPROACH

The impact damage and its propagation behavior under fatigue loading and water environment of T300-3K plain woven and T700S-12K multi-axial knitted CFRP laminates were discussed. Matrix resin was vinylester, and the molding method was vacuum assisted resin transfer molding (VARTM). The damage mechanism within candidate CFRP laminates was evaluated based on the precise observation. Ultrasonic scanning was conducted as a non-destructive observation method, and the cross-sectional observation was also conducted at multiple sections of laminate. The difference between post-impact fatigue (PIF) damage morphology of plain woven and multi-axial knitted CFRP laminates was characterized under dry and wet condition.

RECENT ACHIEVEMENTS

The damage tolerance performance of CFRP laminates for marine use was evaluated. For this purpose, the impact damage mechanism and its propagation behavior of T300 plain woven and T700 multi-axial knitted CFRP laminates were observed by non-destructive and destructive observation methods. Each image observed by these approaches was integrated and 'three-dimensional' damage distribution images were obtained. In addition, environmental effects on mechanical properties of damaged CFRP laminate were evaluated.

1. Introduction

When composites are applied to large-scale structures such as ships, the number of stacking layer becomes larger with conventional thin prepreg or woven fabric, thus long time to molding, labor and cost are necessary. In order to clear these problems, multiaxial knitted fabric which has comparatively thickness and no-crimp is focused as one of new-style reinforcement fabric [1-5]. This fabric has the characteristic configuration in which fiber layers aligned in multiaxial direction are stacked and knitted each other. Therefore thickness and fiber alignment can be obtained with less number of stacking. Additionally, it is thought that no-crimp configuration appears excellent mechanical properties of reinforcement fibers easier than conventional woven fabric etc. On the other hand, as the molding method to be able to facilitate and reduce the price of molding composite for large-scale structures by combining with multiaxial knitted fabric, vacuum assisted resin transfer molding (VARTM) method is paid to attention. Because VARTM does not need the closed mold and pressurized device to the resin either, VARTM is expected as a highly accurate molding method that takes the place of a conventional RTM. Besides, objective large-scale structures are affected by the environment such as variable temperature and humid. The studies of the effect of temperature of polymer composite materials have been conducted [6,7].

In this study, the impact damage and its propagation behavior under fatigue loading and water environment of T300-3K plain woven and T700S-12K multi-axial knitted CFRP laminates were discussed. Matrix resin was vinylester, and the molding method was vacuum assisted resin

transfer molding (VARTM). The damage mechanism within candidate CFRP laminates was evaluated based on the precise observation. Ultrasonic scanning was conducted as a non-destructive observation method, and the cross-sectional observation was also conducted at multiple sections of laminate. The difference between impact damage morphology of plain woven and multi-axial stitched CFRP laminates was characterized three-dimensionally.

2 Materials and Testing Methods

2.1 Materials

The candidate material is a basic type of plain woven fabric, T300B-3K, and newly developed multi-axial knitted fabric, T700S-12K, both of them supplied by Toray Industries, Inc. The innovative multi-axial knitted fabric is expected to apply to the thick and large structural component such as marine ships, because it has much thickness than the conventional T300 fabric (Fig.1(a)), and good mechanical property is expected by its no-crimp configuration and smooth warping performance. Multi-axial knitted fabric consists of several unidirectional or random-mat layers joined by polyester knitting fibers as shown in Fig.1(b). CFRP laminates are molded based on vacuum assisted resin transfer molding (VARTM), which is suitable molding method for large-scale structures. In VARTM, resin is impregnated into reinforcements by atmospheric pressure, unlike conventional RTM with the pressurized resin pot and the rigid closed mold. Figure 2 shows a schematic image of VARTM setup. Resin firstly flows into a flow medium, and then flows into reinforcements. The driving force of resin flow is atmospheric pressure.

Fig.1 Schematic image of plain woven fabric

Fig.2 Schematic image of multi-axial knitted fabric

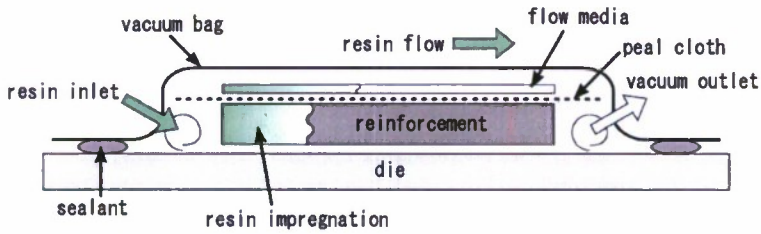

Fig.3 Schematic of vacuum assisted resin transfer molding (VARTM) setup

2.2 Impact test

A drop weight with a steel semi-spherical tip was used as an impactor. The weight of the impactor was 1113.5 g and the diameter of the tip was 16 mm. The specimen was mounted between supporting steel plates with a cutout hole 30 mm in diameter, as shown in Fig. 4, and was subjected to impact energy directly using the impactor. Impact loading of 1 J per mm thickness was applied to the center of the specimen by the impactor. The impact damage in the specimen was observed and characterized by ultrasonic C-scan method and direct cross-section observations.

2.3 Compression after impact (CAI) test and post-impact fatigue (PIF) test

Compressive strength after impact (CAI) and post-impact fatigue (PIF) properties were evaluated. In this study, CAI and PIF tests were conducted with same specimen level as shown in Fig.5. Figure 6 shows a fixture for CAI test. Gauge length was 50 mm. Compressive load was applied by Servopulser EHF-EB100kN-20L (Shimadzu Co., Ltd.). Test speed of CAI was 1.0 mm/min. In PIF tests, stress ratio R was -1, that is, tension-compression test.

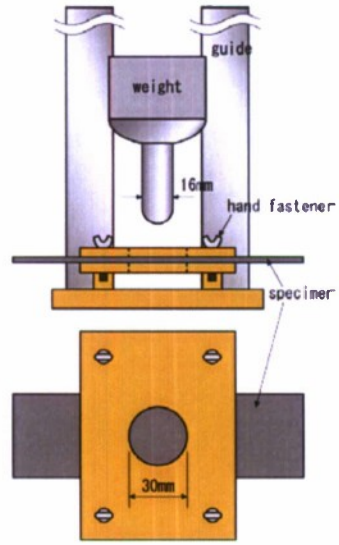

Fig.4 Schematic image of a fixture of impact test

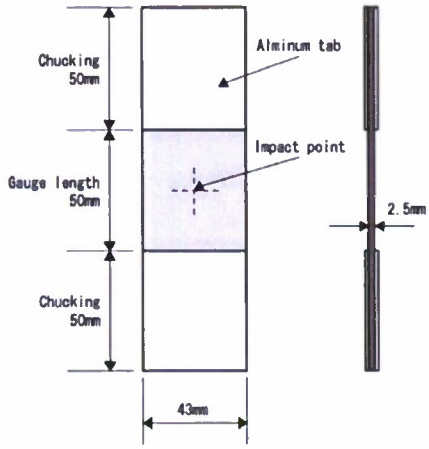

Fig.5 Dimension of the specimen

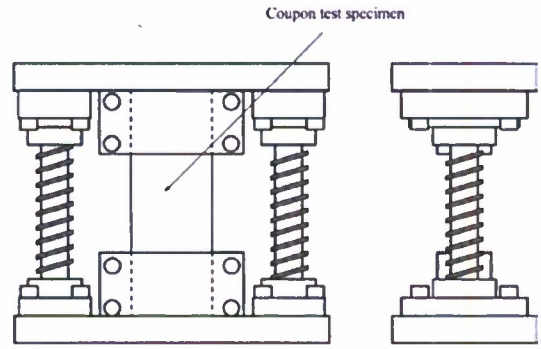

Fig.6 The fixture of CAI test

2.4 Water absorption condition

The effect of water absorption on CAI and PIF strength of CFRP laminates for marine use was evaluated with specimens immersed water bath. Same level coupon specimens as well as normal dry CAI and PIF tests were used for water absorbed CAI and PIF tests. In order to absorb water to specimens up to saturation water content, the accelerated water absorption tests were conducted as shown in Fig.7. Based on these tests, water absorption conditions were

decided as follows; both multi-axial knitted and plain woven CFRP specimens were soaked in a water bath at 95°C for 120 hours up to saturation water content of 0.6wt%. After absorption of water, same level impact (1 J per unit thickness) was applied to these specimens. Specimens after soaking were named as "Wet", as contrasted with "Dry" ones. In order to keep the water content of Wet specimen through the PIF test, gauge region of specimen was covered by plastic bag and filled with water inside of it, as shown in Fig.8. Stress amplitude in PIF tests was 80 %, 70 % and 60 % for both multi-axial knitted and plain woven CFRP.

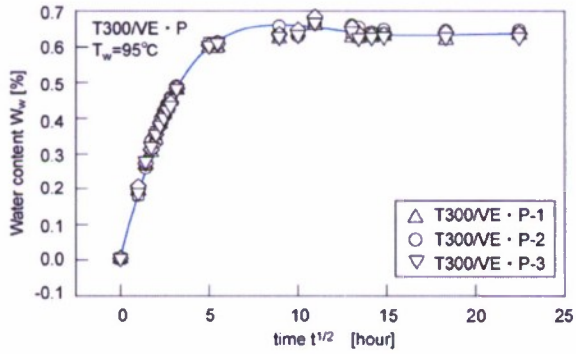

Fig.7 Water content versus time.

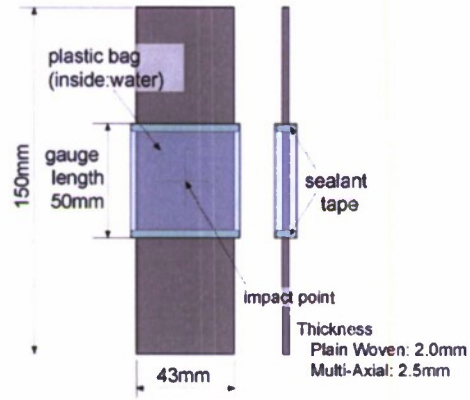

Fig.8 Configuration of Wet specimen.

3. Approach to evaluate damages

3.1 Non-destructive evaluation

Damage progress behavior was observed from the opposite side of impact side of specimens by thermo-elastic stress analyzer (TESA) (JER-8010, JEOL.Ltd) and ultrasonic scanning (UT-2000, Toray Engineering Co., Ltd.). TESA can detect instantaneous changes in a material's surface stress state as instantaneous changes in the material's surface temperature. Therefore 'in-situ' damage propagation behavior can be observed by TESA. Ultrasonic scanning (C-scan) can observe internal damage distribution, especially delamination. C-scan produces an image showing the shape, size, location, and depth of delamination. In this study, the frequency of the transducer was 25 MHz.

3.2 Direct observations

Multiple cross-sections of the same laminate as observed by C-scan, were observed by optical microscope. A square portion with 30-mm sides and with the impact point as the center was cut and embedded in resin to facilitate easy grinding and polishing of the cross section of the laminate. After curing the resin, the face normal to the cross section of the laminate was ground using No. 320 sandpaper, and polished using 9 μm, 3 μm and 1 μm diamond slurry stepwise using a precision polishing machine (TegraPol-15, Struers Co., Ltd.). The mirror-finished cross-section was scanned using a blue-ray microscope (VL2000D, LaserTech Co., Ltd.).

3.3 Three-dimensional characterization of the impact damage within laminate

In order to characterize the impact damage on CFRP laminate, both images observed by ultrasonic C-scan device and cross-sectional observation were compared and integrated as shown in Fig.9. This figure shows the flow in the characterization methodology of the impact damage on CFRP laminate. Both observation methods give different plain information each other about the impact damage, and information obtained is evaluated synthetically. Finally the three-dimensional damage distribution image is estimated.

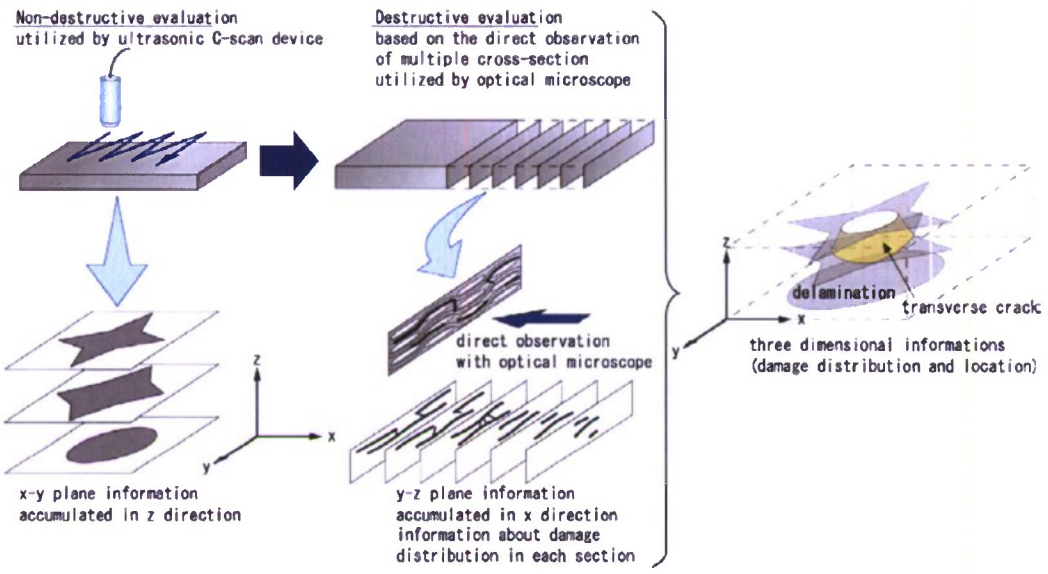

Fig.9 Methodology of the three-dimensional characterization of the impact damage inside laminate

4 Effect of water absorption on post-impact fatigue properties

Figure 10 shows the compressive strength of plain woven and multi-axial knitted CFRP. Here, the specimens without impact damage were named as "bulk" ones, and plain woven and multi-axial knitted CFRP were described as "PW" and "MA", respectively. From this graph, the compressive strength of bulk plain woven and multi-axial knitted CFRP decreased in 59 % and 66 % by the impact damage, respectively. On the other hand, CAI strength of Wet plain woven and multi-axial knitted CFRP were 4.4 % and 7.7 % lower respectively than that of Dry ones. Consequently, the effect of water absorption on CAI strength was little.

Figure 11 shows the result of PIF tests of both plain woven and multi-axial knitted CFRP laminates. All S-N curves in this figure showed approximately inverse linear relation. Both CAI and PIF strength of Dry multi-axial knitted CFRP were higher than that of the other specimens. Slope of approximation line of multi-axial knitted CFRP was smaller than that of plain woven CFRP. Stress amplitude level of Dry multi-axial knitted CFRP was higher than that of Dry plain woven CFRP. Consequently, it is obvious that fatigue performance of MA Dry is fairly higher than that of the others.

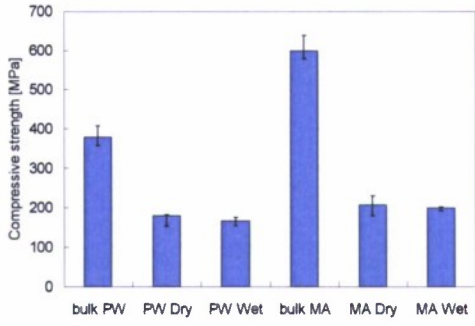

Fig.10 Compressive strength after impact of plain woven and multi-axial knitted CFRP under dry and wet condition.

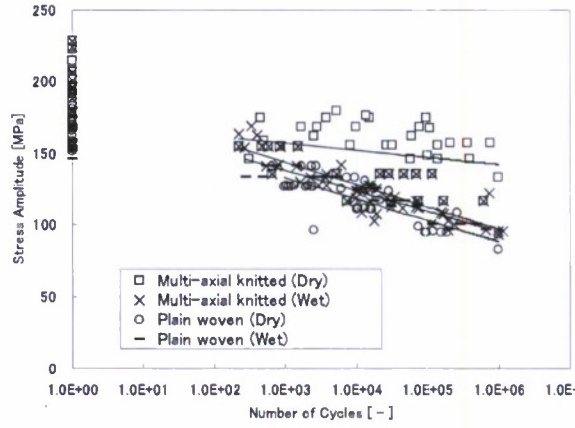

Fig.11 Fatigue strength under water absorption condition of plain woven and multi-axial knitted CFRP laminates

4.1 Plain woven CFRP laminates

For damage propagation observation, specimens were stopped at the cycle just before failure for Dry and Wet conditions, respectively. Here, we measured the stroke variations and also 'the sound of fiber breakage' for helping to determine the 'cycle just before failure'. Figure 12 shows ultrasonic C-scan images of both Dry and Wet specimens before and after fatigue tests. Load was applied in perpendicular direction in these images. In these images, damage propagation was not detected comparing with damage caused by impact only. Actually, plain woven CFRP laminate specimens showed sudden failure at the impact point in the final stage of PIF tests, and almost no-signs were observed before failure.

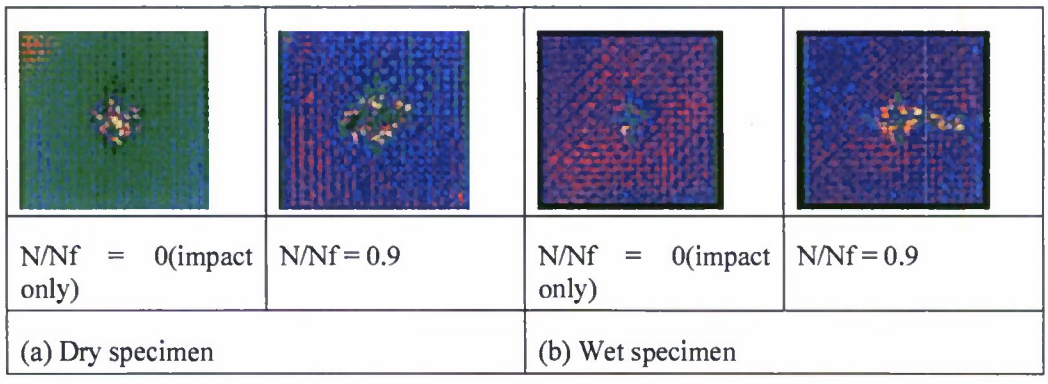

N/Nf = 0(impact only)	N/Nf = 0.9	N/Nf = 0(impact only)	N/Nf = 0.9
(a) Dry specimen		(b) Wet specimen	

Fig.12 Damage propagation shown in ultrasonic C-scan images of plain woven CFRP laminate

Figure 13 shows cross-sectional photographs of both Dry and Wet specimens before and almost final stage of fatigue tests. Cross-sections observed were along the loading direction, which is the perpendicular direction in the ultrasonic scanning images shown in Fig.18. However it is clear that the amount of delamination observed in the cross-sections of Wet specimen was larger than that of Dry specimen, increase of such delamination was not confirmed in the in-plain direction but in the through-thickness direction, as mentioned in Fig.12. Therefore, the characteristic damage morphology in plain woven CFRP is that the

number of delaminations increases almost only in through-thickness direction, not in the in-plain direction.

Figure 14 shows magnified images of cross-section of Dry specimen at both $N/N_f = 0$ (impact only) and $N/N_f = 0.9$. Compared to the section at $N/N_f = 0$, multiple transverse cracks (indicated as arrows in Fig.14) and evolution of delamination initiated from the tip of these cracks were observed.

Figure 15 shows magnified images of cross-section at $N/N_f = 0$ (impact only) in Fig.13. In dry condition, it is obvious that delamination occurred mostly between 'crossed' $0°/90°$ fiber bundles. On the other hand, delamination of Wet specimen occurred between 'parallel' fiber bundles aligned same direction (indicated as arrows in Fig.15) in addition to the interface between 'crossed' fiber bundles. This fact shows an evidence of interfacial degradation caused by water absorption.

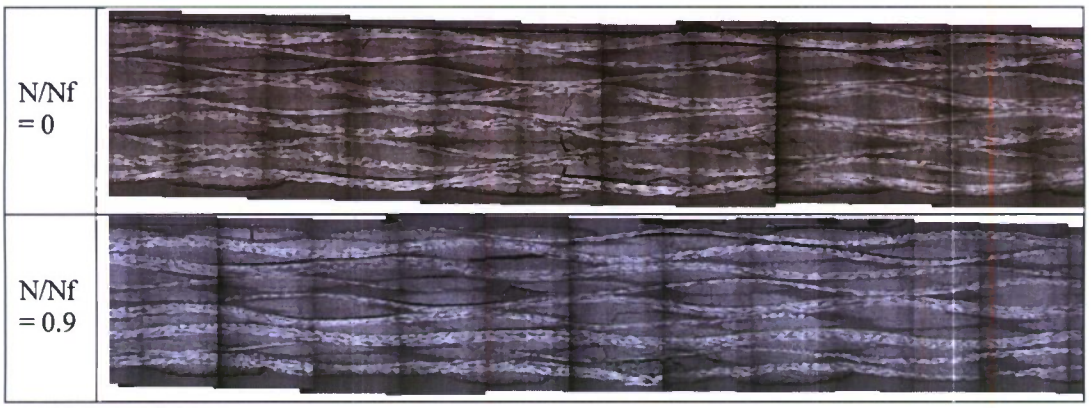

(a) Dry condition

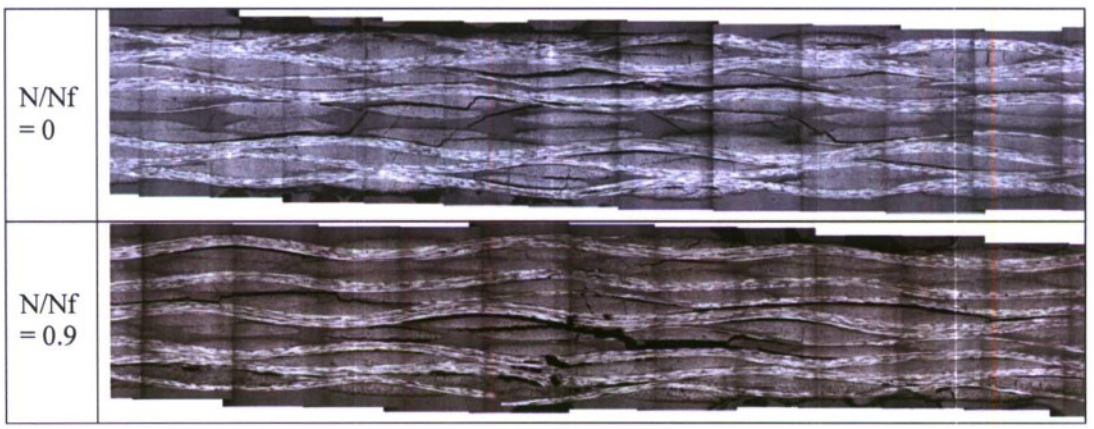

(b) Wet condition

Fig.13 Damage evolution behavior observed in cross-sectional photographs of plain woven CFRP.

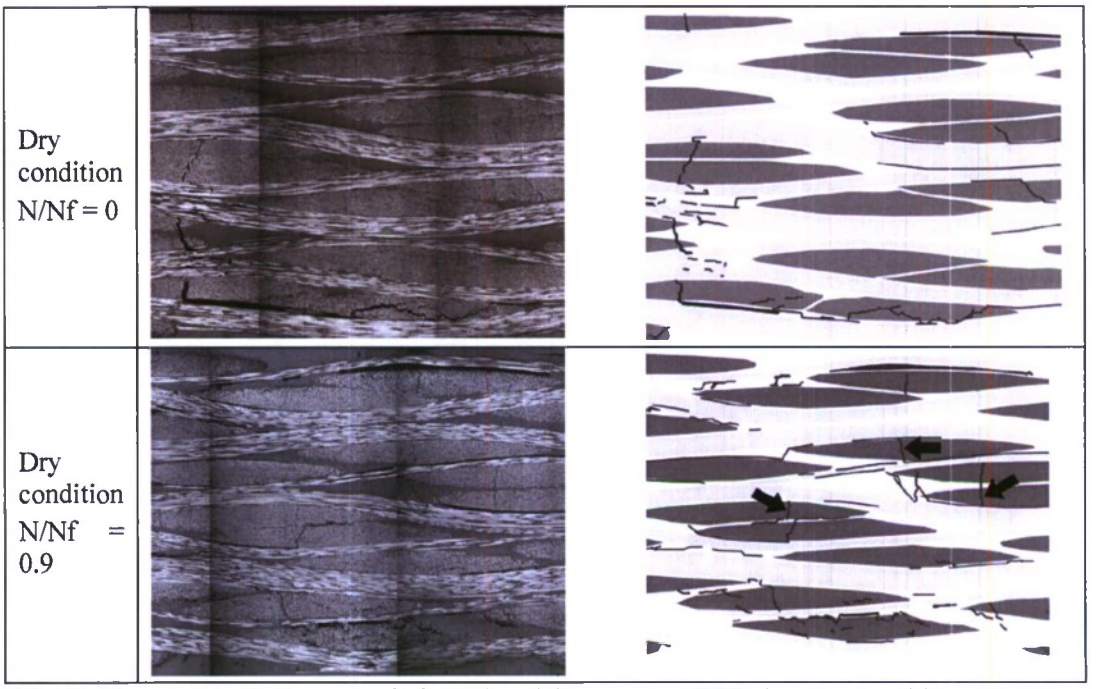

Fig.14 Damage evolution morphology in plain woven CFRP in dry condition. (Arrows indicates the transverse cracks.)

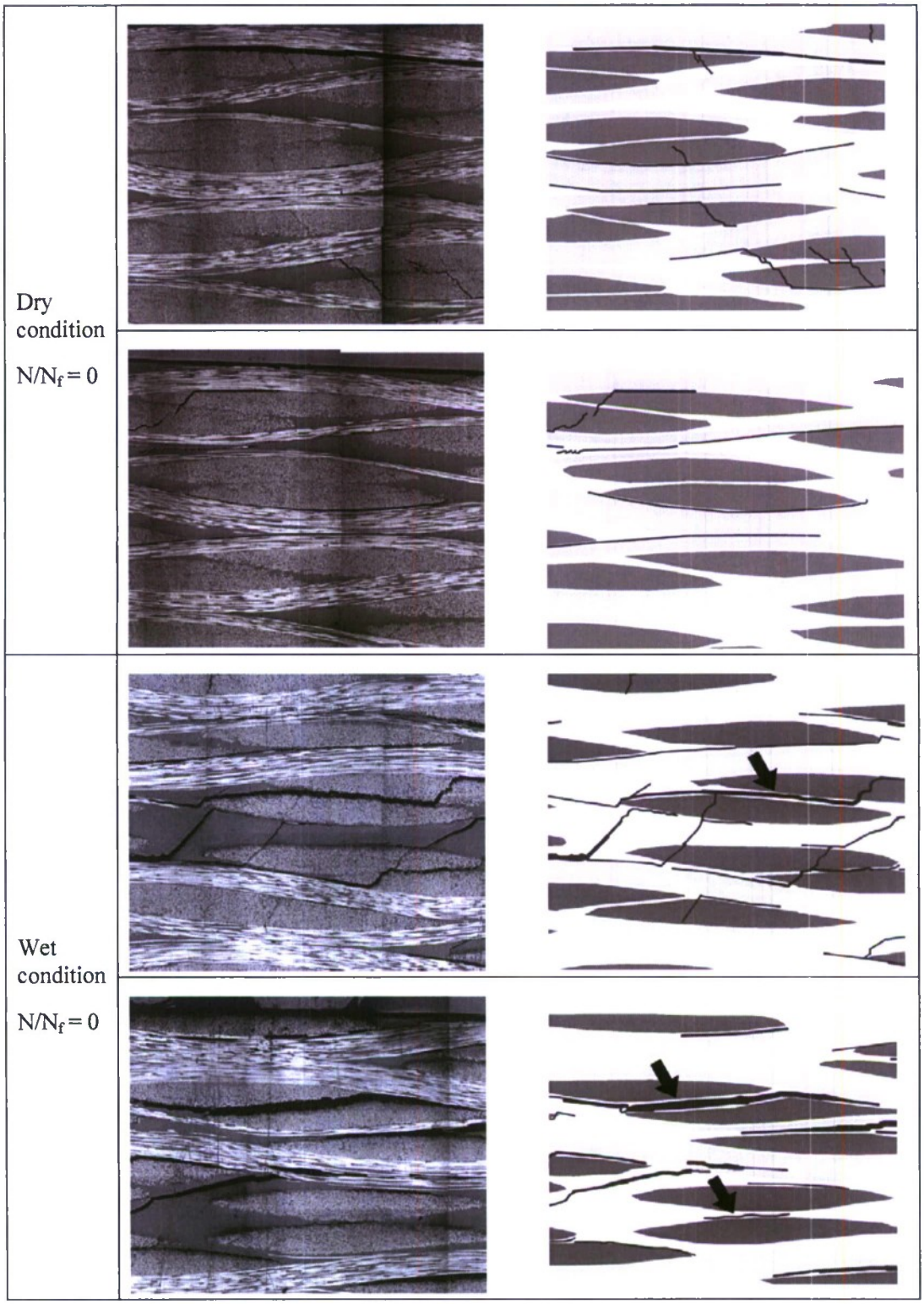

Fig.15 Effects of water absorption on the initial damage of plain woven CFRP. (Arrows indicates the delamination between fiber bundles aligned in same direction.)

4.2 Multi-axial knitted CFRP laminates

Figure 16 shows the ultrasonic C-scan images before and after fatigue test, respectively. Load was applied in perpendicular direction in these images. It is clear that the damage propagated in load direction in both Dry and Wet. However, this large delamination in loading direction propagated just after starting of fatigue test in the back side of impact side. Therefore it is premature to determine that only this large delamination is the damage propagated by fatigue, thus it is not enough to observe damages only with ultrasonic scanning. Final failure occurred in horizontal direction centering on the impact point.

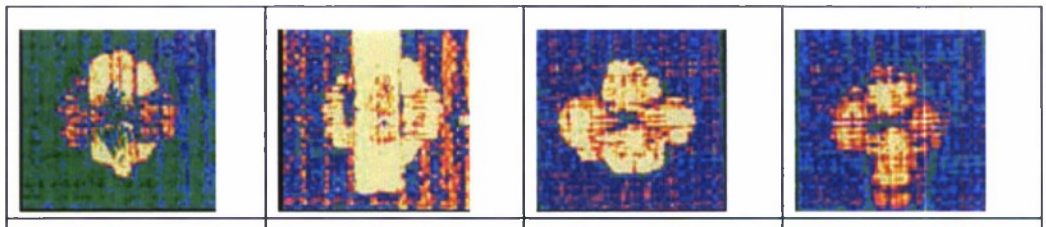

N/Nf = 0(impact only)	N/Nf = 0.9	N/Nf = 0(impact only)	N/Nf = 0.9
(a) Dry specimen		(b) Wet specimen	

Fig.16 Damage propagation shown in ultrasonic C-scan images of multi axial knitted CFRP laminate.

Figure 17 shows cross-sectional photographs of both Dry and Wet specimens before and almost final stage of fatigue tests. Cross-sections observed were along the loading direction, which is the perpendicular direction in the ultrasonic scanning images shown in Fig.16. The increase of transverse crack was dominant damage in the cross-section of both Dry and Wet specimen in PIF tests. On the other hand, delamination growth was little, except the delamination in back-side of impact side.

Figure 18 shows magnified images of cross-section of both Dry and Wet specimens at $N/N_f = 0.9$ (almost final stage in PIF test) in Fig.17. Through the PIF test, multiple transverse cracks occurred, and delaminations propagate from the tip of these cracks. Therefore, delamination area increased with the progress of fatigue.

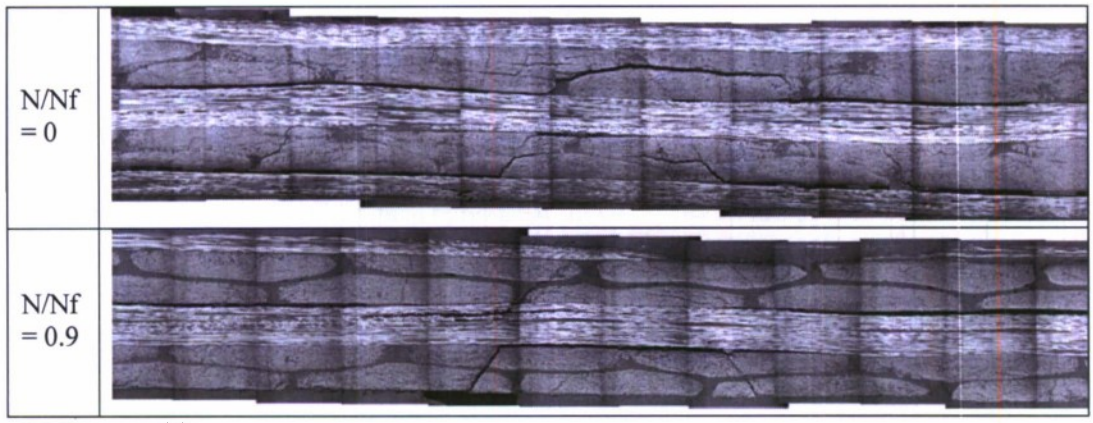

(a) Dry condition

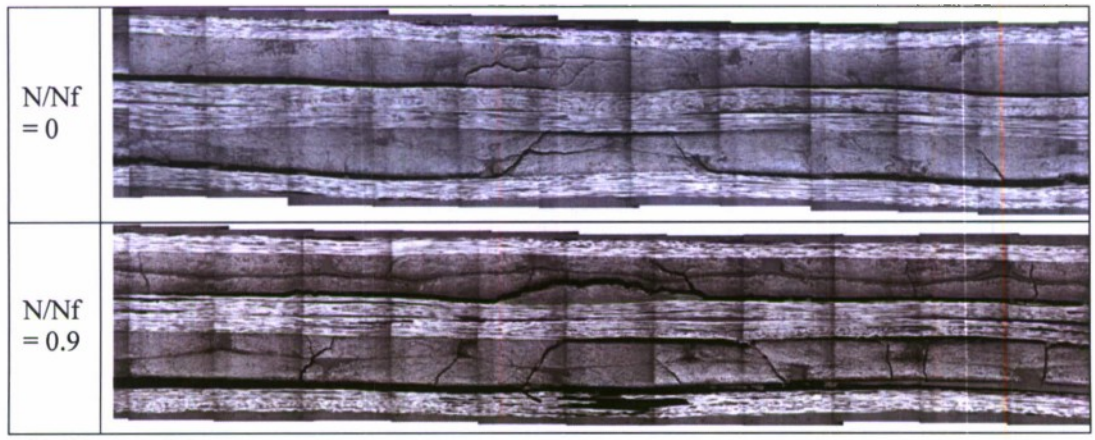

(b) Wet condition

Fig.17 Damage evolution behavior observed in cross-sectional photographs of multi-axial knitted CFRP.

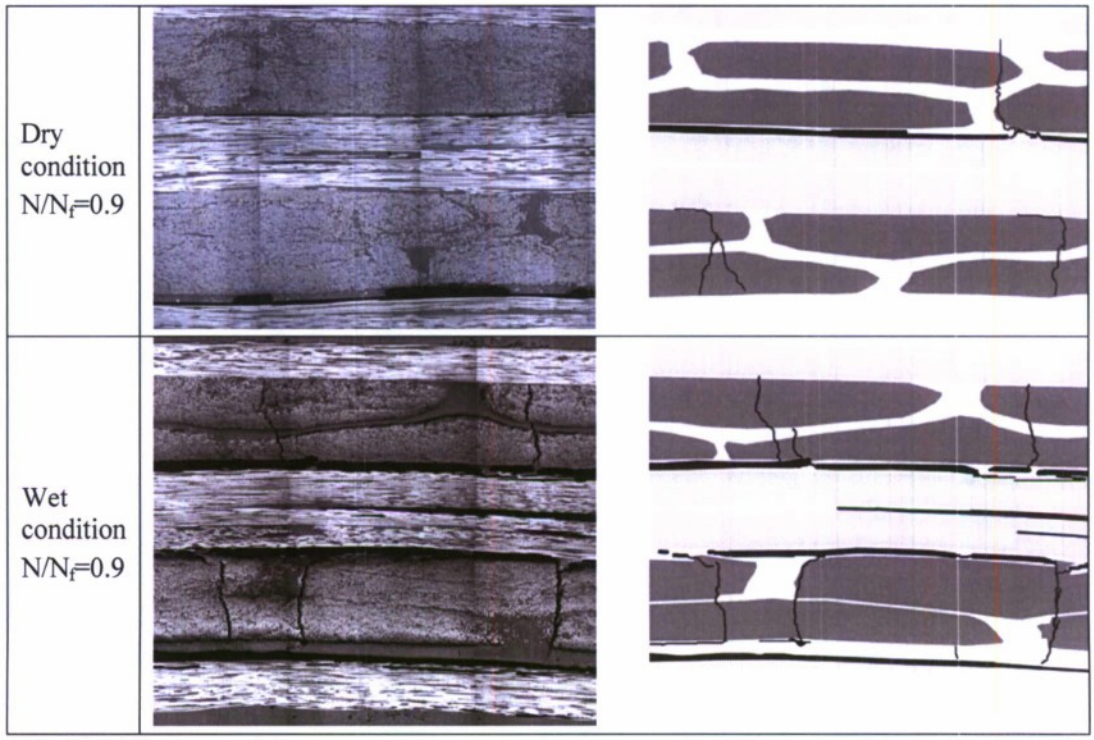

Fig.18 Differences of damage evolution behavior between dry and wet conditions.

5 Conclusions

In this study, the damage evolution behavior under post-impact fatigue and water environment of T300-3k plain woven (PW) and T700S-12k multi-axial knitted (MA) CFRP laminates were evaluated. The effect of water absorption on CAI and PIF properties was small for PW CFRP laminates. Conversely, PIF properties of water absorbed MA CFRP laminates drastically decreased than that of dry ones. CAI strength was not affected by water absorption. PIF performance of dry MA CFRP was fairly higher than that of the others.

Delamination area of PW CFRP is almost unchanged through the PIF test. The characteristic damage morphology in PW CFRP is that the number of delaminations increases almost only in through-thickness direction, not in the in-plain direction. Delamination area of MA CFRP increases with the progress of PIF test. From the observation of cross-sections, it was confirmed that the interface between fibers or fiber bundles could be affected by the water absorption in both PW and MA CFRPs.

Acknowledgements

The authors thank the Office of Naval Research for supporting this work through an ONR award (N000140110949) with Dr. Yapa Rajapakse as the program manager of solid mechanics. The authors thank Professor Richard Christensen at Stanford University as the consultant of this project and Toray Industries, Inc. as the supplier of CFRP laminates. All of experimental data were measured by the graduate students of author's laboratory, in Kanazawa Institute of Technology. The authors thank these graduate students, Mr. Takahiro Nozaki, Mr. Teppei Kimura and Norihiko Ikeda.

References

[1] Kong H, Mouritz AP, Paton R., *Compos Struct*, 66: 249–59 (2004).

[2] Lomov SV, Belov EB, Bischoff T, Ghosh SB, Truong Chi T, Verpoest I., *Compos Part A*, 33: 1171–83 (2002).
[3] Lomov SV, Verpoest I, Barburski M, Laperre J., *Compos Part A*, 34: 359–70 (2003).
[4] Kang TJ, Kim C., *Comp Sci Tech*, 60: 773–84 (2000).
[5] Hu J, Jiang Y., *Compos Part A*, 33: 725–34 (2002).
[6] Matsuda S, Hojo M, Ochiai S., *JSME Int J Series A*, 42(3): 421-428 (1999).
[7] Kootsookos A, Mouritz AP., *Comp Sci Tech*, 64: 1503-1511, (2004).

Part 3

2008 ONR Solid Mechanics Program

Formulation Based on Advanced ATM for Long-Term Fatigue Life Prediction of CFRP Laminates for Marine Use

Yasushi Miyano, Masayuki Nakada and Hongneng Cai
Materials System Research Laboratory
Kanazawa Institute of Technology
3-1 Yatsukaho Hakusan Ishikawa 924-0838, Japan

OBJECTIVES

The main objectives of this research include: (a) proposing theoretically an advanced accelerated testing methodology (advanced ATM) for the long-term fatigue life prediction of polymer composites on the viewpoint of viscoelastic behavior of matrix resin; (b) verifying experimentally the proposed advanced ATM for CFRP laminates for marine use.

TECHNICAL APPROACH

The advanced ATM is proposed based on the viscoelastic behavior of matrix resin. The formulation of long-term fatigue life of polymer composites is established for the advanced ATM. The advanced ATM is verified by applying the formulation to the long-term fatigue of CFRP laminates for marine use.

RECENT ACCOMPLISHMENTS

Previously, authors of this paper have developed an accelerated testing methodology (ATM) to predict the long-term fatigue life of the polymer matrix composites based on the time-temperature superposition principle (TTSP) held for the viscoelastic behavior of matrix resin. The ATM using the TTSP enables us to describe the long-term life by means of master curves covering wide ranges of loading and environmental conditions, including load duration, temperature, frequency of load cycles, load amplitude ratios, etc. The ATM has been applied for various composites and their joint structures, and demonstrated with a great success as a robust and power methodology for the long-term life prediction. This methodology can be applied to the life prediction of polymer composites exposed only to the constant load pattern (load amplitude and frequency) and environmental condition (temperature and water absorption).

In the present paper, we propose an advanced accelerated testing methodology (advanced ATM) which can be applied to the life prediction of polymer composites exposed to an actual load and environment history. First, the four conditions for the advanced ATM are introduced. Second, the long-term fatigue strength of polymer composites exposed to an actual load and environment history is formulated based on the four conditions. Third, the parameters in the formulation are determined for CFRP laminates for marine use. As results, it is verified that the advanced ATM is applicable to the long-term fatigue life prediction of CFRP laminates for marine composites exposed to an actual load and temperature history.

1. Advanced ATM

The advanced ATM is established with four following conditions: (A) the same TTSP is applicable for both non-destructive viscoelastic behavior and destructive strength properties of matrix resin and their composites; (B) strength variation is caused by viscoelastic compliance of matrix resin; (C) failure probability is independent of time, temperature, frequency and stress ratio; (D) strength degradation is caused by linear cumulative damage of cyclic loading.

A key component of the advanced ATM is also the empirical observation (A), which has been demonstrated its applicability for various polymeric composite materials and their structures. Based on the condition (A), the master curves of constant strain rate (CSR), creep and fatigue strengths in the wide range of time and temperature can be determined by the data measured by these tests under the short-term and elevated temperature conditions. With the condition (B), it is possible to calculate the strength variation by the viscoelastic compliance of matrix resin determined by the creep compliance of matrix resin and the history of load and temperature changed with time. With the condition (C), the reference strength and the failure probability can be obtained by measuring CSR strength at an arbitrary strain rate under room temperature. With the condition (D), it is possible to calculate the strength degradation by load cycles undergoing to the linear cumulative damage law. The formulation for long-term fatigue strength of polymer composites exposed to an actual load and environment history are conducted under the four conditions of advanced ATM.

The procedure for determining the materials parameters in the formulation of the advanced ATM is illustrated in Fig. 1. First, the change in modulus or compliance of viscoelastic matrix resin is measured over time at a constant temperature. The tests are repeated for several elevated temperatures, which results in several modulus or compliance curves with the function of time. The time-temperature shift factor are then determined by shifting the viscoelastic modulus or compliance curves at the several temperatures into time scale to form a master curve of the modulus or compliance at a reference temperature. The time-temperature shift factor is thus the measure of the acceleration of the life of matrix resin by means of the elevated temperatures. The next step is to obtain the creep strength master curves. This step consists of two parts. The first part is to determine CSR strength master curve of the composites from the CSR loading tests conducted at a single strain rate and several elevated temperatures using the time-temperature shift factor for matrix resin, and the second part is to convert CSR strength master curve to the creep strength master curve of the composites. Third, the master curves of fatigue strength of the composites at zero stress ratio are determined by conducting the fatigue tests at several stress levels, a single frequency, stress ratio (zero stress ratio) and temperature using CSR strength master curve. Finally, the master curves of fatigue strength at an arbitrary stress ratio are determined by the creep strength master curve and the fatigue strength master curves at zero stress ratio. Through these procedures, all of materials parameters in the formulations can be determined for the long-term fatigue strength at an arbitrary load condition in which the stress and temperature arbitrarily changed with time.

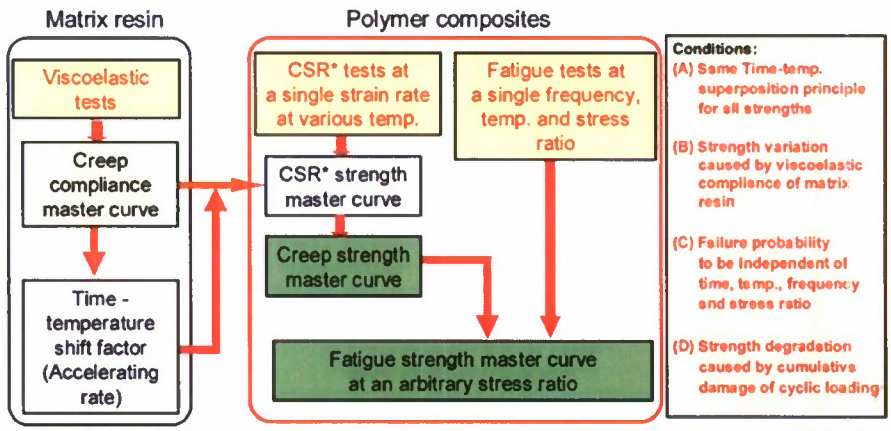

Figure 1 Procedure of advanced accelerated testing methodology (advanced ATM) for polymer composites

2. Formulation

2.1 Long-term fatigue strength of polymer composites under actual loading

The long-term fatigue strength $\sigma_f(t', N_f, R, T_o)$ under actual loading can be formulated based on the four conditions of advanced ATM.

$$\log\sigma_f\left(t', N_f, R, T_o\right) = \log\sigma_s\left(t'_o, T_o\right) + \frac{1}{\alpha}\log\left[-\ln\left(1-P_f\right)\right] - \log\left[\frac{D^*\left(t', T_o\right)}{D_c\left(t'_o, T_o\right)}\right]^{n_r} - \log\left[\frac{N_f}{N_0}\Big/\left(1-k_D\right)\right]^{\frac{(1-R)}{2}n_f} \quad (1)$$

where the first term $\sigma_s(t'_0, T_0)$ is the scale parameter of CSR strength measured at an initial reduced time t'_0 at a reference temperature T_0 which is the static strength at glassy state.

The second term shows Weibull distribution of failure probability P_f in which the shape parameter is α. The α is independent of time to failure, temperature, frequency and stress ratio from the condition (C) based on Christensen's theory.

The third term shows the variation caused by the viscoelastic compliance D^* of matrix resin defined by the following equation based on the condition (B). The n_r in this term is the parameter to be dependent on the failure mechanism.

$$D^*\left(t', T_0\right) = \frac{\varepsilon\left(t', T_0\right)}{\sigma\left(t', T_0\right)} = \frac{\int_0^{t'} D_c\left(t'-\tau', T_0\right)\frac{d\sigma(\tau')}{d\tau'}d\tau'}{\sigma\left(t', T_0\right)} \quad (2)$$

where $D_c(t', T_o)$ is the creep compliance of matrix resin. t' is the reduced time at the reference temperature T_0 which is shown by the following equation based on the condition (A).

$$t' = \int_0^t \frac{d\tau}{a_{To}(T(\tau))} \quad (3)$$

where $a_{T0}(T)$ is the time-temperature shift factor for the creep compliance of matrix resin.

The fourth term shows the degradation caused by cumulative damage of cyclic loading. In this term, N_f and R is the number of cycles to failure and the stress ratio at the final step, respectively. N_o is the reference number of cycles to failure = 1/2 and n_f is the parameter to be dependent on the failure mechanism. k_D is defined as the following equation based on the condition (D).

$$k_D = \sum_{i=1}^{n}\frac{n_i}{N_{fi}} < 1 \quad (4)$$

where n_i and N_{fi} are the number of cycles and the number of cycles to failure at the loading of step i, respectively.

2.2 Creep compliance of matrix resin

The formulation for the master curve of creep compliance of matrix resin $D_c(t', T_o)$ in

Equation (2) and the time-temperature shift factor of matrix resin $a_{To}(T)$ in Equation (3) should be performed for the long-term fatigue strength of polymer composites under actual loading. The master curve of $D_c(t',T_o)$ can be represented by two tangential lines, whose slopes are m_g and m_r, respectively. With these parameters, the master curve of $D_c(t',T_o)$ can be fit with the following equation,

$$\log D_c(t',T_o) = \log D_c\left(t'_o, T_o\right) + \log\left[\left(\frac{t'}{t'_o}\right)^{m_g} + \left(\frac{t'}{t'_g}\right)^{m_r}\right], \tag{5}$$

where t'_o is an initial reduced time at a reference temperature T_o. t'_g is the reduced glassy time at a reference temperature T_o. m_g and m_a are the parameters.

The time-temperature shift factor $a_{To}(T)$ that is the amount of the horizontal shift, can be fit with the following equation,

$$\begin{aligned}\log a_{To}(T) = {} & \frac{\Delta H_1}{2.303G}\left(\frac{1}{T} - \frac{1}{T_o}\right)\mathrm{H}(T_g - T) \\ & + \left[\frac{\Delta H_1}{2.303G}\left(\frac{1}{T_g} - \frac{1}{T_o}\right) + \frac{\Delta H_2}{2.303G}\left(\frac{1}{T} - \frac{1}{T_g}\right)\right]\left(1 - \mathrm{H}(T_g - T)\right),\end{aligned} \tag{6}$$

where G is the gas constant, 8.314×10^{-3} [kJ/(Kmol)], ΔH_1 and ΔH_2 are the activation energies below and above the glass transition temperature T_g, respectively, and H is the Heaviside step function. The temperature shift factor, $b_{To}(T)$, which is the amount of the vertical shift, can be fit with the following equation,

$$\begin{aligned}\log b_{To}(T) = {} & b_1\left(T - T_o\right)\mathrm{H}(T_g - T) \\ & + \left[b_1\left(T_g - T_o\right) + b_2\left(T - T_g\right)\right]\left(1 - \mathrm{H}(T_g - T)\right),\end{aligned} \tag{7}$$

where b_1 and b_2 are slopes of two line segments below and above T_g.

Alternatively, the viscoelastic behaviors of the matrix resin can be represented by the storage modulus E' which can easily be measured with experimental devices such as the dynamic mechanical analyzer (DMA) conducted at various frequencies and temperatures. Note that D_c can approximately be obtained from E' by using

$$D_c = 1/E'. \tag{8}$$

2.3 CSR, creep and fatigue strength of polymer composites

For the CSR strength $\sigma_s(t',T_o)$, the Equation (1) can be simplified to following equation,

$$\log \sigma_s(t',T_o) = \log \sigma_s\left(t'_o, T_o\right) + \frac{1}{\alpha_s}\log\left[-\ln\left(1 - P_f\right)\right] - \log\left[\frac{D_c\left(t'/2, T_o\right)}{D_c\left(t'_o, T_o\right)}\right]^{n_r}. \tag{9}$$

For the creep strength $\sigma_c(t',T_o)$, the Equation (1) can be simplified to following equation,

$$\log\sigma_c(t',T_o)=\log\sigma_s(t'_o,T_o)+\frac{1}{\alpha_s}\log\left[-\ln\left(1-P_f\right)\right]-\log\left[\frac{D_c(t',T_o)}{D_c(t'_o,T_o)}\right]^{n_r} \quad (10)$$

For the fatigue strength $\sigma_f(t',T_o)$ under cyclic loading which stress ratio R is zero, the Equation (1) can be simplified to following equations,

$$\log\sigma_f(t',f',T_o)=\log\sigma_s(t'_o,T_o)+\frac{1}{\alpha_f}\log\left[-\ln\left(1-P_f\right)\right]-\log\left[\frac{D^*(t',T_o)}{D_c(t'_o,T_o)}\right]^{n_r}$$
$$-\frac{1}{2}\log\left[\frac{N_f}{N_0}\right]^{n_f} \quad (11)$$

where

$$D^*(t',T_o)=\frac{1}{2}D_c(t',T_o)+\frac{1}{2}D_c\left(\frac{1}{4f'},T_o\right) \quad (12)$$

where f' is the reduced frequency at the reference temperature T_o.

3. Long-term fatigue strength of CFRP laminates for marine use

All parameters in the formulation for the long-term fatigue strength under actual loading for three kinds of CFRP laminates are determined in this section. Three kinds of CFRP laminates are plain woven T300 carbon fibers fabric/vinylester (T300/VE), plain woven T700 carbon fibers flat fabric/vinylester (T700/VE-F) and multi-axial knitted T700 carbon fibers fabric/vinylester (T700/VE-K) for marine use.

3.1 Creep compliance and time-temperature shift factors

The creep compliances of matrix resin at various temperature were measured by the three-point bending creep tests. The storage moduli at various temperatures were also measured by the dynamic mechanical analyzer (DMA) in order to get the accurate shift factors in the wide range of temperature.

The creep compliances at various temperatures shown in the left of Figure 2 were shifted horizontally and vertically to construct the smooth master curve of creep compliance shown in the right of this figure. The activation energy ΔH_1 in the horizontal time-temperature shift factor $a_{To}(T)$ shown by Equation (6) and the parameter b_1 in the vertical temperature shift factor $b_{To}(T)$ shown by Equation (7) were determined through the construction of creep compliance master curve as shown in Figure 4.

The storage moduli at various temperatures shown in the left of Figure 3 were shifted horizontally and vertically to construct the smooth master curve of storage modulus shown in the right of this figure. The activation energy ΔH_2, the parameter b_2 and the glass transition temperature T_g in Equations (6) and (7) were determined through the construction of storage modulus master curve.

The material parameters of $D_c(t'_0, T_0)$, t'_g, m_g and m_a in the creep compliance master curve shown by Equation (5) are determined after the reconstruction of creep compliance master curve by shifting horizontally and vertically the creep compliances at various temperatures as shown in Figure 2.

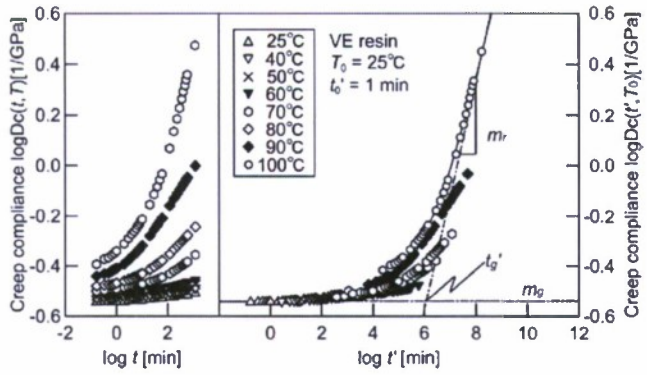

Figure 2 Master curve of creep compliance of matrix resin

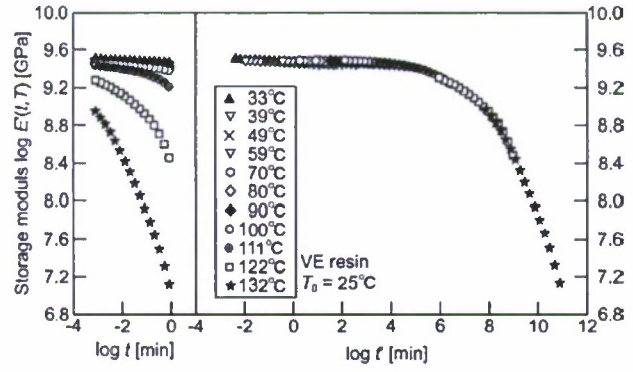

Figure 3 Master curve of storage modulus of matrix resin

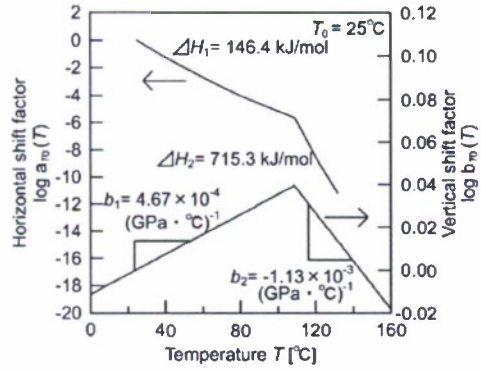

Figure 4 Master curves of horizontal shift factor and vertical shift factor of matrix resin

3.2 Flexural CSR strength of CFRP laminates

The left side of each graph in Figure 5 shows the flexural CSR strength σ_s versus time to failure t_s at various temperatures T for three kinds of CFRP laminates, where t_s is the time period from initial loading to maximum load during testing. The master curves of σ_s versus the reduced time to failure t_s' were constructed by shifting σ_s at various constant temperatures along the log scale of t_s using the same time-temperature shift factors for D_c and E' of matrix resin shown in Figure 4. It is cleared from Figure 5 that the σ_s for all three CFRP laminates strongly decreases with increasing time and temperature.

The flexural CSR strength for three kinds of CFRP laminates were formulated using Equation (9), whose parameters are listed in Table 1. Weibull plots of the CSR strength data are also shown in Figure 5. During the formulation, the parameter n_r was fixed to 0.5 for the micro-buckling failure mechanism.

The formulated curves of CSR strength of all three kinds of CFRP laminates agree well with the experimental data.

Weibull shape parameters α_s in the case that the material parameter n_r is fixed to 0.5 were compared with those in the case that the material parameter n_r as shown in Figure 6. The shape parameters from both methods are very close. Therefore, the CSR strength formulation with fixed n_r is reasonable as the standardized formulation method.

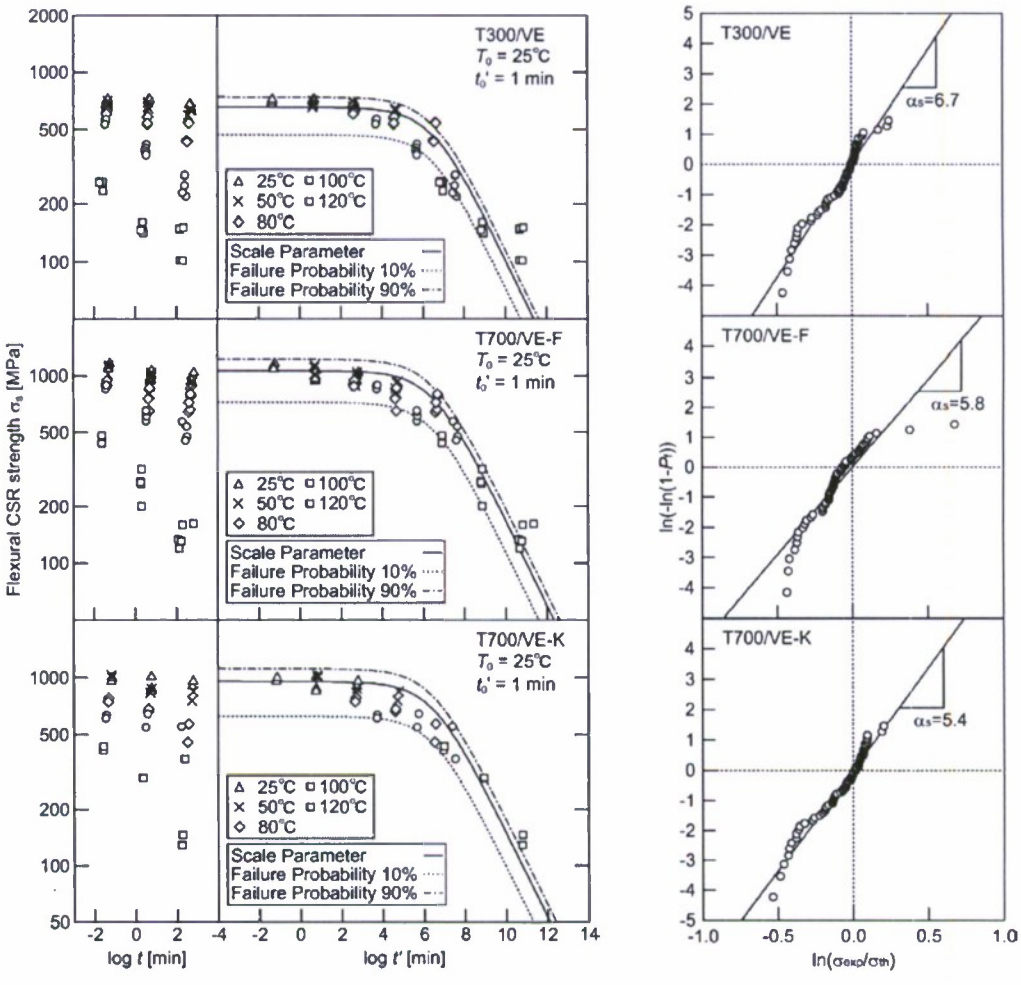

Figure 5 Master curves of flexural CSR strength and Weibull distributions

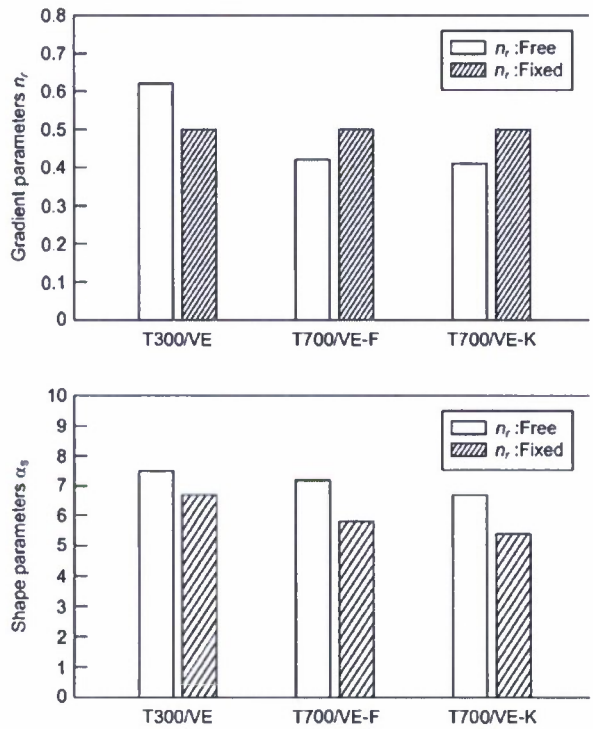

Figure 6 Comparison of shape parameters α_s with different gradient parameters n_r

3.3 Master curves of fatigue strength of CFRP laminates

To construct the master curve of flexural fatigue strength σ_f, we need the reduced frequency f' in addition to the reduced time to failure t_f' defined by the following equations

$$f' = f \cdot a_{T_0}(T) \quad , \qquad t_f' = \frac{t_f}{a_{T_0}(T)} = \frac{N_f}{f'} \tag{13}$$

where N_f is the number of cycles to failure.

S-N curves showing the relations of σ_f and N_f at frequency f=2Hz at various temperatures were measured for three kinds of CFRP laminates shown in Figure 7. These S-N curves were formulated using the Equation (11). The time-temperature shift factors $a_{T0}(T)$ of the creep compliance of matrix resin was used to convert f and N_f into f' and t_f' for each CFRP laminates. The formulation parameters for fatigue strength of three kinds of CFRP laminates are listed in Table 1. The formulated curves of fatigue strength of all three kinds of CFRP laminates agree well with the experimental data.

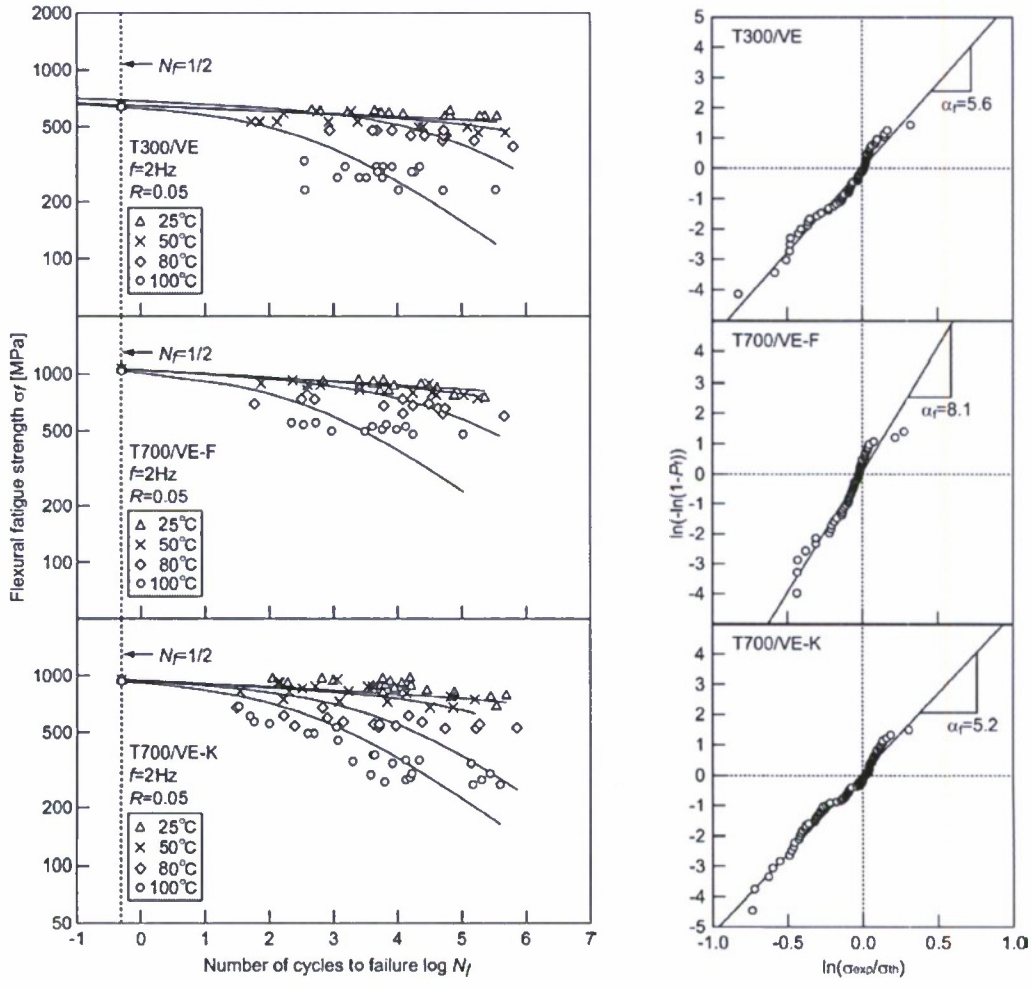

Figure 7 S-N curves at various temperatures and Weibull distributions

Using the formulation parameters, the master curves of fatigue strength versus the reduced time t' for distinct N_f can be constructed as depicted in solid line in Figure 8. It is cleared from Figures 7 and 8 that the σ_f of all three CFRP laminates strongly decreases with time to failure, temperature although the σ_f decreases scarcely with N_f.

The scale parameters σ_s of CSR strength for three kinds of CFRP laminates at an initial reduced time at a reference temperature are clearly different from each other, as shown on Table 1, because the carbon fibers and weave structure are different. The shape parameters α_s and α_f of both CSR and fatigue strengths, the formulation parameters n_r and $n_f$have approximately the same values for three kinds of CFRP laminates. The n_f is very small. From these facts that the failure mechanism is the same for these CFRP laminates and the degradation of these fatigue strengths is controlled by matrix resin. The effect of number of load cycles on the flexural strength of these CFRP laminates is negligible small.

Table 1 Formulation parameters of three kinds of CFRP laminates

	T_0 [℃]	25		
	t_0' [min]	1		
	$D_{c0}(t_0', T_0)$ [1/GPa]	0.287		
	m_g	0.0003		
Resin	m_r	0.455		
	t'_g at T_0 [min]	1.50×10^6		
	ΔH_1 [KJ/mol]	146.4		
	ΔH_2 [KJ/mol]	648.7		
	T_g [℃]	109		
		T300/VE	T700/VE-F	T700/VE-K
	$\sigma_s(t_0', T_0)$	652	1061	951
	α_s	6.7	5.8	5.4
	α_f	5.6	8.1	5.2
CFRP	n_r	0.5	0.5	0.5
	n_f	0.028	0.038	0.033

NAVY RELEVANCE

The proposed methodology has effectively combined the effects of time and temperature on the strength and life of composite materials. It can be confirmed that the methodology is applicable to the innovative CFRP laminates for marine use.

PUBLICATIONS

1. Y. Miyano, M. Nakada J. Ichimura and E. Hayakawa, "Accelerated testing for long-term strength of innovative CFRP laminates for marine use", Composites Part B, Vol.39,pp.5-12 (2008)
2. H. Cai, Y. Miyano, M. Nakada and S. K. Ha, " Long-term fatigue strength prediction of CFRP structure based on micromechanics of failure", Jour. of Composite Materials, Vol.42, pp.825-844 (2008)
3. J. Noda, M. Nakada and Y. Miyano, "Temperature dependence of accumulation of fiber breakages under tensile loading for unidirectional CFRP", Jour. of Reinforced Plastics and Composites, Vol.27, pp. 1005-1019 (2008)
4. J. Noda, M. Nakada and Y. Miyano, "Statistical formulation for time-temperature dependent flexural strength of CFRP laminates", Jour. of Reinforced Plastics and Composites, Vol.26, pp. 1881-1891 (2007)
5. J. Noda, M. Nakada and Y. Miyano, "Fatigue life prediction under variable cyclic loading based on statistical linear cumulative damage rule for CFRP laminates", Jour. of Reinforced Plastics and Composites, Vol.26, pp.665-680 (2007)
6. M. Nakada and Y. Miyano, "Accelerated testing for long-term fatigue strength of various FRP laminates for marine use", Composites Science and Technology (to be published)
7. H. Cai, Y. Miyano and M. Nakada, "long-term open-hole compression strength of CFRP laminates based on strain invariant failure theory", Jour. Thermoplastic Composite Materials (to be published)

Part 4

2008 ONR Solid Mechanics Program

EDGE OBSERVATION OF DAMAGE GROWTH BEHAVIOR OF CFRP LAMINATES

Isao Kimpara, Masayuki Nakada and Hiroshi Saito

Research Laboratory for Integrated Technological Systems,
Kanazawa Institute of Technology
3-1 Yatsukaho, Hakusan, Ishikawa 924-0838, Japan

Objectives

The aim of this study is the verification of the accelerated testing methodology to FRP laminates from the point of view of damage propagation behavior. It is essentially important to verify the mechanism of acceleration per increment of elevated temperature on deformation, strength, damage growth in CFRP laminates.

Technical approach

Verification of the accelerated testing methodology to FRP laminates is supported by the observation of failure process and the statistical estimation of fatigue strength. In this study, applicability of ATM on the crack propagation behavior was verified by the Mode I interlaminar fracture toughness test as the first step. The effect of temperature on the Mode I interlaminar fracture toughness was evaluated at the various temperatures.

Recent accomplishments

The effect of impact damage and water absorption on both the compressive strength after impact (CAI strength) and the post-impact fatigue (PIF) performance was evaluated with plain woven T300B-3k (PW) and multi-axial knitted T700S-12k (MA), respectively. The effect of water absorption on the performances of compression after impact (CAI) and PIF were small in PW CFRP laminates. Conversely, PIF properties of water-absorbed MA CFRP laminates drastically decreased than that of dry ones. CAI strength was not affected by water absorption. PIF performance of dry MA CFRP was fairly higher than that of the others. However the delamination area of PW CFRP was almost unchanged through the PIF test, the transverse cracks and delaminations were increased not in the in-plane direction but in the through-thickness direction. Delamination area of MA CFRP was almost unchanged through the PIF test however increase of the number of transverse cracks was recognized. In Wet condition, it is clear that delaminations were propagated between 0° and 90° fiber bundles. Therefore, it is thought that the large decrease in S-N curves in the PIF test was caused by the incidence of these "critical" delaminations.

Static and fatigue Mode I and Mode II interlaminar fracture toughness and the crack growth property under thermal and water environments of multiaxial knitted CFRP laminates were clarified.

Impact 3-point bending was applied to the CFRP specimen in order to induce penetrating damage in the through-width direction, and then 3-point bending loading was applied to the specimen. Damage evolution mechanism was evaluated by monitoring of damages appearing on the edge face of specimen.

1. introduction

Over the past 5 years, our KIT group has conducted the research works about the evaluation of "the accelerated testing methodology (ATM) for long-term durability and the damage tolerance performance of marine composites", as a project of the Office of Naval Research (ONR) (ONR Award Number: N000140110949). Through these works, it was cleared that the time-temperature superposition principle (TTSP), which is the most important scientific base of the accelerated testing methodology, holds for the flexural fatigue strength of CFRP laminates under water absorption condition, and that the long-term fatigue life is performed by using the master curves of the flexural fatigue strength constructed. Besides, the integrated damage evaluation methodology (IDEM) was established by the observation of damaged CFRP laminates under dry and wet condition through the compression after impact (CAI) tests and the post impact fatigue (PIF) tests. 3-D damage observation of FRP has been conducted based on both the non-destructive and direct observation methods.

For establishing more reliable ATM for the prediction of long-term creep and fatigue life for CFRP laminates for marine use under temperature and water environments, it is important to clear theoretically and experimentally that the time-temperature superposition principle (TTSP) holds for the damage growth under constant and cyclic loadings as well as the creep and fatigue lives. Therefore it is necessary that the damage evolution behavior in the accelerated testing is clarified based on the damage evaluation technique established. That is, the integration of ATM and damage evaluation approaches is very important as shown in Fig.1.

However, in the past damage evaluation technique, continuous observation is not conducted in one specimen because this is a destructive observation method. Therefore the scattering of damage evolution behavior in each specimen should be considered.

In order to solve these issues, the best way is the establishment of direct 'in-situ' damage observation. However complete NDE, such as radiography, is suitable method for these demands, complex and expensive apparatus should be necessary. On the other hand, the edge face observation is traditional but easy and simple way to follow up the damage evolutions. In addition, especially 3-point or 4-point bending tests are suitable for accelerated testing at elevated temperature and long-term fatigue testing.

The aim of this study is the verification of the applicability of ATM on the crack propagation behavior. For the first step of this objective, the effect of temperature on the Mode I interlaminar fracture toughness was evaluated at the various temperatures.

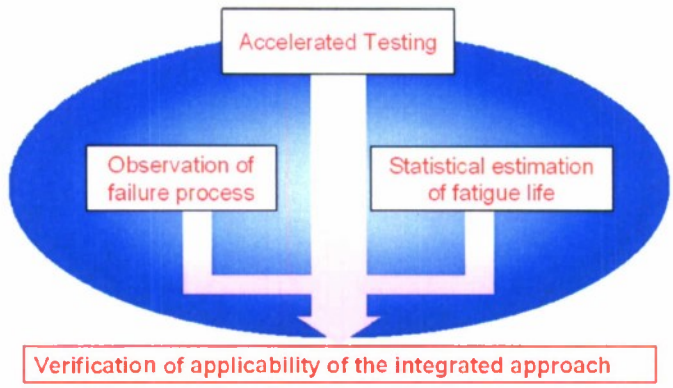

Fig.1 Verification of applicability of ATM with the integrated approach.

2. Materials and testing methods

Materials used in this study were a laminate consisted of T300-3k plain woven fabric and vinylester resin (Neopole 8250L, U-PICA Company. Ltd.). Stacking sequence was $[0/90]_{18}$ and the thickness of laminate was approximately 4mm. Molding method of CFRP

laminate was the vacuum assisted resin transfer molding (VARTM) process.

2.1. Dynamic viscoelastic test

First, the dynamic viscoelastic measurement test was conducted in order to obtain the time-temperature shift factor of the storage modulus of matrix resin. Resin specimen was prepared at the same curing condition as CFRP laminate. Geometry of specimen was 45.0mm in length, 6.4mm in width and 1.6mm in thickness. Dynamic viscoelastic measurement was conducted by RSA III (TA Instruments), and test mode was dual cantilever bending. Span of the fulcrums was 36.7mm.

2.2. Mode I interlaminar fracture toughness test

Specimen was prepared pursuant to the Japanese Industrial Standard (JIS) K7086 "Testing methods for interlaminar fracture toughness of carbon fibre reinforced plastics". Polytetrafluoroethylene film of 25μm in thickness was placed in the neutral plane of this laminate in order to insert a precrack. Dimension of the specimen of double cantilever bending (DCB) test was follows: 25mm in width, 100mm in length and 4mm in thickness (Fig.2). Because it was necessary that DCB test was conducted in the thermostatic chamber, the length of specimen was reduced than that of JIS. In addition, the thickness of specimen was increased by 1mm in order to prevent bending failure of DCB specimen in the high temperature condition.

All tests were conducted with servohydraulic testing machine (EHF-FB05-4LE 5kN, Shimadzu Corporation). The temperature dependency on the Mode I interlaminar fracture toughness was evaluated in the constant testing speed of 5.0mm/min. Temperature conditions were varied as follows: 25°C, 70°C, 80°C, 90°C, 100°C, 105°C, 110°C and 115°C.

On the other hand, the test speed dependency on the Mode I interlaminar fracture toughness was evaluated at the following conditions: 0.05mm/min, 0.5mm/min, 5.0mm/min and 50mm/min at 25°C; 0.5mm/min, 5mm/min and 50mm/min at 105°C. Test specimen caused bending failure before crack propagation under test condition of 0.05mm/min at 105°C. All testing conditions were shown in Table 1.

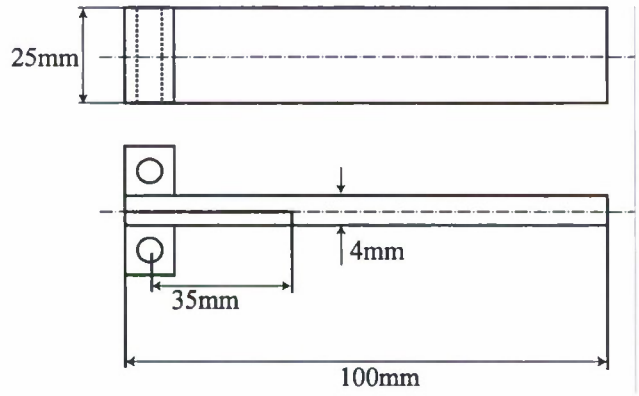

Fig.2 Geometry of the specimen for Mode I interlaminar fracture toughness test.

Table 1 Testing conditions conducted.

		Temperature [°C]							
		25	70	80	90	100	105	110	115
Speed [mm/min]	0.05	x							
	0.5	x		x	x	x	x		
	5.0	x	x	x	x	x	x	x	x
	50	x				x	x		

3. Results and discussions

3.1. Viscoelastic properties of matrix resin

Figure 3 shows the measurement results of glass transition temperature (T_g) of matrix resin through the dynamic viscoelastic measurement test. From the measurement result of tanδ, T_g of vinylester used in this study was 118.1°C.

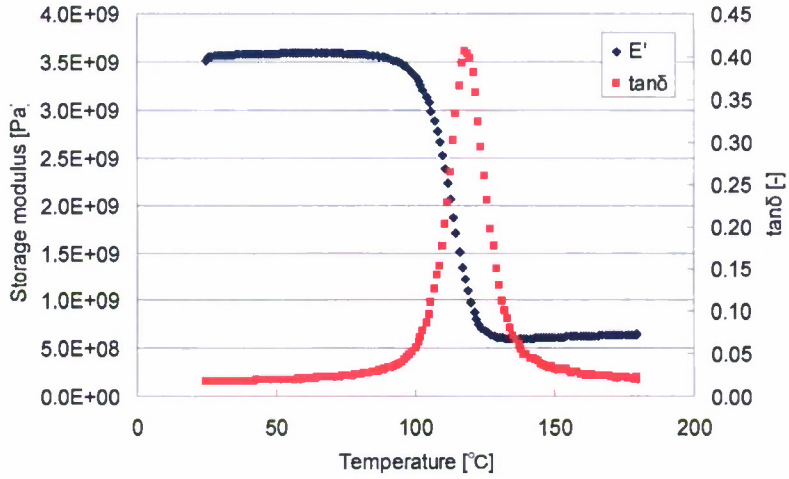

Fig.3 Results of dynamic viscoelastic measurement test.

The left side of Fig.4 shows the storage modulus E' versus testing time t at various temperatures T. The master curves of E' versus the reduced time t' were constructed by shifting E' at various constant temperatures along the log scale of t. Since the smooth master curve of E' for each specimen can be obtained as shown in the right side of each graph, the TTSP is applicable for each E'.

The horizontal time-temperature shift factor $a_{To}(T)$ and the vertical temperature shift factor $b_{To}(T)$ at a reference temperature T_0 are defined by follows:

$$\log a_{T_0}(T) = \log t - \log t' \tag{1}$$

$$\log b_{T_0}(T) = \log E'(t,T) - \log E'(t',T_0) \tag{2}$$

Both the $a_{To}(T)$ and $b_{To}(T)$ for each E' obtained experimentally in Fig.4 are plotted in Fig.5 and Fig.6. The $a_{To}(T)$ and $b_{To}(T)$ for each E' are described by two Arrhenius' equations with different activation energies ΔH:

$$\log a_{T_0}(T) = \frac{\Delta H}{2.303G}\left(\frac{1}{T} - \frac{1}{T_0}\right) \tag{3}$$

where G is the gas constant 8.314×10^{-3} [kJ/(K·mol)].

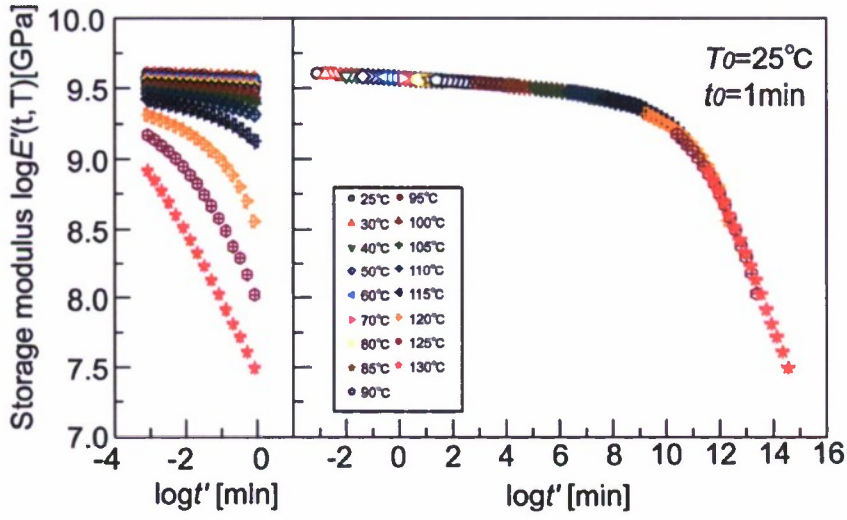

Fig.4 Master curve of storage modulus for neat vinylester resin.

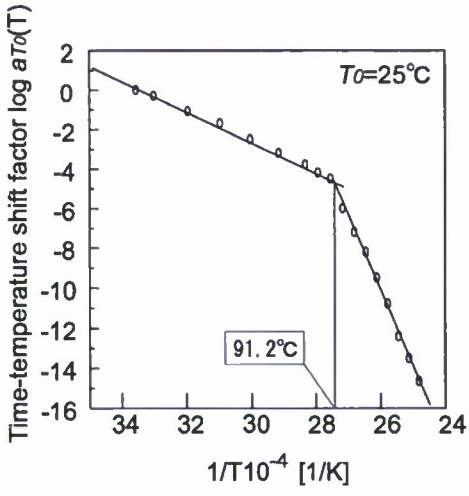

Fig.5 Time-temperature shift factors of storage modulus.

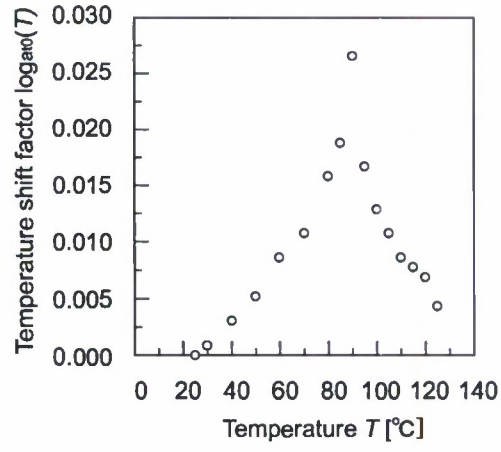

Fig.6 Temperature shift factors of storage modulus.

3.2. Temperature dependency on Mode I interlaminar fracture toughness

Figure 7 shows the energy release rate values measured at various temperatures in the test speed of 5.0mm/min. Both G_{IC} and G_{IR} increased drastically at above 115°C, which corresponds to T_g measured by the dynamic viscoelastic test.

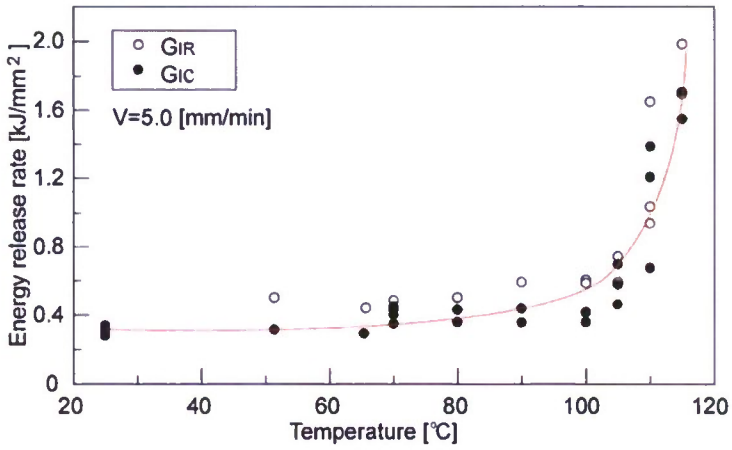

Fig.7 Effect of temperature on Mode I energy release rate.

3.3. Test speed dependency on Mode I interlaminar fracture toughness

Figure 8 shows the energy release rate values measured at 25°C and 105°C in the test speed of 0.05mm/min, 0.5mm/min, 5.0mm/min and 50mm/min. Energy release rate was not affected by the test speed at 25°C. On the other hand, energy release rate increased at 105°C, especially in the test speed of 0.5mm/min. However, scatter was increased at the higher temperature.

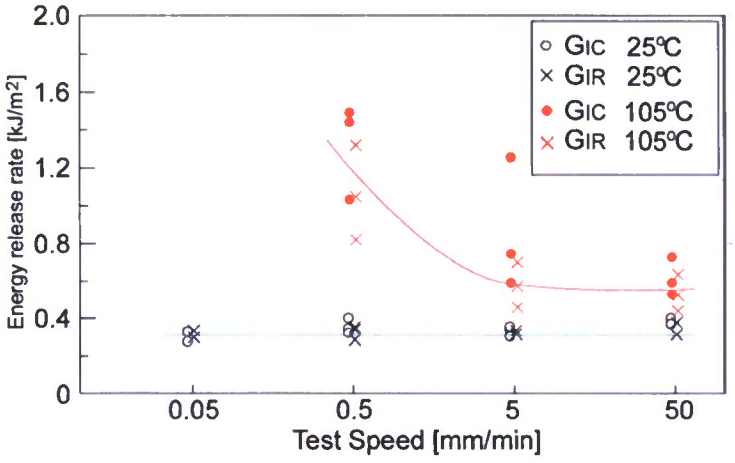

Fig.8 Effect of test speed on Mode I energy release rate.

3.4. Application of time-temperature superposition principle

Figures 9 and 10 show the Mode I energy release rate versus log scale of time to failure t at various temperatures T. The master curves of G_{IC} and G_{IR} versus the reduced time to failure t' were constructed by shifting G_{IC} and G_{IR} at various constant temperatures along the log scale of t and the log scale of G_{IC} using the same time-temperature shift factors for E' of matrix resin shown in Fig.9 and Fig.10. Since the smooth master curve of G_{IC} and G_{IR} for each specimen can be obtained as shown in the right side of each graph, the TTSP for E' of matrix resin is also applicable for the G_{IC} and G_{IR} of corresponding FRP laminates. It is cleared from Fig.9 that the G_{IC} and G_{IR} drastically increases with increasing time and temperature.

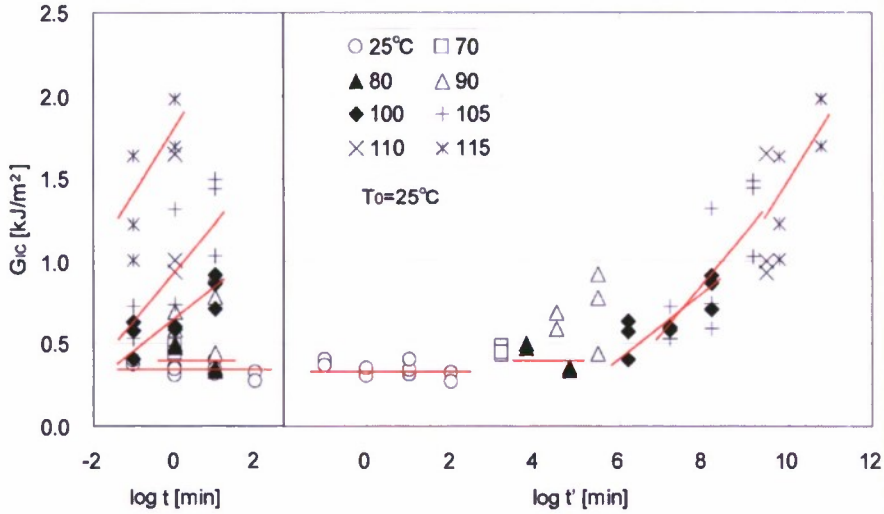

Fig.9 Effect of temperature on G_{IC}.

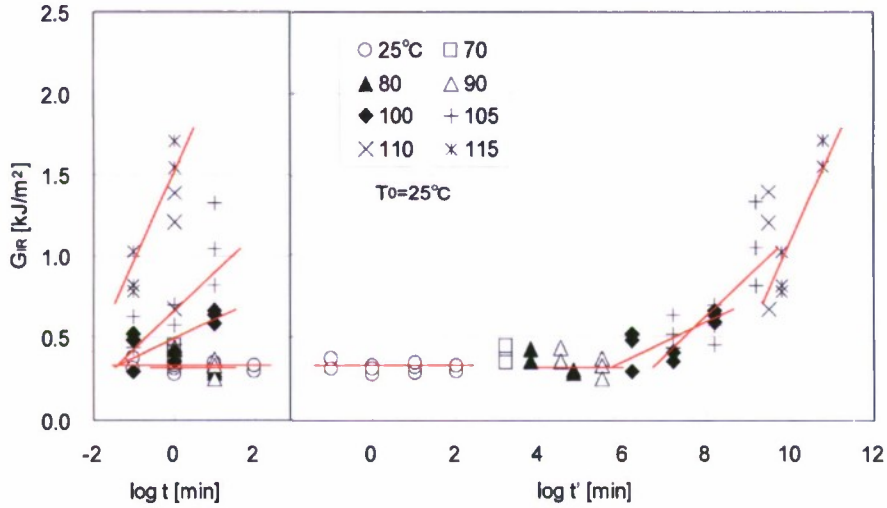

Fig.10 Effect of temperature on G_{IR}.

4. observation of crack propagation behavior

R-curves obtained at various temperatures are shown in Fig.11. Scatters of energy release rate (G_I) were drastically increased at the temperature above 90°C. From this result, it was cleared that crack propagation behavior was largely affected by temperature. Besides, however crack propagated in the resin at less than 70°C, crack path was gradually changed to the interface between reinforcement carbon fabric and matrix resin at 90°C as shown in Fig.12. Finally at 110°C, crack propagated in the interface between reinforcement and matrix. Consequently, the master curve was drawn by the shift factor of matrix resin, however, fracture morphology of Mode I test was affected gradually by increasing temperature.

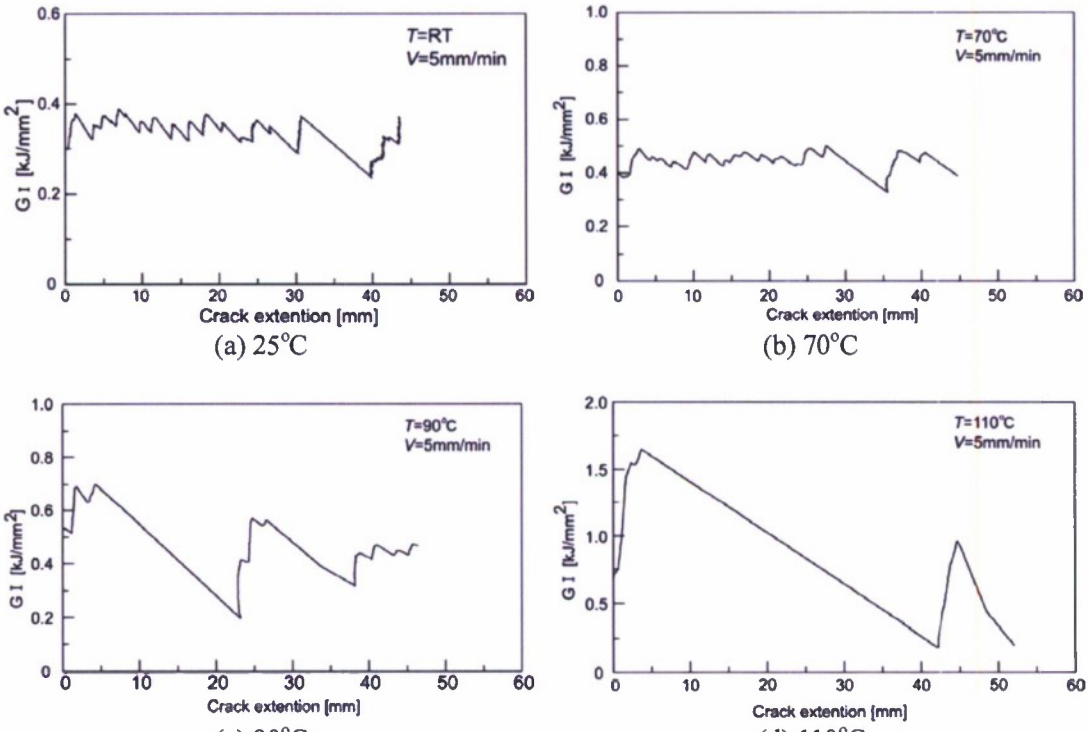

Fig.11 R-curves obtained at various temperatures.

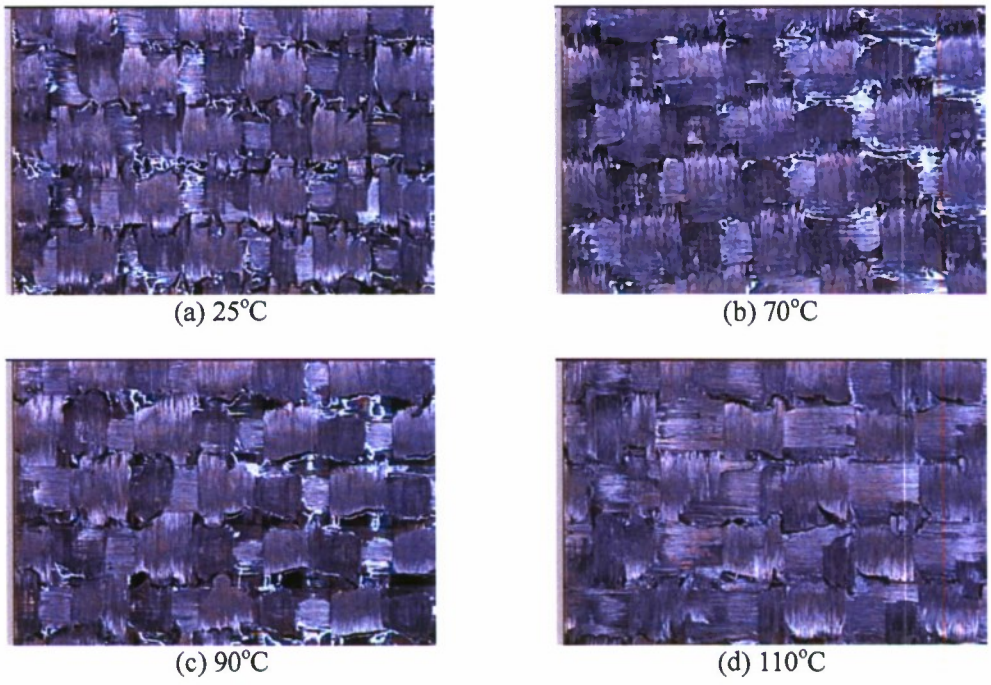

Fig.12 Fracture surfaces of the DCB specimen at various temperatures.

Conclusions

In this study, the verification of the applicability of ATM on the crack propagation behavior was evaluated. For the first step of this objective, the effect of temperature on the Mode I interlaminar fracture toughness was evaluated at the various temperatures. In the evaluation of temperature dependency on Mode I interlaminar fracture toughness, both G_{IC} and G_{IR} increased drastically at above 115°C, which corresponds to T_g measured by the dynamic viscoelastic test. In the evaluation of test speed dependency, G_I was not affected by the test speed at 25°C but increased at 105°C, especially in the test speed of 0.5mm/min. However, scatter was increased at the higher temperature.

By using the same time-temperature shift factors for E' of matrix resin, the smooth master curve of G_{IC} and G_{IR} for each specimen was obtained. Therefore the TTSP for E' of matrix resin is also applicable for the G_{IC} and G_{IR} of corresponding FRP laminates. However, fracture morphology of Mode I test was affected gradually by increasing temperature.

The relationship between temperature and fracture morphology will be studied more precisely in the future work. Especially the crack initiation and its propagation behavior will be followed up by the edge observation at the various temperatures.

References

1. Y. Miyano and M. Nakada, Marine Composites and Structures: Proc. 2006 ONR Review on Solid Mechanics Program, May 17-18, 2006, The Inn and Conference Center, University of Maryland University College, Adelphi, MD, 38-50 (2006).
2. M. Nakada, Y. Miyano, M. Kinoshita and R. Muki, Journal of Composite Materials, 36: 2567-2581 (2002).
3. R. Christensen and Y. Miyano, International Journal of Fracture, 137: 77-87 (2006).
4. I. Kimpara and H. Saito, Marine Composites and Structures: Proc. 2006 ONR Review on Solid Mechanics Program, May 17-18, 2006, The Inn and Conference Center, University of Maryland University College, Adelphi, MD, 51-58 (2006).

Part 5

2009 ONR Solid Mechanics Program

Advanced Accelerated Testing Methodology for Long-Term Life Prediction of CFRP Laminates for Marine Use

Yasushi Miyano, and Masayuki Nakada
Materials System Research Laboratory
Kanazawa Institute of Technology
3-1 Yatsukaho Hakusan Ishikawa 924-0838, Japan

OBJECTIVES

The main objectives of this research include: (a) proposing theoretically an advanced accelerated testing methodology (advanced ATM) for the long-term fatigue life prediction of polymer composites on the viewpoint of viscoelastic behavior of matrix resin; (b) applying experimentally the proposed advanced ATM for CFRP laminates for marine use.

TECHNICAL APPROACH

The advanced ATM is proposed based on the viscoelastic behavior of matrix resin. The formulation of long-term fatigue life of polymer composites is established for the advanced ATM. The advanced ATM is applied to the formulation for the long-term fatigue of CFRP laminates for marine use under the actual environmental and load conditions.

RECENT ACCOMPLISHMENTS

The advanced ATM for the long-term life prediction of polymer composites exposed to the actual loading of variable stress and temperature history was proposed based on the fact that the time and temperature dependence on the strength of polymer composites is controlled by the viscoelastic modulus of matrix resin.

The modified time-temperature superposition principle was proposed for the determination of reliable master curve for the viscoelastic modulus of matrix resin.

The applicability of advanced ATM for the long-term life prediction of CFRP laminates for marine use was confirmed under dry and wet conditions.

The applicability of advanced ATM for the long-term life prediction of CFRP laminates was confirmed under the cyclic loading in which loading and unloading are repeated as one of examples of actual loading.

1. Advanced Accelerated Testing Methodology (Advanced ATM)

1.1 Concept of advanced ATM

The advanced ATM is established with four following conditions: (A) the same time-temperature superposition principle (TTSP) is applicable for both non-destructive viscoelastic behavior and destructive strength properties of matrix resin and their composites; (B) the strength variation is caused by the viscoelastic compliance of matrix resin; (C) the failure probability is independent of time, temperature, frequency and stress ratio; (D) the strength degradation is caused by the linear cumulative damage of cyclic loading.

A key component of the advanced ATM is also the empirical observation (A), which has been demonstrated its applicability for various polymeric composite materials and their structures. Based on the condition (A), the master curves of static, creep and fatigue strengths in the wide range of time and temperature can be determined by the data measured by these tests under the short-term and elevated temperature conditions. With the condition (B), it is possible to calculate the strength variation by the viscoelastic compliance of matrix resin determined by the creep compliance of matrix resin and the history of load and temperature

changed with time. With the condition (C), the reference strength and the failure probability can be obtained by measuring static strength at an arbitrary strain rate under room temperature. With the condition (D), it is possible to calculate the strength degradation by load cycles undergoing to the linear cumulative damage law. The formulation for long-term fatigue strength of polymer composites exposed to an actual load and environment history are conducted under the four conditions of advanced ATM.

The procedure for determining the materials parameters in the formulation of the advanced ATM is illustrated in Figure 1. First, the change in modulus or compliance of viscoelastic matrix resin is measured over time at a constant temperature. The tests are repeated for several elevated temperatures, which results in several modulus or compliance curves with the function of time. The time-temperature shift factor are then determined by shifting the viscoelastic modulus or compliance curves for several temperatures into time scale to form a master curve of the modulus or compliance at a reference temperature. The time-temperature shift factor is thus the measure of the acceleration of the life of matrix resin by means of the elevated temperatures. The next step is to obtain the creep strength master curves. This step consists of two parts. The first part is to determine static strength master curve of the composites from the static loading tests conducted at a single strain rate and several elevated temperatures using the time-temperature shift factor for matrix resin, and the second part is to convert the static strength master curve to the creep strength master curve of the composites. Third, the master curves of fatigue strength of the composites at zero stress ratio are determined by conducting the fatigue tests at several stress levels, a single frequency, stress ratio (zero stress ratio) and temperature using static strength master curve. Finally, the master curves of fatigue strength at an arbitrary stress ratio are determined by the creep strength master curve and the fatigue strength master curves at zero stress ratio. Through these procedures, all of materials parameters in the formulations can be determined for the long-term fatigue strength at an arbitrary load condition in which the stress and temperature arbitrarily changed with time.

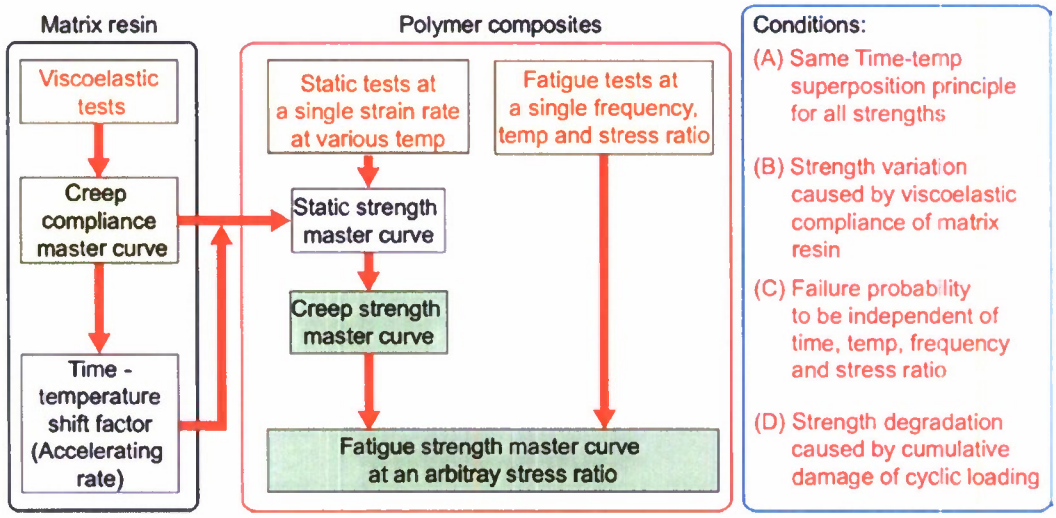

Figure 1 Procedure of advanced ATM for polymer composites

1.2 Formulation of long-term fatigue strength of polymer composites under actual loading

The long-term fatigue strength $\sigma_R(t', T_0)$ under the actual loading can be formulated based on the four conditions of advanced ATM.

$$\log\sigma_f\left(t',f',N_f,R\right)=\log\sigma_s\left(t'_o,T_o\right)+\frac{1}{\alpha}\log\left[-\ln\left(1-P_f\right)\right]-\log\left[\frac{D^*\left(t',f',R\right)}{D_c\left(t'_o\right)}\right]^{n_r}$$
$$-\log\left[\frac{N_f}{N_0}\Big/\left(1-k_D\right)\right]^{\frac{(1-R)}{2}n_f}, \tag{1}$$

where the first term $\sigma_s(t'_0, T_0)$ is the scale parameter of static strength measured at an initial reduced time t'_0 at a reference temperature T_0 which is the static strength at glassy state.

The second term shows Weibull distribution of failure probability P_f in which the shape parameter is α. The α is independent of time to failure, temperature, frequency and stress ratio from the condition (C) based on Christensen's theory.

The third term shows the variation caused by the viscoelastic compliance D^* of matrix resin defined by the following equation based on the condition (B). The n_r in this term is the parameter to be dependent on the failure mechanism.

$$D^*\left(t',T_0\right)=\frac{\varepsilon\left(t',T_0\right)}{\sigma\left(t',T_0\right)}=\frac{\int_0^{t'}D_c\left(t'-\tau',T_0\right)\frac{d\sigma\left(\tau'\right)}{d\tau'}d\tau'}{\sigma\left(t',T_0\right)}, \tag{2}$$

where D_c is the creep compliance of matrix resin. t' is the reduced time at the reference temperature T_0 which is shown by the following equation based on the condition (A).

$$t'=\int_0^t\frac{d\tau}{a_{T_o}(T(\tau))}, \tag{3}$$

where a_{T_o} is the time-temperature shift factor for the creep compliance of matrix resin.

The fourth term shows the degradation caused by cumulative damage of cyclic loading. In this term, N_f and R is the number of cycles to failure and the stress ratio at the final step, respectively. N_0 is the reference number of cycles to failure = 1/2 and n_f is the parameter to be dependent on the failure mechanism. The k_D is defined as the following equation based on the condition (D).

$$k_D=\sum_{i=1}^{n}\frac{n_i}{N_{fi}}<1, \tag{4}$$

where n_i and N_{fi} are the number of cycles and the number of cycles to failure at the loading of step i, respectively.

2. Modified time-temperature superposition principle

The formulation for the master curve of creep compliance of matrix resin D_c in Equation (1) and the time-temperature shift factor of matrix resin $a_{T_o}(T)$ in Equation (3) should be performed for the long-term fatigue strength of polymer composites under the actual loading. The master curve of D_c can be represented by two tangential lines, whose slopes are m_g and m_r, respectively. With these parameters, the master curve of D_c can be fit with the following equation,

$$\log D_c=\log D_c\left(t'_o,T_o\right)+\log\left[\left(\frac{t'}{t'_o}\right)^{m_g}+\left(\frac{t'}{t'_g}\right)^{m_r}\right], \tag{5}$$

where t'_o is an initial reduced time at a reference temperature T_o. The t'_g is the reduced glassy

time at a reference temperature T_o. The m_g and m_r are the parameters.

The modified time-temperature superposition principle was proposed for the determination of reliable master curve for the viscoelastic modulus or compliance of matrix resin. The vertical shifting as well as the horizontal shifting should be performed for getting the reliable master curve of viscoelastic modulus or compliance of matrix resin. The necessity of vertical shift was cleared theoretically and experimentally. The details of results are beyond the scope of this paper.

The horizontal time-temperature shift factor $a_{To}(T)$ that is the amount of the horizontal shift, can be fit with the following equation,

$$\log a_{T_o}(T) = \frac{\Delta H_1}{2.303G}\left(\frac{1}{T} - \frac{1}{T_o}\right)\mathrm{H}(T_g - T) + \left[\frac{\Delta H_1}{2.303G}\left(\frac{1}{T_g} - \frac{1}{T_o}\right) + \frac{\Delta H_2}{2.303G}\left(\frac{1}{T} - \frac{1}{T_g}\right)\right]\left(1 - \mathrm{H}(T_g - T)\right), \tag{6}$$

where G is the gas constant, 8.314×10^{-3} [kJ/(Kmol)], ΔH_1 and ΔH_2 are the activation energies below and above the glass transition temperature T_g, respectively, and H is the Heaviside step function. The vertical temperature shift factor, $b_{To}(T)$, which is the amount of the vertical shift, can be fit with the following equation,

$$\log b_{T_o}(T) = b_1(T - T_o)\mathrm{H}(T_g - T) + \left[b_1(T_g - T_o) + b_2(T - T_g)\right]\left(1 - \mathrm{H}(T_g - T)\right), \tag{7}$$

where b_1 and b_2 are the slopes of two line segments below and above T_g.

Alternatively, the viscoelastic behaviors of matrix resin can be represented by the storage modulus E' which can easily be measured with experimental devices such as the dynamic mechanical analyzer (DMA) conducted at various frequencies and temperatures. Note that D_c can approximately be obtained from E' by using

$$D_c(t) = 1/E'(f). \tag{8}$$

where it can be considered that the frequency f is equal to the inverse of time $1/t$.

3. Long-term life prediction of CFRP laminates under dry and wet conditions

The long-term fatigue strength for three kinds of CFRP laminates under dry and wet conditions are formulated by substituting the measured data in Equation (1). Three kinds of CFRP laminates are plain woven T300 carbon fibers fabric/vinylester (T300/VE), plain woven T700 carbon fibers flat fabric/vinylester (T700/VE-F) and multi-axial knitted T700 carbon fibers fabric/vinylester (T700/VE-K) for marine use. These CFRP laminates were prepared under two conditions of Dry and Wet after molding. Dry specimens by holding the cured specimens at 150°C for 2 hours in air, Wet specimens by soaking Dry specimens in hot water of 95°C for 120 hours were respectively prepared.

3.1 Creep compliance and time-temperature shift factors

The creep compliances at various temperatures under Dry and Wet conditions shown in the left side of Figure 2 were shifted horizontally and vertically to construct the smooth master curve of creep compliance shown in the right side of this figure. The activation energy ΔH_1 in the horizontal time-temperature shift factor $a_{To}(T)$ shown by Equation (6) and the parameter b_1 in the vertical temperature shift factor $b_{To}(T)$ shown by Equation (7) were determined through the construction of creep compliance master curve. Additionally, the storage moduli under Dry condition measured at various temperatures in the relative high temperature range were also

shifted horizontally and vertically to construct the smooth master curve of storage modulus. The activation energy ΔH_2, the parameter b_2 and T_g in Equations (6) and (7) which are the parameters in the high temperature range were determined through the construction of storage modulus master curve.

The material parameters of $D_c(t'_0, T_0)$, t'_g, m_g and m_r in the creep compliance master curve shown by Equation (5) are determined by fitting the creep compliance master curves under Dry and Wet conditions shown in Figure 2.

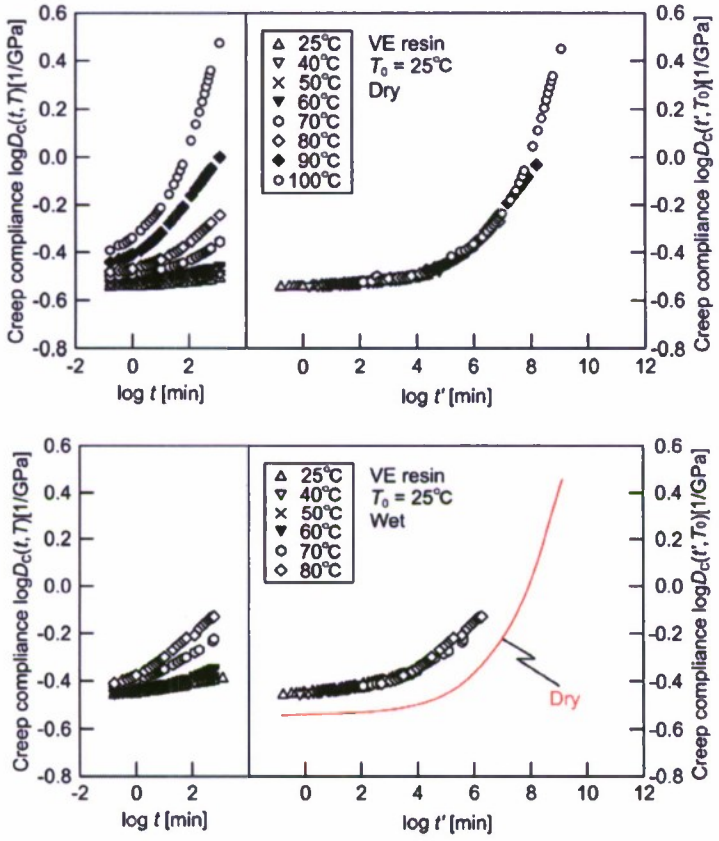

Figure 2 Master curves of creep compliance of matrix resin under Dry and Wet conditions

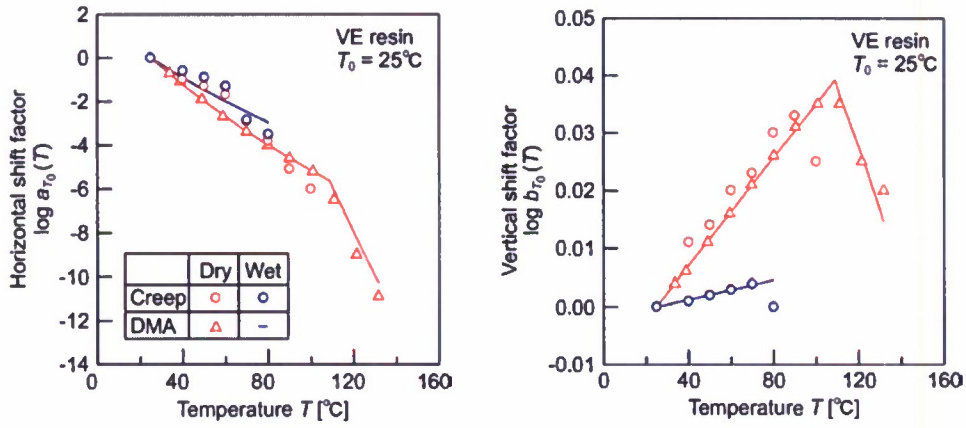

Figure 3 Horizontal and vertical shift factors under Dry and Wet conditions based on the modified time-temperature superposition principle

3.2 Flexural static strength of CFRP laminates under Dry and Wet conditions

The left side of each graph in Figure 4 shows the flexural static strength σ_s versus time to failure t_s at various temperatures T for three kinds of CFRP laminates under Dry and Wet conditions, where t_s is the time period from initial loading to maximum load during testing. The master curves of σ_s versus the reduced time to failure t_s' were constructed by shifting σ_s at various constant temperatures along the log scale of t_s using the same time-temperature shift factors for D_c and E' of matrix resin shown in Figure 3. The flexural static strength for three kinds of CFRP laminates under both of Dry and Wet conditions were formulated by using Equation (1). The formulated curves of flexural static strength of all three kinds of CFRP laminates under both conditions agree well with the experimental data. It is cleared from Figure 4 that the σ_s for all of three CFRP laminates under both of Dry and Wet conditions strongly decreases with increasing time, temperature and water absorption and that the time, temperature and water absorption dependent behavior for the flexural static strength is just the same for three kinds of CFRP laminates although the scale parameters σ_s of static strength for three kinds of CFRP laminates at an initial reduced time at a reference temperature are clearly different from each other, because the carbon fibers and weave structure are different. It is concluded that the time, temperature and water absorption dependent behavior for the flexural static strength of CFRP laminates is perfectly controlled by the viscoelastic behavior of matrix resin.

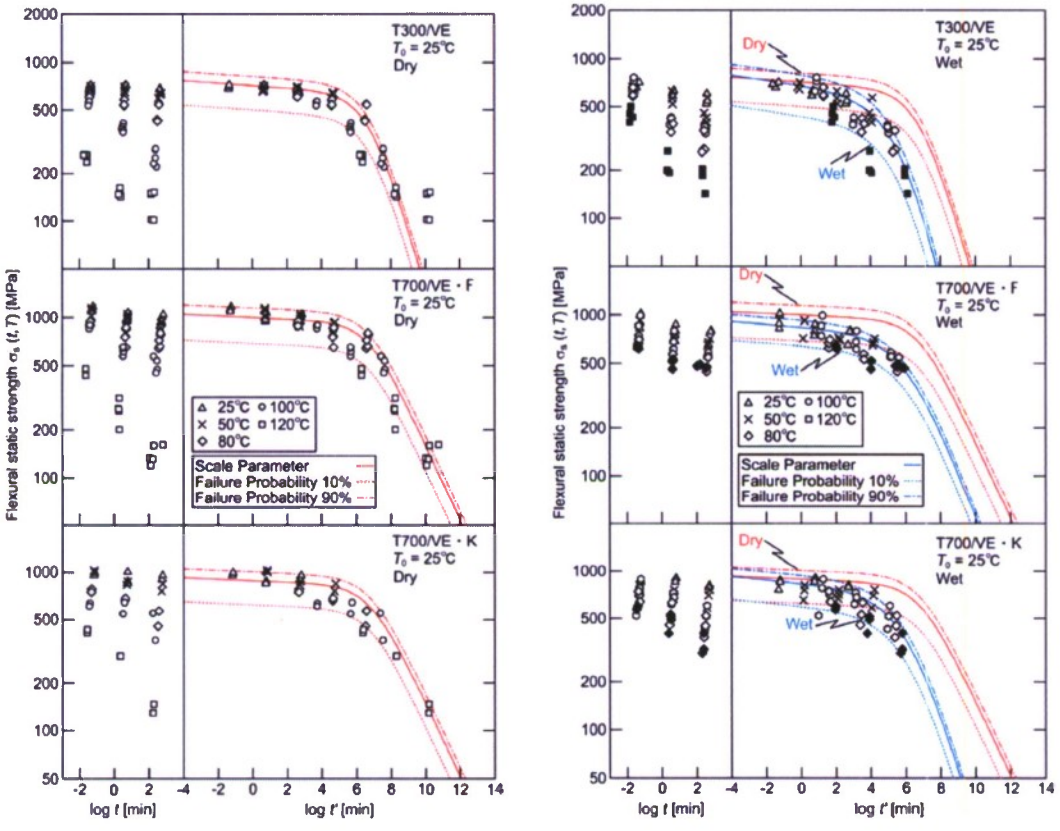

Figure 4 Master curves of flexural static strength of three kinds of CFRP laminates under Dry and Wet conditions

3.3 Flexural fatigue strength of CFRP laminates under Dry and Wet conditions

To construct the master curve of flexural fatigue strength σ_f, we need the reduced frequency f' in addition to the reduced time to failure t_f' defined by the following equations

$$f' = f \cdot a_{T_0}(T) \quad , \qquad t_f' = \frac{t_f}{a_{T_0}(T)} = \frac{N_f}{f'} \tag{9}$$

where N_f is the number of cycles to failure. The master curves of fatigue strength versus the reduced time t' for distinct N_f can be constructed as depicted in solid curves in Figure 5. It is cleared from this figure that the σ_f of all three CFRP laminates strongly decreases with time to failure, temperature although the σ_f decreases scarcely with N_f. The effect of number of load cycles on the flexural strength of these CFRP laminates is negligible small.

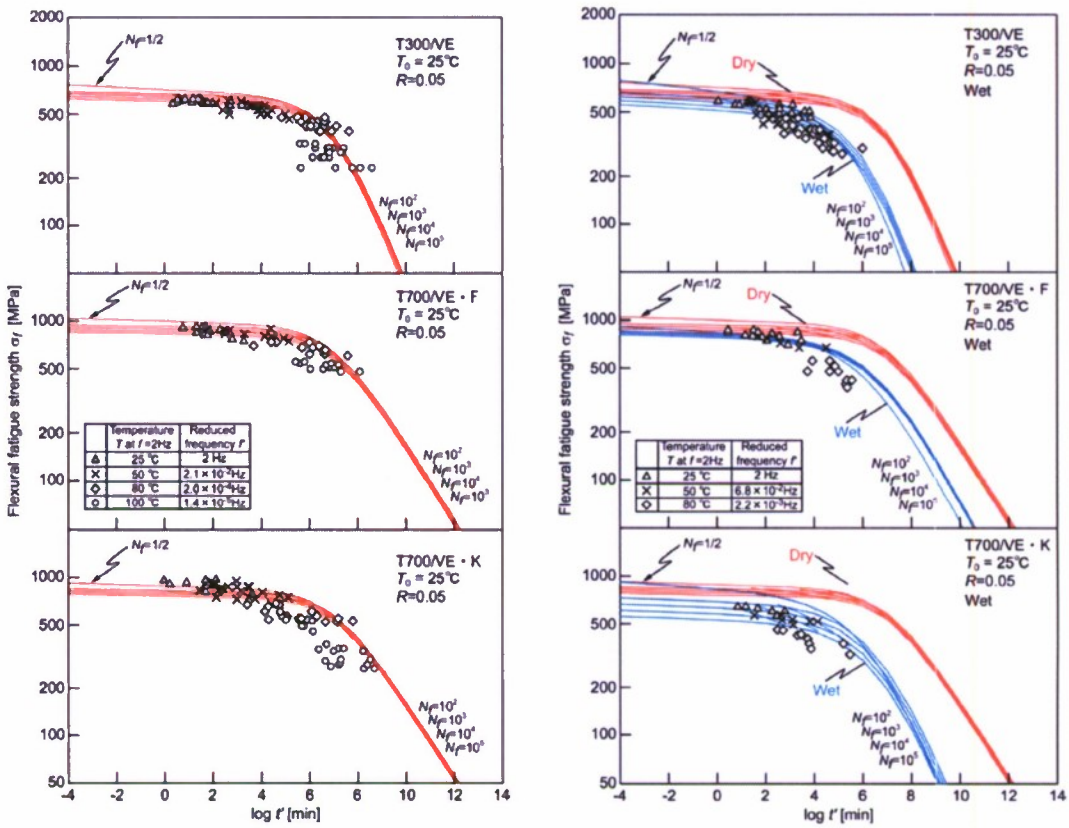

Figure 5 Master curves of flexural fatigue strength of three kinds of CFRP laminates under Dry and Wet conditions

4. Prediction of flexural cyclic fatigue and creep lives of CFRP laminates

The applicability of advanced ATM was confirmed for the long-term life prediction of CFRP laminates under the cyclic loading in which loading and unloading are repeated as one of examples of actual loading. The upper portion of Figure 6 shows the constant and cyclic load conditions in the flexural fatigue tests for CFRP laminates of T300/VE. The lower portion shows the failure probability versus number of cycles to failure under constant and cyclic fatigue loads. The i in this figure shows the cycles of loading and unloading at the cyclic fatigue load. The fatigue lives for both of constant and cyclic fatigue loadings predicted by Equation (1) are shown with the experimental data measured at the fatigue tests. It is cleared from this figure that the fatigue life increases by cyclic loading because of the creep recovery during unloading.

	Constant fatigue	Cyclic fatigue
Maximum stress [MPa]	160	160
Frequency [Hz]	2	2
Temperature [℃]	116	116
Stress ratio	0.05	0.05
Loading time [min]	—	10
Non loading time [min]	—	30
Number of specimen	20	20

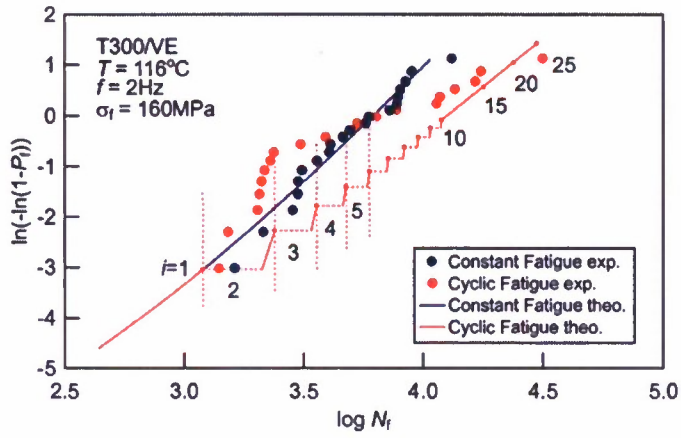

Figure 6 Test conditions and failure probability versus number of cycles to failure under constant and cyclic fatigue loads

The upper portion of Figure 7 shows the constant and cyclic load conditions in the flexural creep tests for CFRP laminates of T300/VE. The lower portion shows the failure probability versus time to failure under constant and cyclic creep loads. The i in this figure shows also the cycles of loading and unloading at the cyclic fatigue load. The creep lives for both of constant and cyclic creep loadings predicted by Equation (1) are shown with the experimental data measured at the creep tests. It is also cleared from this figure that the creep life increases by cyclic loading because of the creep recovery during unloading.

	Constant creep	Cyclic creep
Maximum stress [MPa]	240	240
Temperature [°C]	105	105
Loading time [min]	—	10
Non loading time [min]	—	30
Number of specimen	20	20

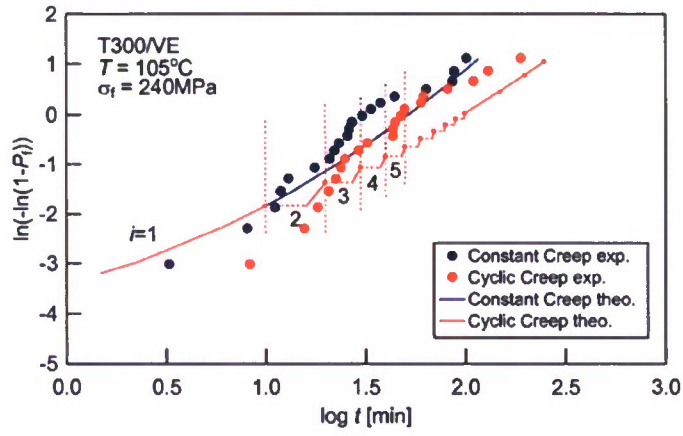

Figure 7 Failure probability versus time to failure under constant and cyclic creep loads

Navy Relevance

The proposed advanced accelerated testing methodology has effectively combined the effects of time, temperature and water absorption on the strength and life of composite materials. It was confirmed that the methodology is applicable to the innovative CFRP laminates for marine use exposed to active loading of variable stress and temperature history.

Publications

1. Miyano, Y., Nakada, M., Ichimura, J., and Hayakawa, E., "Accelerated testing for long-term strength of innovative CFRP laminates for marine use", *Composites Part B,* Vol.39, pp.5-12 (2008).
2. Cai,H., Miyano, Y., Nakada, M., and Ha, S.K., "Long-term fatigue strength prediction of CFRP structure based on micromechanics of failure", *Jour. of Composite Materials,* Vol.42, pp.825-844 (2008).
3. Noda, J., Nakada, M., and Miyano, Y., "Temperature dependence of accumulation of fiber breakages under tensile loading for unidirectional CFRP laminates", *Jour. of Reinforced Plastics and Composites,* Vol.27, pp.1005-1019 (2008).
4. Miyano, Y., Nakada, M., and Cai, H., "Formulation of long-term creep and fatigue strengths of polymer composites based on accelerated testing methodology", *Jour. of Composite Materials,* Vol.42, pp.1897-1919 (2008).
5. Miyano, Y., Nakada, Masayuki, N., and Cai, H., "Formulation of long-term creep and fatigue strengths based on ATM", *Strength & Life of Composites*, Tsai (ed.), Composites Design Group, Department of Aeronautics and Astronautics, Stanford University, ISBN: 978-0-9819-143-0-5 , pp.4.1-4.28 (2008).
6. Noda, J., Nakada, M., and Miyano, Y., "Statistical scatter of creep and fatigue failure times for CFRP laminates", *Jour. of Reinforced Plastics and Composites,* Vol.28, pp.1139-1148 (2009).
7. Cai, H., Miyano, Y., and Nakada, M., "Long-term open hole compression strength of CFRP laminates based on strain invariant failure theory", *Jour. of Thermoplastic Composite Materials,* Vol.22, pp.63-81 (2009).
8. Nakada, M. and Miyano, Y., "Accelerated testing for long-term fatigue strength of various FRP laminates for marine use", *Composites Science and Technology*, Vol.69, pp.805-813 (2009).

Part 6

2010 ONR Solid Mechanics Program

Verification of Accelerated Testing Methodology for Long-term Durability of CFRP Laminates for Marine Use

Yasushi Miyano
Materials System Research Laboratory, Kanazawa Institute of Technology
3-1 Yatsukaho Hakusan Ishikawa 924-0838, Japan
miyano@neptune.kanazawa-it.ac.jp

OBJECTIVES

The advanced accelerated testing methodology (advanced ATM) for the fatigue life prediction of CFRP laminates proposed and verified theoretically and experimentally in the previous studies is expanded to the fatigue life prediction of the structures made of CFRP laminates.

TECHNICAL APPROACH

1. The procedure of MMF/ATM method combined with our advanced ATM and the micromechanics of failure (MMF) developed by Professor Sung-Kyu Ha and others is proposed for the fatigue life prediction of the structures made of CFRP laminates.
2. The master curves of MMF/ATM critical parameters of CFRP are determined by measuring the static and fatigue strengths at elevated temperatures in the longitudinal and transverse, tension and compression directions of unidirectional CFRP.
3. The fatigue strengths of quasi-isotropic CFRP laminates with a central hole under compression load as an example of CFRP structures are measured at elevated temperatures, and these experimental data are compared with the predicted results by using the master curves of MMF/ATM critical parameters of CFRP based on MMF/ATM method.

SUMMARY OF RECENT ACCOMPLISHMENTS

1. The procedure of MMF/ATM method for the fatigue life prediction of the structures made of CFRP laminates was proposed as shown in Figures 1 and 2.
2. The master curves of MMF/ATM critical parameters of CFRP were actually determined by measuring the static and fatigue strengths at elevated temperatures in the longitudinal and transverse, tension and compression directions of unidirectional CFRP as shown in Figure 1.
3. The fatigue strengths of quasi-isotropic CFRP laminates with a central hole under compression load as an example of CFRP structures measured at elevated temperatures agreed well with the predicted results by using the master curves of MMF/ATM critical parameters of CFRP based on MMF/ATM method as shown in Figure 2. The reliability of proposed MMF/ATM method was confirmed experimentally.

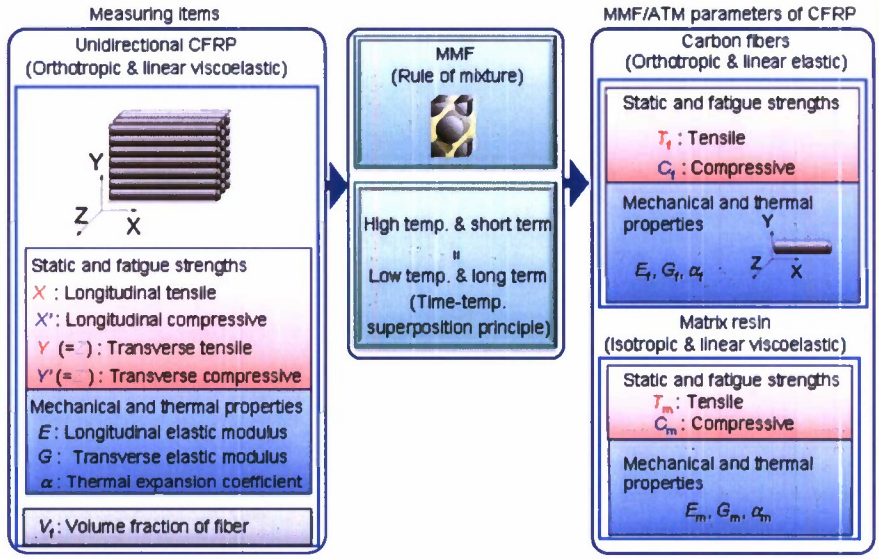

Figure 1 First step for prediction procedure by MMF/ATM method
Determination of MMF/ATM critical parameters

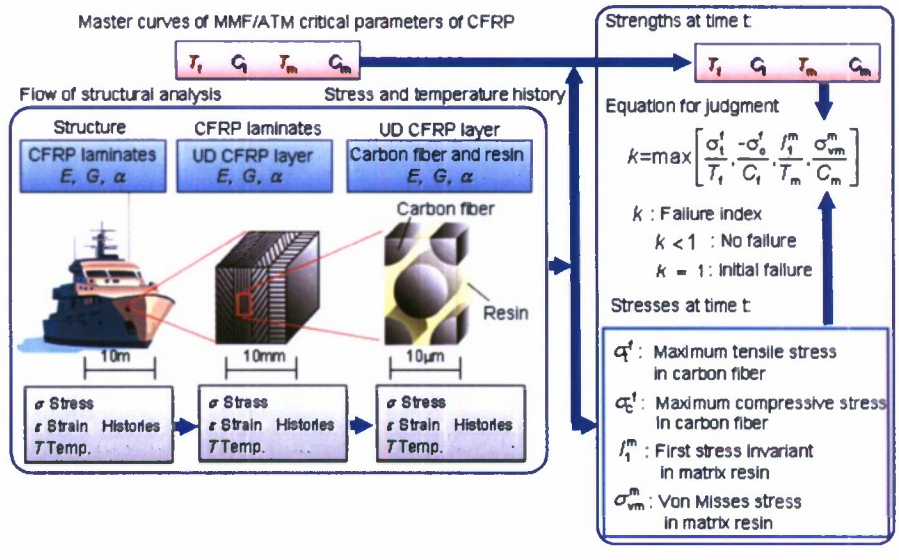

Figure 2 Second step for prediction procedure by MMF/ATM method
Life determination of CFRP structures

TECHNICAL DETAILS

1. Introduction

The accelerated testing methodology (ATM) [1] was proposed for the prediction of long-term fatigue strength of CFRP laminates based on the time-temperature superposition principle (TTSP). Based on ATM, the long-term fatigue strength for CFRP laminates and structures can be predicted by measuring the short-term fatigue strengths at elevated temperatures. The applicability of ATM was confirmed for CFRP laminates and structures combined with PAN based carbon fibers and thermosetting resins [2-4]. Furthermore, the

advanced accelerated testing methodology (advanced ATM) was proposed in which the formulation for the master curves of time-temperature dependent fatigue strength was performed based on Christensen's theory [5] which describes statistically the crack kinetics in viscoelastic body.

The failure criteria of separated fiber and matrix in polymer composites have been developed and the failure of composite structures has been predicted based on the analyses on micromechanics, laminates and structure levels. Recently, the stress-based micromechanics of failure (MMF) have been proposed by Sung-Kyu Ha and others [6] for polymer composite with viscoelastic matrix.

In this paper, the procedure of MMF/ATM method combined with our advanced ATM and MMF is proposed for the fatigue life prediction of the structures made of CFRP laminates. The validity of MMF/ATM method is confirmed through the following two steps. As the first step, the master curves of MMF/ATM critical parameters of CFRP are determined by measuring the static and fatigue strengths at elevated temperatures in the longitudinal and transverse, tension and compression directions of unidirectional CFRP. As the second step, the fatigue strengths of quasi-isotropic CFRP laminates with a central hole under compression load as an example of CFRP structures are measured at elevated temperatures, and these experimental data are compared with the predicted results by using the master curves of MMF/ATM critical parameters of CFRP based on MMF/ATM method.

2. Procedure of MMF/ATM method

The procedure of proposed MMF/ATM method is shown schematically in Figures 1 and 2.

Figure 1 shows the first step for the prediction procedure by MMF/ATM method that is the process of determination of MMF/ATM critical parameters. First, the viscoelastic modulus in the transverse direction of unidirectional CFRP is measured at various temperatures. The master curve and the time-temperature shift factor are determined by using these test data based on the TTSP. Second, the static and fatigue strengths in the typical four directions of unidirectional CFRP are measured at various temperatures at a single loading rate and single loading frequency, respectively. The strengths in four directions are longitudinal tension X, longitudinal compression X', transverse tension Y and transverse compression Y', respectively. Third, the master curves of these strengths are determined by using the measured data and the time-temperature shift factor for viscoelastic modulus. Fourth, the master curves of four MMF/ATM critical parameters, fiber tensile strength T_f, fiber compressive strength C_f, matrix tensile strength T_m, and matrix compressive strength C_m are determined through the method described in [7].

Figure 2 shows the second step for the prediction procedure by MMF/ATM method that is the life determination of CFRP structures. With the master curves of the MMF/ATM critical parameters, long-term strength prediction of CFRP becomes possible. Three-step stress analyses are necessary to process the test result, including stress analysis for "homogenous" CFRP structures and CFRP laminates in macro level and stress analysis for the constituents in micro level by stress amplification. From the master curves of MMF/ATM critical parameters and failure criteria for fiber and matrix, the strength of CFRP structure under arbitrary time to failure and temperature can be determined.

3. Experimental procedure

The test specimens were fabricated from unidirectional CFRP and quasi-isotropic CFRP laminate (QIL) $[45/0/-45/90]_{2s}$ of MR60H/1053 which consists MR60H carbon fiber and epoxy resin 1053. The unidirectional CFRP were used to back-calculate the constituent properties. The QIL was used for strength prediction verification. All the laminates were made by the autoclave technique. The curing procedure includes 180°C for 2 hours and then

postcured at 160°C for 70 hours. The volume fraction of fiber is approximately 0.55. The laminates were cut by diamond-grit wheel to the specific size for the tests. The dynamic viscoelastic tests were performed for various frequencies and temperatures for the transverse direction of unidirectional CFRP. The shift factors for constructing master curve hold for strength master curve of CFRP and constituent critical parameters' master curves. The static and fatigue tests for four directions of unidirectional CFRP were carried out to extract constituent critical parameters' master curves by micromechanical amplification. Longitudinal tension tests under static and fatigue loadings were carried out at various temperatures according with ISO 527 to get the longitudinal tensile static and fatigue strengths. Longitudinal bending tests under static and fatigue loadings were carried out at various temperatures according with ISO 14125 to get the longitudinal compressive static and fatigue strengths. Transverse bending tests under static and fatigue loadings were carried out at various temperatures according with ISO 14125 to get the transverse tensile static and fatigue strengths. 20° off-axis tension tests under static and fatigue loadings were carried out at various temperatures to get the transverse compressive static and fatigue strengths. The compression tests for QIL under static and fatigue loadings were carried out at various temperatures using the open hole compression test specimens as shown in Figure 3. The experimental results have been already reported on [8-10].

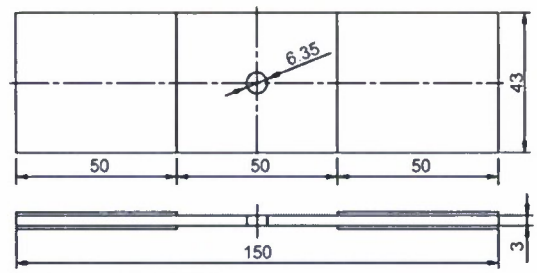

Figure 3 Open hole compression (OHC) tests for QIL

4. Determination of MMF/ATM critical parameters

4.1 Creep compliance of matrix resin

The left side of Figure 4 shows the master curve of the storage modulus E' for the transverse direction of unidirectional CFRP versus time t, where time t is the inverse of frequency. The right side shows the master curve of E' which is constructed by shifting E' at various constant temperatures along the logarithmic scale of t and logarithmic scale of E' until they overlapped each other, for the reduced time t' at the reference temperature T_0=25°C. Since E' at various constant temperatures can be superimposed so that a smooth curve is constructed, the TTSP is applicable for the storage modulus for the transverse direction of unidirectional CFRP. The time-temperature shift factor $a_{T_0}(T)$ which is the horizontal shift amount is shown by rectangular symbols in Figure 5, and the temperature shift factor, $b_{T_0}(T)$, which is the amount of vertical shift, is shown by circular symbols in this figure. The creep compliance D_c of matrix resin is back-calculated from the storage modulus E' for the transverse direction of unidirectional CFRP, and the master curve of D_c of matrix resin is shown in Figure 6.

4.2 Master curves of MMF/ATM critical parameters

Figures 7 and 8 show the master curves of static and fatigue strengths for longitudinal tension X, longitudinal compression X', transverse tension Y and transverse compression Y' for unidirectional CFRP obtained from the strength data at various temperatures by using the time-temperature shift factors a_{T_0} shown in Figure 5.

The MMF/ATM critical parameter master curves T_f, C_f, T_m and C_m are shown in Figures 9 and 10. The critical parameter of T_f was back-calculated from the tensile strength X of unidirectional CFRP. This process was repeated to construct other critical parameter master curves, the X', Y and Y' yielding the critical parameters C_f, T_m and C_m, respectively.

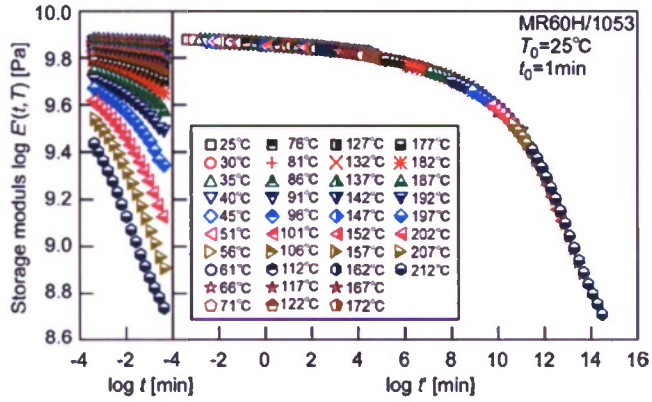

Figure 4 Master curve of storage modulus for transverse direction of unidirectional CFRP

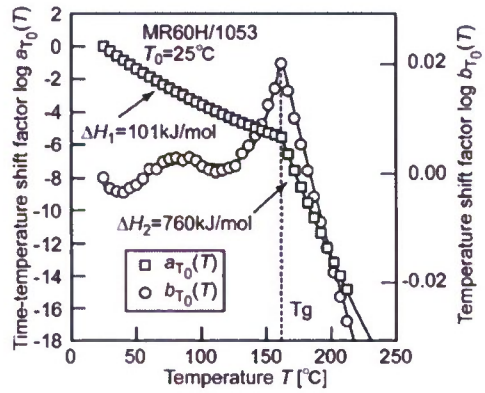

Figure 5 Shift factors of the storage modulus for the transverse direction of unidirectional CFRP

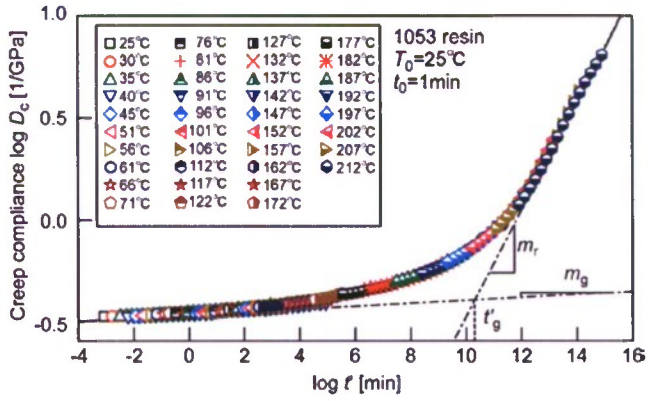

Figure 6 Master curve of creep compliance for matrix resin calculated from the storage modulus for the transverse direction of unidirectional CFRP

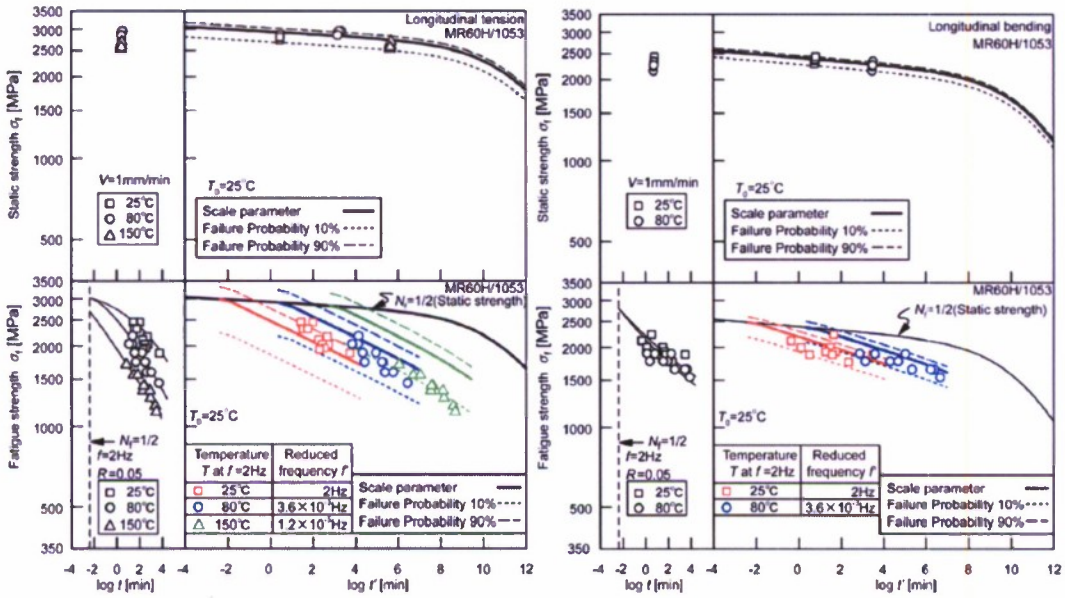

Figure 7 Master curves of tensile and bending static and fatigue strengths in the longitudinal direction of unidirectional CFRP

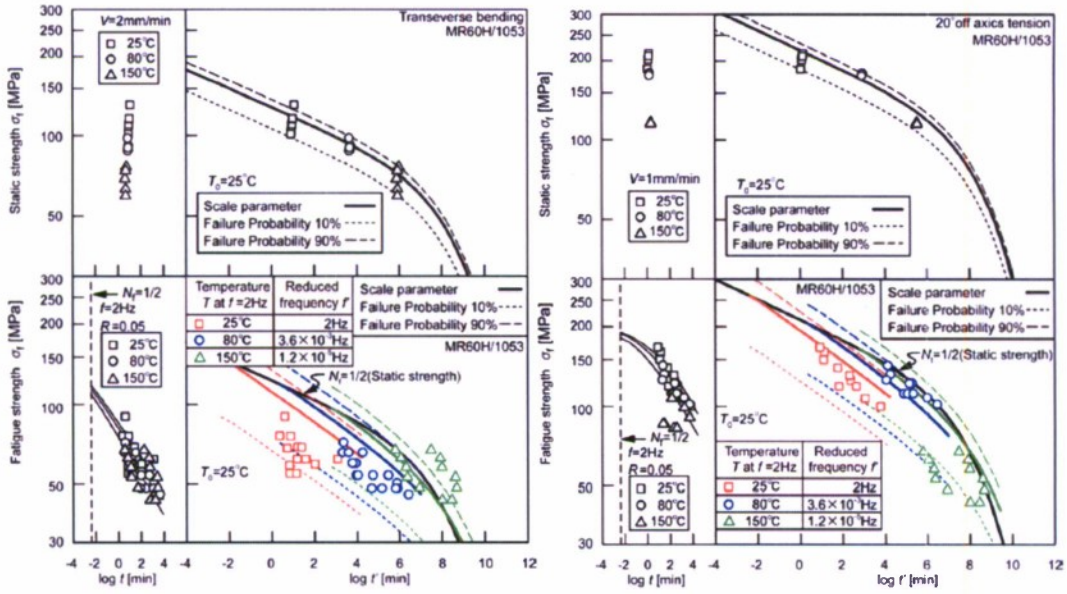

Figure 8 Master curves of bending and 20° off-axis tensile static and fatigue strengths in the transverse direction of unidirectional CFRP

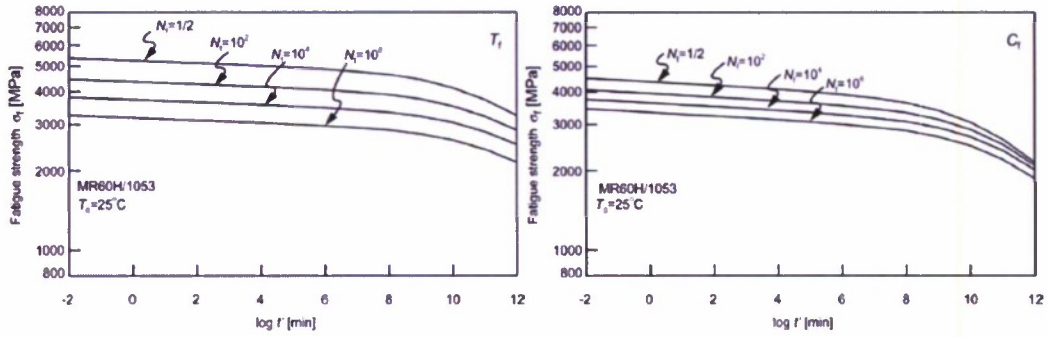

Figure 9 Master curves of MMF/ATM critical parameters T_f and C_f

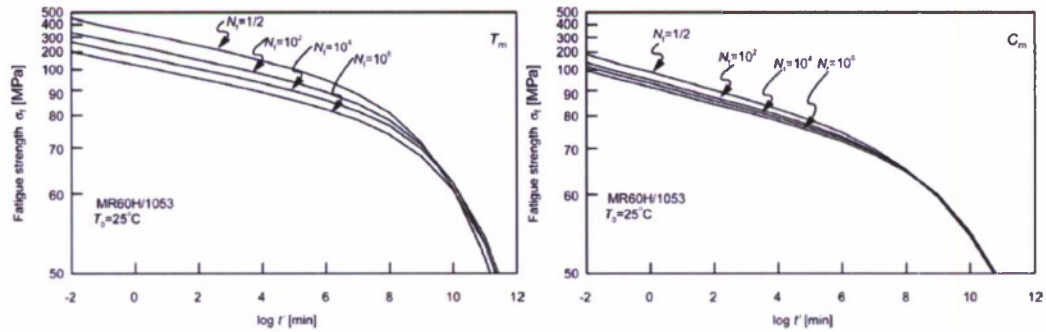

Figure 10 Master curves of MMF/ATM critical parameters T_m and C_m

5. Life determination of CFRP structures

As an example of application of MMF/ATM critical parameters master curves, long-term OHC strength for QIL was predicted. Figure 11 shows the initial failure mechanism for static loading by comparing the failure indexes of MMF/ATM parameters under, for example, T=25°C. k_{Tf} is failure index of fiber under tension, k_{Cf} is failure index of fiber under compression, and k_{Tm}* is failure index of matrix under tension, and k_{Cm}* is failure index of matrix under compression [7]. When one of these failure indexes reaches to unity, the initial failure of laminate occurs. It is cleared from this figure that the OHC failure of QIL was triggered by fiber compressive failure in 0° layer.

Figure 12 shows the initial failure of OHC for QIL under static loading observed from the specimen in which the OHC test was stopped at 98% level of maximum stress under T=25 °C. The microbuckling of fiber in 0° layer as well as the transverse crack in 45° layer are observed. In the -45° and 90° layers, any failures can not be observed. Furthermore, any failures can not be observed for the specimen in which the OHC test was stopped at 95% stress level of maximum stress under all temperatures tested.

For all temperature conditions tested, the same failure was observed with the above simulation. Therefore, the predicted master curves of OHC strength for QIL were constructed based on the MMF/ATM parameter of compressive strength of fiber. Figure 13 shows the predicted master curves of OHC strength for QIL with experimental data. The predicted strength agrees well with the experimental data for all region of time to failure t'.

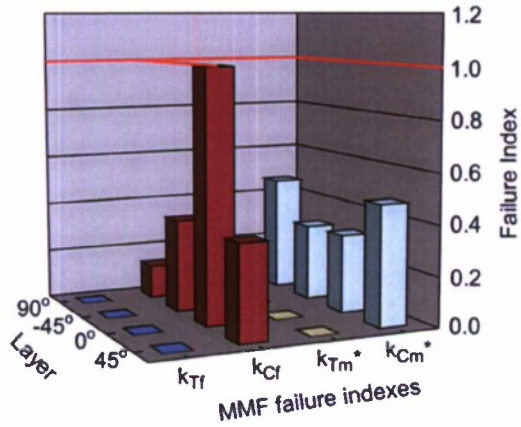

Figure 11 Judgment of initial failure of OHC for QIL under static loading (T=25°C, t'=1 min)

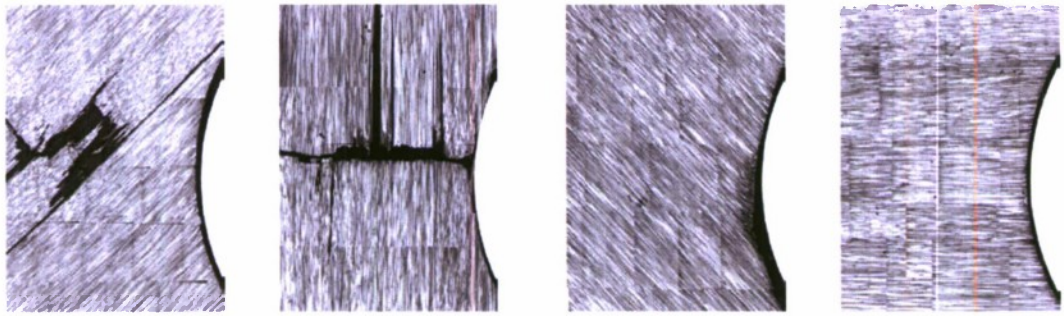

(a) 45°layer (b) 0°layer (c) -45°layer (d) 90°layer

Figure 12 Observation of initial failure of OHC for QIL under static loading (σ_{max}=0.98σ_s, T=25 °C, V=0.1mm/min)

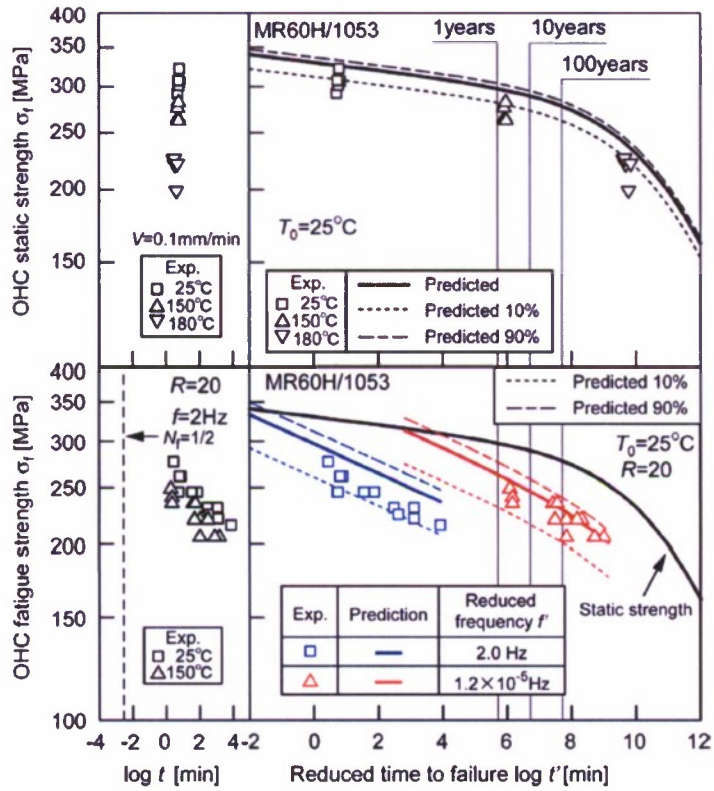

Figure 13 Predicted OHC static and fatigue strengths for QIL

6. Conclusion

The time-temperature dependent master curves of MMF/ATM critical parameters were constructed for CFRP laminates MR60H/1053 by tensile and compressive tests under static and fatigue loadings for the longitudinal and transverse directions of unidirectional CFRP under various temperatures based on the time-temperature superposition principle which holds for the viscoelastic behavior of matrix resin. It was confirmed experimentally that the long-term OHC strength of quasi-isotropic CFRP laminates $[45/0/-45/90]_{2s}$ can be predicted using these master curves of MMF/ATM critical parameters. Therefore, the verification of proposed MMF/ATM method was confirmed experimentally.

7. References

1. Miyano, Y., Nakada, M., McMurray, M. K. and Muki, R. "Prediction of Flexural Fatigue Strength of CFRP Composites under Arbitrary Frequency, Stress Ratio and Temperature", Journal of Composite Materials, 31: 619-638, 1997.
2. Miyano, Y., Nakada, M. and Muki, R. "Applicability of Fatigue Life Prediction Method to Polymer Composites", Mechanics of Time-Dependent Materials, 3: 141-157, 1999.
3. Miyano, Y., Nakada, M., Kudoh, H. and Muki, R., "Prediction of Tensile Fatigue Life under Temperature Environment for Unidirectional CFRP", Advanced Composite Materials, 8: 235-246, 1999
4. Miyano, Y., Nakada, M. and Sekine, N., "Accelerated Testing for Long-term Durability of FRP Laminates for Marine Use", Journal of Composite Materials, 39: 5-20, 2005.
5. Christensen, R. and Miyano, Y., "Stress Intensity Controlled Kinetic Crack Growth and Stress History Dependent Life Prediction with Statistical Variability", International Journal of Fracture, 137: 77-87, 2006.

6. Ha, S. K., Jin, K. K. and Huang Y., "Micro-Mechanics of Failure (MMF) for Continuous Fiber Reinforced Composites", Journal of Composite Materials, 42: 1873-1895, 2008.
7. Cai, H., Miyano, Y., Nakada, M. and Ha, S. K., "Long-trem Fatigue Strength Prediction of CFRP Structure Based on Micromechanics of Failure", Journal of Composite Materials, 42: 825-844, 2008.
8. Iwai, K., Cai, H., Nakada, M. and Miyano, Y., "Prediction of Long-term Fatigue Strength of Quasi-isotropic CFRP Laminates with A Hole Under Compressive Loading", 8th International Conference on Durability of Composite Systems (DURACOSYS 08), Porto, Portugal, July 2008
9. Miyano, Y., Nakada, M. and Cai, H., "Formulation of Long-term Creep and Fatigue Strengths of Polymer Composites Based on Accelerated testing Methodology", Journal of Composite Materials, 42: 1897-1919, 2008.
10. Hiraoka, M., Iwai, K., Cai, H., Nakada, M. and Miyano, Y., "Long-term Life Prediction of Quasi-isotropic CFRP Laminates with A Hole Under Compressive Loading", 17th International Conference of Composite Materials (ICCM-17), Edinburgh, UK, July 2009.
11. Tsai, S. W. and Hahn, H. T., Introduction to composite materials, Westport, Technomic, 1980.

NAVY RELEVANCE

The proposed MMF/ATM method is effectively combined the effects of time and temperature on the strength and life of composite structures exposed to an actual loading having general stress and temperature history. The methodology is useful to the durability analysis and design for the marine composite structures.

AKNOWLEDGEMENTS

The authors thank the Office of Naval Research for supporting this work through an ONR award with Dr. Yapa Rajapakse as the ONR Program Officer. Our award is numbered to N000140611139 and titled "Verification of Accelerated Testing Methodology for Long-Term Durability of CFRP laminates for Marine Use". The authors thank Professor Richard Christensen, Stanford University as the consultant of this project and Toray Industries, Inc. as the supplier of CFRP laminates.

PUBLICATIONS (ONR supported)

1. Journal Papers

1. Noda, J., Nakada, M., and Miyano, Y., "Statistical Scatter of Creep and Fatigue Failure Times for CFRP Laminates", Jour. of Reinforced Plastics and Composites, Vol.28, pp.1139-1148 (2009).
2. Cai, H., Miyano, Y., and Nakada, M., "Long-term Open Hole Compression Strength of CFRP Laminates Based on Strain Invariant Failure Theory", Jour. of Thermoplastic Composite Materials, Vol.22, pp.63-81 (2009).
3. Nakada, M. and Miyano, Y., "Accelerated Testing for Long-term Fatigue Strength of Various FRP Laminates for Marine Use", Composites Science and Technology, Vol.69, pp.805-813 (2009).
4. Cai, H., Miyano, Y. and Nakada, M., "Prediction of Long Term Flexural Fatigue Strength of Honeycomb Sandwich Composites", Jour. of Reinforced Plastics and Composites, Vol.29, pp.266-277 (2010).
5. Cai, H., Miyano, Y., Nakada, M. and Sihn, S., "Master Curves of Residual Creep and Fatigue Strengths for Damaged CFRP Composites", Jour. of Reinforced Plastics and Composites, Vol.29, pp.1009-1019 (2010).
6. Nakada, M., Miyano, Y., Cai, H., and Kasamori, M., "Modified Time-temperature Superposition Principle for Viscoelastic Behavior of Amorphous Resin", Mechanics of

Time-Dependent Materials, (Submitted April 2010)

7. Cai, H., Nakada, M. and Miyano, Y., "Simplified Determination Method of Long-term Viscoelastic Behavior of Amorpous Resin", Mechanics of Time-Dependent Materials, (Submitted June 2010)

2. Conference Papers

1. Miyano, Y., Nakada, M. and Hanatani, Y., "Advanced Accelerated Testing Methodology for Life Prediction of Polymer Composites", SEM Annual Conference & Exposition on Experimental and Applied Mechanics, Albuquerque, USA, 2009.6.
2. Miyano, Y., Nakada, M. and Cai, H., "Formulation Based on Advanced ATM for Long-term Fatigue Life Prediction of CFRP Laminates for Marine Use", 17th International Conference on Composite Materials, Edinburgh, UK, 2009.7.
3. Nakada, M., Hanatani, Y. and Miyano, Y., "Advanced Accelerated Testing Methodology for Long-term Life Prediction of Polymer Composites", 17th International Conference on Composite Materials, Edinburgh, UK, 2009.7.
4. Fukushima, K., Cai, H., Nakada, M. and Miyano, Y., "Determination of Time-temperature Shift Factor for Long-term Life Prediction of Polymer Composites,", 17th International Conference on Composite Materials, Edinburgh, UK, 2009.7.
5. Hiraoka, M., Iwai, K., Cai, H., Nakada, M. and Miyano, Y., "Long-term Life Prediction of Quasi-isotropic CFRP Laminates with A Hole under Compressive Loading", 17th International Conference on Composite Materials, Edinburgh, UK, 2009.7.
6. Nakada, M. and Miyano, Y., Advanced Accelerated Testing Methodology for Long-Term Life Prediction of Polymer Composites, 14th International Workshop on Advances in Experimental Mechanics, Portoroz, Slovenia, 2009.8.
7. Nakada, M. and Miyano, Y., Advanced Accelerated Testing Methodology for Long-Term Life Prediction of Polymer Composites, 7th Japan-Korea Joint Symposium on Composite Materials, pp.195-196, Nonoichi, Ishikawa, 2009.9.
8. Hiraoka, M., Cai, H., Nakada, M. and Miyano, Y., Prediction of Long-term Fatigue Strength of Quasi-isotropic CFRP Lamanates with A Hole under Compressive Load, 11th Japan International SAMPE Symposium & Exhibition, AS-1-4, Tokyo, 2009.11.
9. Fukushima, K., Cai, H., Nakada, M. and Miyano, Y., "Modified Time-temperature Superposition Principle for Viscoleastic Behavior of Amorphous Resin, 11th Japan International SAMPE Symposium & Exhibition, PMC-1-2, Tokyo, 2009.11.
10. Nakada, M., Saito, H., Kimpara, I. and Miyano, Y., "Time and Temperature Dependence on Mode I Interlaminar Fracture Behavior of CFRP Laminates", 11th Japan International SAMPE Symposium & Exhibition, PMC-3-1, Tokyo, 2009.11.
11. Miyano, Y. and Nakada, M., "Advanced Accelerated Testing Methodology for Life Prediction of CFRP Laminates", SEM Annual Conference & Exposition on Experimental & Applied Mechanics, Indianapolis, 2010.6.

AWARD

Fellow Award from Society of Advanced Materials and Process Engineering (SAMPE) (2010)

Part 7

2011 ONR Solid Mechanics Program

Verification of Accelerated Testing Methodology for Long-term Durability of CFRP Laminates for Marine Use

Yasushi Miyano and Masayuki Nakada
Materials System Research Laboratory, Kanazawa Institute of Technology
3-1 Yatsukaho Hakusan Ishikawa 924-0838, Japan
miyano@neptune.kanazawa-it.ac.jp

OBJECTIVES

The accelerated testing methodology (ATM) for the fatigue life prediction of CFRP laminates proposed and confirmed experimentally in the previous ONR project of Grant # N000140110949 is verified theoretically and refined quantitatively based on the viscoelasticity of matrix resin in this ONR project.

TECHNICAL APPROACH

1. The advanced accelerated testing methodology (ATM-2) in which the role of viscoelastic behavior of matrix resin on the long-term fatigue life of CFRP laminates is cleared statistically and quantitatively is proposed and the formulation of long-term fatigue life of CFRP laminates is constructed based on ATM-2.
2. The formulations by ATM-2 is applied to the flexural fatigue strengths of three kinds of CFRP laminates for marine use used in the previous ONR project and the parameters in the formulations is determined.
3. The flexural fatigue strengths of quasi-isotropic CFRP laminates exposed to general loading of variable stress and temperature history in which the stress and temperature are changed with time is predicted by the formulation by ATM-2 and measured experimentally. The validity of ATM-2 is confirmed by comparing of the predicted ones and the measured data.

SUMMARY OF RECENT ACCOMPLISHMENTS

1. The formulation of long-term life under an actual loading was shown by the multiplication of four terms. These terms are the static strength at room temperature and its failure probability at room temperature, the power function of normalized viscoelatic compliance of matrix resin determined by the stress and temperature history, and the strength degradation caused by the damage linearly cumulated by the maximum stress, stress ratio and number of cycles on cyclic loading.
2. The formulations by ATM-2 were applied to the flexural fatigue strengths of three kinds of CFRP laminates for marine use and the parameters in the formulations were determined. The influence of viscoelasticity of matrix resin on these fatigue strength was cleared. Furthermore, the influence of water absorption on these fatigue strength was quantitatively obtained based on the viscoelasticity of matrix resin.
3. The flexural fatigue strengths of quasi-isotropic CFRP laminates exposed to general loading of variable stress and temperature history in which the stress and temperature are changed with time was predicted by the formulation by ATM-2 and measured experimentally. The validity of ATM-2 was confirmed by comparing of the predicted ones and the measured data.
4. ATM-2 for the fatigue life prediction of CFRP laminates was expanded to MMF/ATM method for the fatigue life prediction of the structures made of CFRP laminates. The procedure of proposed MMF/ATM method is shown schematically in Figures 1 and 2. Figure 1 shows the first step for the prediction procedure by MMF/ATM method that is the process of determination of MMF/ATM critical parameters. Figure 2 shows the second step for the

prediction procedure by MMF/ATM method that is the life determination of CFRP structures.

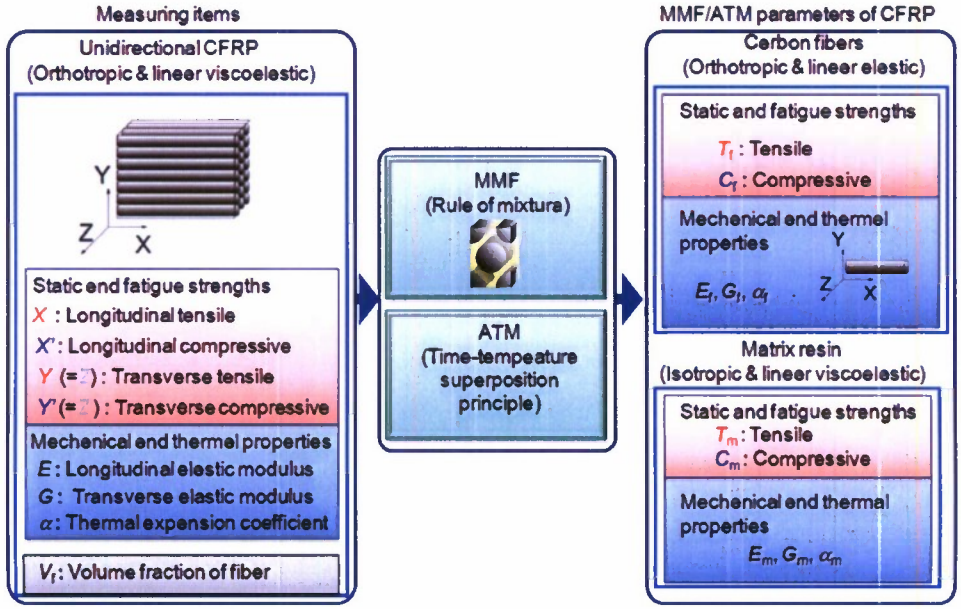

Figure 1 First step of MMF/ATM method: Determination of MMF/ATM parameters

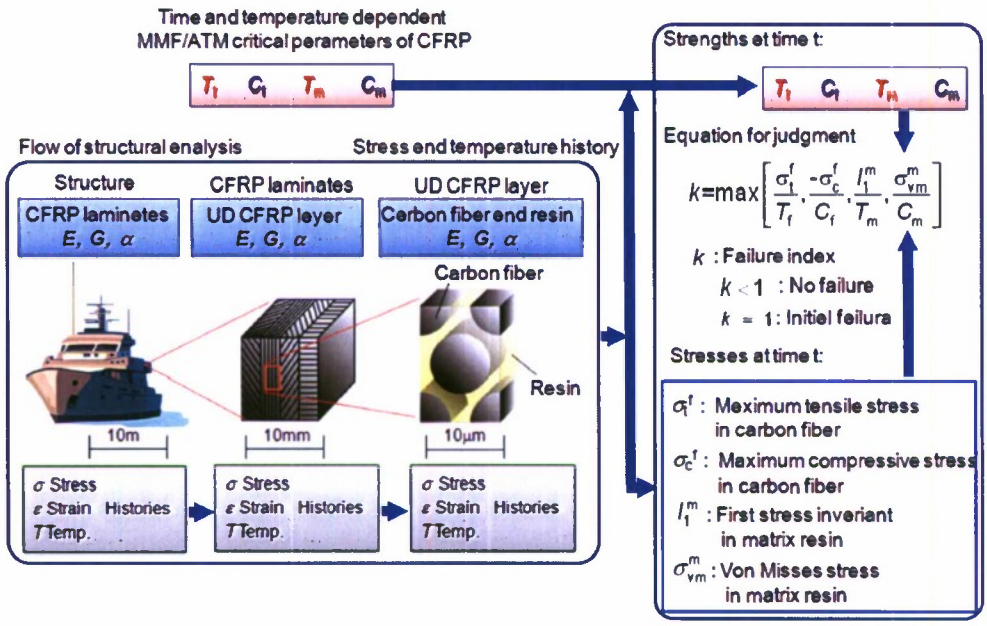

Figure 2 Second step of MMF/ATM method: Life determination of CFRP structures

TECHNICAL DETAILS

1. Introduction

The accelerated testing methodology (ATM) [1] was proposed for the prediction of long-term fatigue strength of CFRP laminates based on the time-temperature superposition

principle (TTSP). Based on ATM, the long-term fatigue strength for CFRP laminates can be predicted by measuring the short-term fatigue strengths at elevated temperatures. The applicability of ATM was confirmed for CFRP laminates and structures combined with PAN based carbon fibers and thermosetting resins [2-4].

The most important condition for the accelerated testing methodology (ATM) for the fatigue life prediction of CFRP laminates is the fact that the same time-temperature superposition principle for the viscoelastic behavior of matrix resin is hold for that for the fatigue strength as well as the static and creep strengths. The applicability of this condition was experimentally cleared for the flexural fatigue strength as well as the static and creep strengths for CFRP laminates combined with carbon fibers and vinylester resin for marine use under dry and wet conditions and the validity of ATM was confirmed for these strengths in the previous ONR project.

This ATM is verified theoretically and refined quantitatively based on the viscoelasticity of matrix resin in this ONR project. The long-term fatigue life of CFRP laminates is formulated as the function of the viscoelasticity of matrix resin including the load and temperature history under the following approachs. First, the advanced accelerated testing methodology (ATM-2) in which the role of viscoelastic behavior of matrix resin on the long-term fatigue life of CFRP laminates is cleared statistically and quantitatively is proposed and the formulation of long-term fatigue life of CFRP laminates is constructed based on ATM-2. Second, the flexural fatigue strengths of quasi-isotropic CFRP laminates exposed to general loading of variable stress and temperature history in which the stress and temperature are changed with time is predicted by the formulation by ATM-2 and measured experimentally. The validity of ATM-2 is confirmed by comparing of the predicted ones and the measured data.

As mentioned above, the first and third recent accomplishments are focused in the technical details and the second and fourth recent accomplishments are omitted from the technical details.

2. Advanced accelerated testing methodology (ATM-2) and formulation

The ATM-2 is established with three following conditions, (A) the failure probability is independent of temperature and load histories, (B) the time and temperature dependence of strength of CFRP is controlled by the viscoelasticity of matrix resin. Therefore, the time-temperature superposition principle for the viscoelasticity of matrix resin holds for the strength of CFRP, (C) the strength degradation of CFRP holds the linear cumulative damage law as the cumulative damage under cyclic loading. The fatigue strength can be formulated by the following equation under three conditions.

$$\sigma_f = \sigma_{f_0} \cdot f_A \cdot f_B \cdot f_C \quad \text{or} \quad \log \sigma_f = \log \sigma_{f_0} + \log f_A + \log f_B + \log f_C \qquad (1)$$

where σ_{fo} is the static strength at reference time and temperature and is determined by types of fiber and weave, volume fraction, load direction and others. f_A is the scatter of strength as a function of failure probability and is determined by types of fiber and weave, volume fraction, load direction and others. f_B is the time and temperature dependent strength and is determined by viscoelasticity of matrix resin. f_C is the strength degradation by the load amplitude and number of cycles to failure.

The details of f_A, f_B and f_C are explained in the following sections.

2.1 Failure probability to be independent of time, temperature and load history

The static strength can be shown by the following equation of Weibull distribution:

$$f_A = \frac{\sigma(P_f)}{\sigma_{f_0}} = [-\ln(1-P_f)]^{\frac{1}{\alpha}} \tag{2}$$

where P_f is the failure probability and α is the shape parameter. Christensen and Miyano found theoretically and experimentally that α is independent of time and temperature [5].

2.2 Time and temperature dependence of strength controlled by the viscoelasticity of matrix resin

Figure 3 shows the static strengths for typical three directions of unidirectional CFRP versus the inverse of compliance of matrix resin D^*. CFRP LT, LB and TB show longitudinal tension and bending and transverse bending for unidirectional CFRP, respectively. These strengths against the inverse of compliance of matrix resin $1/D^*$ are uniquely determined and these slopes are constant, respectively. Then, it is clear that the time and temperature dependence of these static strengths is controlled by the viscoelastic behavior of matrix resin.

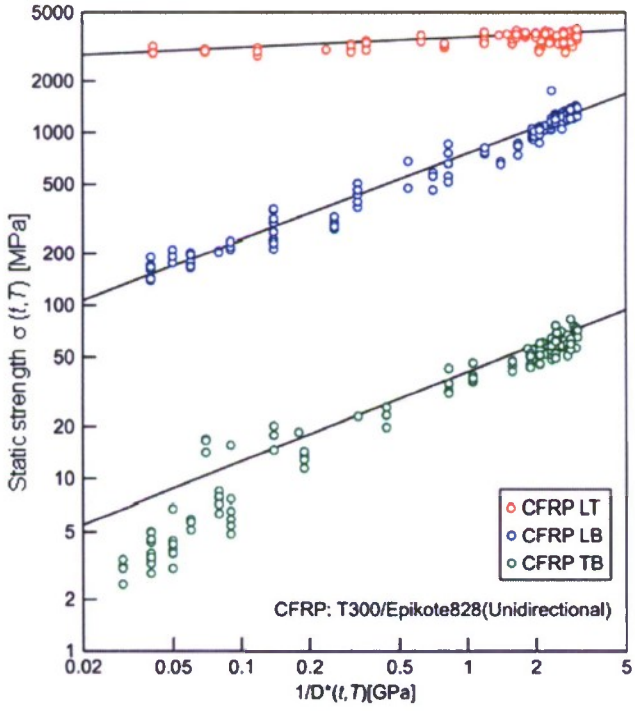

Figure 3 Static strengths for three directions of CFRP versus the inverse of compliance of matrix resin [6, 7].

Based on the facts mentioned above, the strength of CFRP σ_f varies with the viscoelastic compliance of matrix resin D^* under arbitrary load and temperature histories as expressed by

$$f_B = \frac{\sigma_f(t', T_0)}{\sigma_f(t'_0, T_0)} = \left(\frac{1/D^*(t', T_0)}{1/D_c(t'_0, T_0)}\right)^{n_r} \tag{3}$$

where,

$$D^*(t',T_0)=\frac{\varepsilon(t',T_0)}{\sigma(t',T_0)}=\frac{\int_0^{t'} D_c(t'-\tau',T_0)\dfrac{d\sigma(\tau')}{d\tau'}d\tau'}{\sigma(t',T_0)}, \qquad t'=\int_0^{t}\frac{d\tau}{a_{T_0}(T(\tau))} \tag{4}$$

where $\sigma_f(t'_0,T_0)$ shows the static strength at reduced reference time t_0' under the reference temperature T_0. $D_c(t'_0,T_0)$ is the creep compliance of matrix resin at t_0' under T_0. n_r is the parameter determined by failure mode which is independent of time and temperature. $\sigma(\tau')$ shows the stress history. a_{T_0} shows the time-temperature shift factor of matrix resin and $T(\tau)$ shows the temperature history.

2.3 Strength degradation caused by cyclic loading

Based on the condition that the slope of S-N curve depends on the stress amplitude determined by maximum stress and stress ratio and is independent of time, temperature and frequency, the strength degradation of CFRP is expressed by

$$f_C=\frac{\sigma_f(N_f)}{\sigma_f(N_0)}. \tag{5}$$

Then, f_c is formulated by the following equation:

$$\log\frac{\sigma_f(N_f)}{\sigma_f(N_0)}=-\frac{(1-R)}{2}\cdot n_f\cdot\log\left(\frac{N_f}{N_0}\right)+n_f^*\cdot\log(1-k_D), \tag{6}$$

where N_0 is equal to 1/2, $\sigma_f(N_0)$ is equal to the strength under monotonic loading. N_f and R are the number of cycles to failure and the stress ratio. n_f and n_f^* are the material parameters. k_D shows the accumulation index of damage defined by the following equation:

$$k_D=\sum_{i=1}^{n}\frac{n_i}{N_{fi}}<1, \tag{7}$$

where n_i and N_{fi} are the number of cycles and the number of cycles to failure at the loading of step i, respectively.

2.4 Formulation procedure based on ATM-2

The long-term fatigue strength under an actual loading history of stress $\sigma(\tau)$ and temperature $T(\tau)$ for CFRP can be expressed by the following equation:

$$\log\sigma_f(t',T_0,N_f,R,P_f)=\log\sigma_{f0}(t_0',T_0)+\frac{1}{\alpha}\log[-\ln(1-P_f)]-n_r\log\left[\frac{D^*(t',T_0)}{D_c(t_0',T_0)}\right]$$
$$-\frac{(1-R)}{2}n_f\log(2N_f)+n_f^*\log(1-k_D) \tag{8}$$

The determination of material parameters in formulation for ATM-2 should be done by determining the parameters of a_{T_0} and D_c of matrix resin as the first step and determining the parameters of σ_{f0}, α, n_r and n_f of CFRP as the second step shown in Figure 4. First, the viscoelastic test for matrix resin is carried out at various temperatures and the master curve of

creep compliance D_c is constructed using measured data based on the time-temperature superposition principle and the time-temperature shift factor a_{To} is determined. Second, the master curve of static strength is constructed by using the static strengths measured at various temperatures for CFRP and the time-temperature shift factor a_{To} of matrix resin. The master curve of creep strength is determined from the master curve of static strength. The fatigue strength master curve is constructed by using the fatigue strengths measured at various temperatures for CFRP and the time-temperature shift factor a_{To} of matrix resin. The parameters of σ_{f0}, α, n_r and n_f of CFRP are determined from these master curves.

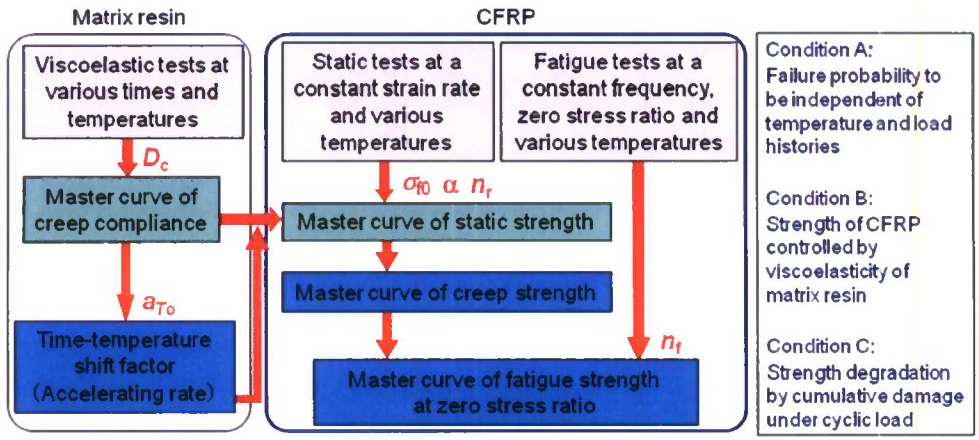

Figure 4 Determination of parameters in formulation for ATM-2

3. Flexural fatigue strength for CFRP laminates exposed to general loading

This section is concerned with the applicability of formulation of ATM-2 for predicting the fatigue life under variable cyclic loading for CFRP laminates. The flexural static and fatigue strengths were measured at a constant loading rate at various temperatures and the long-term fatigue life were formulated based on ATM-2 using the creep compliance and the time-temperature shift factor of matrix resin as the first step. The flexural fatigue life for quasi-isotropic CFRP laminates under various cyclic loadings with constant and variable temperature, frequency, maximum stress and stress ratio were predicted and compared with the experimental ones as the second step.

3.1 Preparation of specimens

The CFRP laminates employed in this study is T800S/3900-2B quasi-isotropic laminate, which consists of unidirectional T800S carbon fiber and 3900 epoxy resin with toughened interlayer by polymer particles. The stacking sequence of CFRP laminates is $[45/0/-45/90]_{2s}$. The CFRP laminates is cured at 180 °C for 2hours and then post cured at 170 °C for 10hours. The thickness of CFRP laminate was approximately 3.0mm.

3.2 Formulation of flexural fatigue strength

Table 1 shows the specimen size and the test conditions for T800S/3900-2B laminates. The first is the dynamic viscoelastic tests for obtaining the storage modulus at various frequencies and temperatures. The second is the static bending tests at a constant deflection rate at various temperatures. The third is the fatigue bending tests at a frequency and stress ratio at various temperatures.

The storage modulus for the transverse direction of unidirectional CFRP measured at various frequencies and temperatures are transferred to the creep compliance of matrix resin

based on the average approximating method [8]. The left side of Figure 5 shows the creep compliance of matrix resin of T800/3900-2B against time at various temperatures and the right side shows the master curve of creep compliance against the reduced time at a reference temperature. Figure 6 shows the time-temperature shift factor as the horizontal shift factor $a_{T0}(T)$ and the temperature shift factor as the vertical shift factor $b_{T0}(T)$ for the creep compliance of T800/3900-2B.

Table 1 Specimen size and test condition

	Material	Frequency f [Hz]	Temperature T [℃]	Test method
Viscoelastic test	 T800S/3900-2B $[90]_8$	0.01~10	25~250	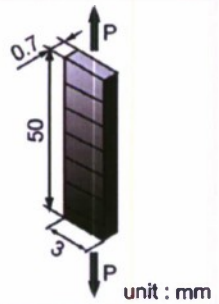 unit : mm
Static test	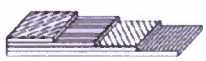 T800S/3900-2B $[45/0/-45/90]_{2S}$	—	25, 50, 80, 110, 140, 170	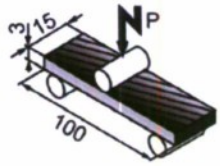 unit : mm
Fatigue test		2	25, 110	

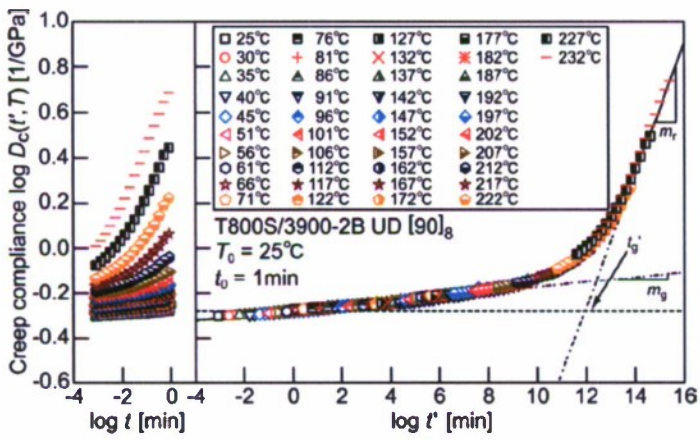

Figure 5 Master curve of creep compliance for the matrix resin of T800/3900-2B

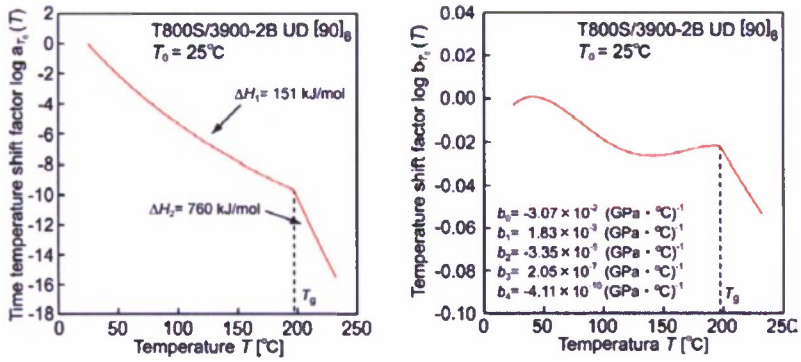

Figure 6 Time-temperature shift factor $a_{T0}(T)$ and temperature shift factor $b_{T0}(T)$

The left side of Figure 7 shows the static strength of quasi-isotropic CFRP laminates of T800/3900-2B against the time to failure at various temperatures and the right side shows the master curve of static strength against the reduced time to failure at a reference temperature obtained by shifting horizontally the static strengths with the amount of the time-temperature shift factor of the creep compliance of matrix resin of T800/3900-2B. Figure 8 shows the master curves of the fatigue strength of quasi-isotropic CFRP laminates.

The solid curves of both figures are the static and fatigue strengths predicted by the equation (8). Figure 9 shows Weibull distributions for the static strength at room temperature and for the fatigue strength at various temperatures, respectively. All of the parameters of equation (8) were determined successfully for the flexural fatigue strength of quasi-isotropic CFRP laminates by using the measured static and fatigue strengths.

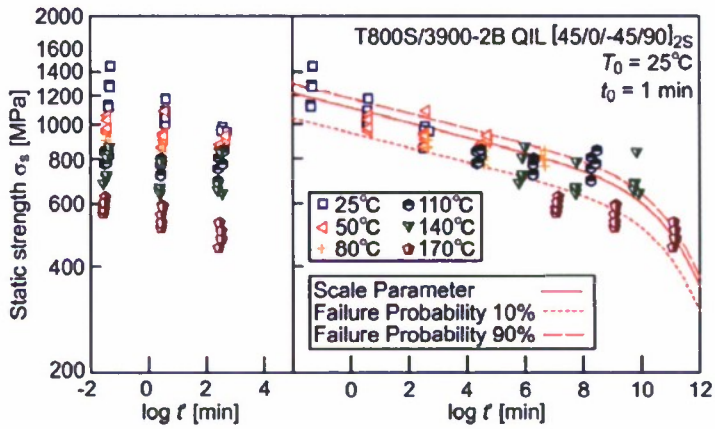

Figure 7 Master curve of static strength for quasi-isotropic CFRP laminates

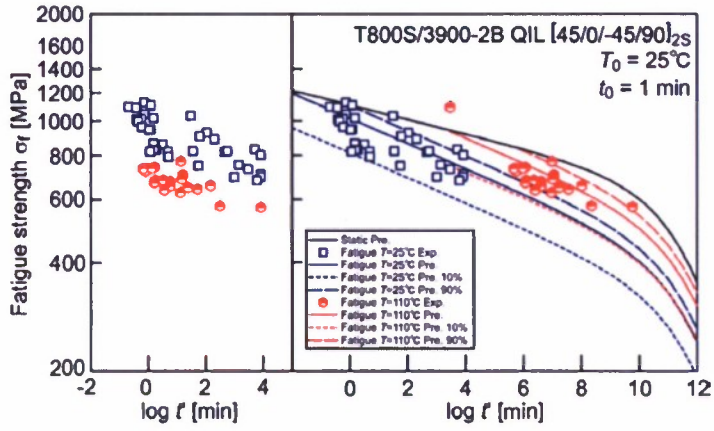

Figure 8 Master curves of fatigue strength for quasi-isotropic CFRP laminates

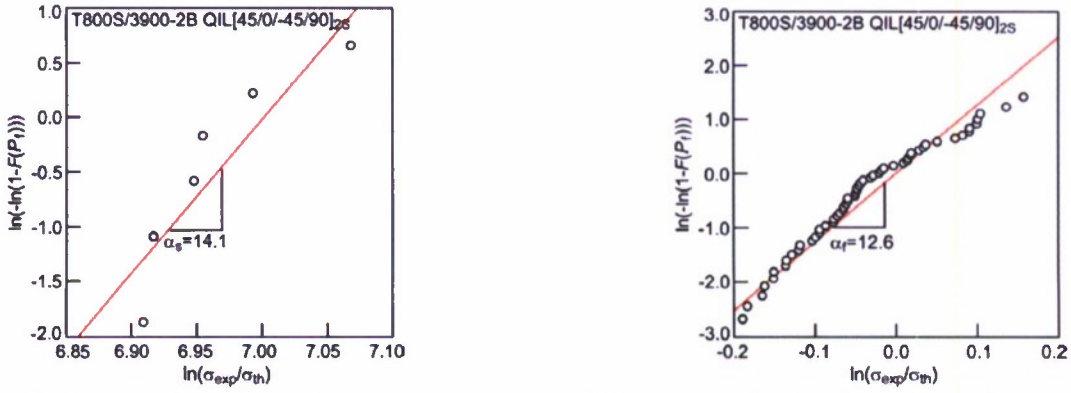

Static strengths at room temperature

Fatigue strengths at various temperatures

Figure 9 Weibull distribution of strengths

5.3 Prediction of fatigue time to failure at variable loadings

The flexural fatigue time to failure of quasi-isotropic CFRP laminates at variable loadings are predicted by using the formulation with parameters determined at the previous section. The conditions of constant and variable loadings as shown on Table 2 are constant low, constant high, variable low-high and variable high-low conditions of temperature, frequency, maximum stress and stress ratio.

Weibull distribution curves of the fatigue time to failure under constant and variable temperature, frequency, maximum stress and stress ratio for quasi-isotropic CFRP laminates predicted are shown with the data measured experimentally at the same conditions in Figure 10. The solid predicted curves and the solid experimental points show the time to failure under constant loadings, and the dotted curves and the hollow points show the time to failure after changing the load. The blue curves and points show low and low-high conditions, and the red curves and points show high and high-low conditions.

As results, the predicted flexural fatigue time to failure under variable loadings as well as constant loadings agree well with the experimental ones. The fatigue time to failure remarkably depend on temperature, frequency, maximum stress and stress ratio. The time to failure under low-high condition of temperature decreases comparing with that under low condition of temperature, and the time to failure under high-low condition of temperature

increases comparing with that under high condition of temperature. The same tendency is observed in the other conditions.

Table 2 Constant and variable fatigue test conditions

Variable parameter		Temperature T [℃]	Frequency f [Hz]	Stress σ [MPa]	Stress ratio R [-]
Temperature	Low	25	2	780	0.05
	High	45			
	Low→High	25→45	2	780	0.05
	High→Low	45→25			
Frequency	Low	25	0.02	880	0.05
	High		2		
	Low→High	25	0.02→ 2	880	0.05
	High→Low		2 →0.02		
Stress	Low	25	2	780	0.05
	High			880	
	Low→High	25	2	780→880	0.05
	High→Low			880→780	
Stress ratio	Low	25	2	880	0.05
	High				1
	Low→High	25	2	880	0.05→ 1
	High→Low				1 →0.05

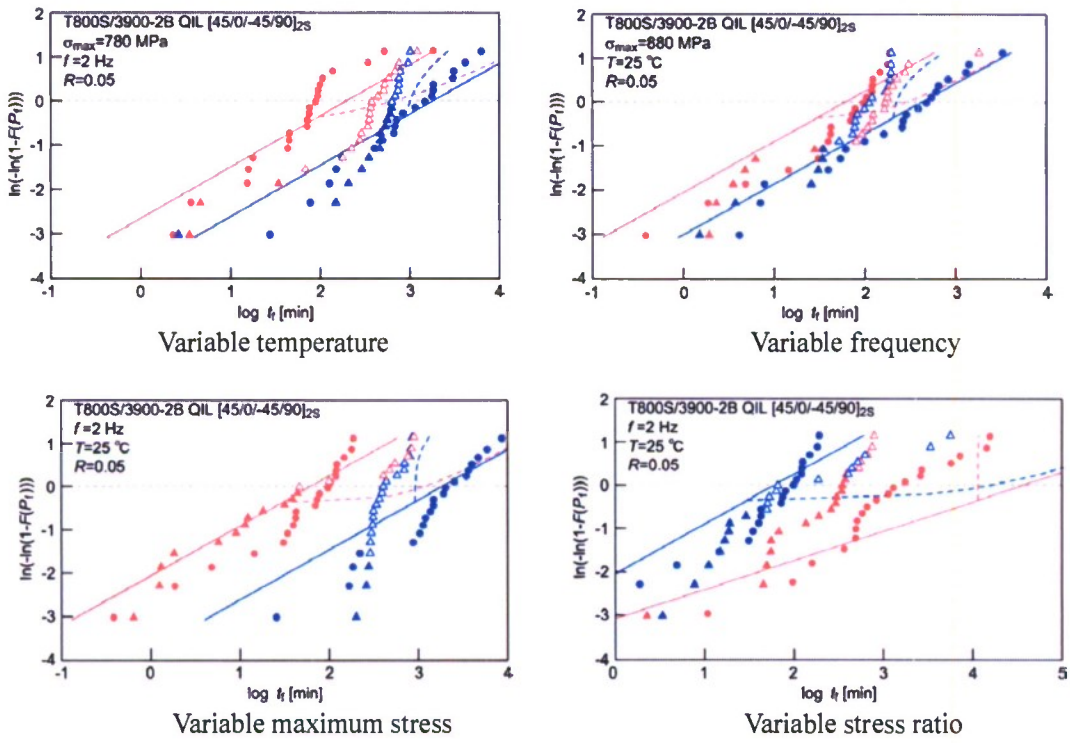

Variable temperature　　Variable frequency

Variable maximum stress　　Variable stress ratio

Figure 10 Weibull distribution of the fatigue time to failure under variable temperature, frequency, maximum stress and stress ratio for quasi-isotropic CFRP laminates

6. Conclusion

The accelerated testing methodology for the fatigue life prediction of CFRP laminates confirmed experimentally in the previous ONR project is verified theoretically and refined quantitatively based on the viscoelasticity of matrix resin in this ONR project.

1.. The advanced accelerated testing methodology (ATM-2) in which the role of viscoelastic behavior of matrix resin on the long-term fatigue life of CFRP laminates is cleared statistically and quantitatively was proposed and the formulation of long-term fatigue life of CFRP laminates was constructed based on ATM-2.

2. The flexural fatigue strengths of quasi-isotropic CFRP laminates exposed to general loading of variable stress and temperature history in which the stress and temperature are changed with time was predicted by the formulation by ATM-2 and measured experimentally. The validity of ATM-2 was confirmed by comparing of the predicted ones and the measured data.

7. References

1. Miyano, Y., Nakada, M., McMurray, M. K. and Muki, R. "Prediction of Flexural Fatigue Strength of CFRP Composites under Arbitrary Frequency, Stress Ratio and Temperature", Journal of Composite Materials, 31: 619-638, 1997.
2. Miyano, Y., Nakada, M. and Muki, R. "Applicability of Fatigue Life Prediction Method to Polymer Composites", Mechanics of Time-Dependent Materials, 3: 141-157, 1999.
3. Miyano, Y., Nakada, M., Kudoh, H. and Muki, R., "Prediction of Tensile Fatigue Life under Temperature Environment for Unidirectional CFRP", Advanced Composite Materials, 8: 235-246, 1999
4. Miyano, Y., Nakada, M. and Sekine, N., "Accelerated Testing for Long-term Durability of FRP Laminates for Marine Use", Journal of Composite Materials, 39: 5-20, 2005.
5. Christensen, R. and Miyano, Y., "Stress Intensity Controlled Kinetic Crack Growth and Stress History Dependent Life Prediction with Statistical Variability", International Journal of Fracture, 137: 77-87, 2006.
6. Nakada, M., Yoshioka, K. and Miyano, Y., "Prediction of Long-Term Creep Life for Unidirectional CFRP", Proceedings of the 6th International Conference on Mechanics of Time Dependent Materials (MTDM 2008), Monterey, 2008.
7. Miyano, Y., Kanemitsu, M., Kunio, T. and Kuhn, A. H., "Role of Matrix Resin on Fracture Strengths of Unidirectional CFRP", Journal of Composite Materials, 20: 520-538, 1986.
8. Uemura, M. and Yamada, N., "Elastic constants of carbon fiber reinforced plastic materials", Journal of the Society of Materials Science, Japan, 24: 156-163, 1975.

NAVY RELEVANCE

The proposed accelerated testing methodology is effectively combined the effects of time and temperature on the strength and life of CFRP laminates and structures exposed to an actual loading having general stress and temperature history. The methodology is useful to the durability analysis and design for the marine composite structures.

AKNOWLEDGEMENTS

The authors thank the Office of Naval Research for supporting this work through an ONR award with Dr. Yapa Rajapakse as the ONR Program Officer. Our award is numbered to N000140611139 and titled "Verification of Accelerated Testing Methodology for Long-Term Durability of CFRP laminates for Marine Use". The authors thank Professor Richard Christensen, Stanford University as the consultant of this project and Toray Industries, Inc. as the supplier of CFRP laminates.

PUBLICATIONS (ONR supported)

1. Journal Papers

1. Cai, H., Miyano, Y. and Nakada, M., "Prediction of Long Term Flexural Fatigue Strength of Honeycomb Sandwich Composites", Jour. of Reinforced Plastics and Composites, Vol.29, pp.266-277 (2010).
2. Cai, H., Miyano, Y., Nakada, M. and Sihn, S., "Master Curves of Residual Creep and Fatigue Strengths for Damaged CFRP Composites", Jour. of Reinforced Plastics and Composites, Vol.29, pp.1009-1019 (2010).
3. Miyano, Y., Nakada, M. and Sekine, N. "Life Prediction of CFRP/Metal Bolted Joint Under Water Absorption Condition", Journal of Composite Materials, Vol.44, pp.2393-2411 (2010).
4. Iwai, K., Cai, H., Nakada, M. and Miyano, Y., "Prediction of Long-term Fatigue Strength of Quasi-isotropic CFRP Laminates with a Hole Under Compressive Loading", Science and Engineering of Composite Materials, Vol.17, pp.227-241 (2010).
5. Hanatani, Y., Nakada, M. and Miyano, Y., "Validation of Fatigue Life Prediction Method under Variable Fatigue Loading for CFRP Laminates", Science and Engineering of Composite Materials, Vol.17, pp.261-269 (2010).
6. Miyano, Y., Nakada, M. and Cai, H., "Accelerated Testing Methodology for Long-term Fatigue Life Prediction of Polymer Composites", Science and Engineering of Composite Materials, Vol.17, pp.313-335 (2010).
7. Nakada, M., Miyano, Y., Cai, H., and Kasamori, M., "Prediction of long-term viscoelastic behavior of amorphous resin based on the time-temperature superposition principle", Mechanics of Time-Dependent Materials, (in print)
8. Cai, H., Nakada, M. and Miyano, Y., "Simplified Determination Method of Long-term Viscoelastic Behavior of Amorpous Resin", Mechanics of Time-Dependent Materials, (Submitted June 2010)

2. Conference Papers

1. Nakada, M. and Miyano, Y., "Accelerated Testing Methodology for Long-Term Life Prediction of Polymer Composites Based on the Time-Temperature Superposition Principle", 6th Annual European Rheology Conference, Gothenburg, 2010.4.
2. Miyano, Y. and Nakada, M., "Advanced Accelerated Testing Methodology for Life Prediction of CFRP Laminates", Society for Experimental Mechanics (SEM) Annual Conference & Exposition on Experimental & Applied Mechanics, Indianapolis, 2010.6.
3. Miyano, Y., "ACCLERATED TESTING METHODOLOGY FOR LONG-TERM CURABILITY OF CFRP LAMINATES FOR MARINE USE", 2010 Office of Naval Research Solid Mechanics Program – Marine Composites and Sandwich Structures -, Adelphi, MD, 2010.9.
4. Nakada, M. and Miyano, Y., "ADVANCED ACCELERATED TESTING METHODOLOGY FOR LIFE PREDICTION OF POLYMER COMPOSITES", 7th International Conference on Mechanics of Time-Dependent Materials, Portroz, 2010.9.
5. Nakamura, M., Nakada, M. and Miyano, Y., "APPLICABILITY OF TIME-TEMPRATURE SUPERPOSITION PRICIPLE TO MODE I INTERLAMINAR FATIGUE CRACK PROPAGATION OF CFRP LAMINATE", 7th International Conference on Mechanics of Time-Dependent Materials, Portroz, 2010.9.
6. Nakane, T., Nakada, M. and Miyano, Y., "LIFE PREDICTION OF CFRP LAMINATES UNDER CYCLIC FATIGUE LOADING BASED ON ADVANCED ATM", 7th International Conference on Mechanics of Time-Dependent Materials, Portroz, 2010.9.
7. Ogata, M., Nakada, M. and Miyano, Y., "QUANTITATIVE EVALUATION OF PHYSICAL AGING ON VISCOELASTIC BEHAVIOR OF EPOXY RESIN", 7th International Conference on Mechanics of Time-Dependent Materials, Portroz, 2010.9.
8. Harada, T., Nakada, M. and Miyano, Y., "TEMPERATURE-WATER ABSORPTION

DEPENDENT STRENGTH IN VARIOUS LOADING DIRECTION OF UNIDIRECTIONAL CFRP", 7th International Conference on Mechanics of Time-Dependent Materials, Portroz, 2010.9.

9. Miyano, Y., Nakada, M. and Cai, H., "ADVANCED ACCELERATED TESTING METHODOLOGY FOR LONG-TERM LIFE PREDICTION OF CFRP LAMINATES", 9th International Conference on Durability of Composites Systems (DURACOSYS-2010), Patras, 2010.9.
10. Miyano, Y., Nakada, M. and Cai, H., "Long-term Life Prediction of CFRP Structures Based on MMF/ATM Method", 15th Composites Durability Workshop (CDW-15), Kanazawa, 2010.10.
11. Nakada, M., Miyano, Y. and Cai, H., "Advanced Accelerated Testing Methodology for Long-term Life Prediction of CFRP", 15th Composites Durability Workshop (CDW-15), Kanazawa, 2010.10.
12. Cai, H., Miyano, Y. and Nakada, M., "Modified Time-temperature Superpositiom Principle for Viscoelasticity of Thermosetting Resins", 15th Composites Durability Workshop (CDW-15), Kanazawa, 2010.10.
13. Nakada, M. and Miyano, Y., "Advanced Accelerated Testing Methodology for Life Prediction of CFRP Laminates for Marine Use", 7th Asian-Australasian Conference on Composite Materials (ACCM-7), 2010.11.
14. Miyano, Y. and Nakada, M., "Time and Temperature Dependence on Mode I Interlaminar Fracture Behavior of CFRP Laminates", 7th Asian-Australasian Conference on Composite Materials (ACCM-7), 2010.11.

AWARD

Fellow Award to Yasushi Miyano from Society of Advanced Materials and Process Engineering (SAMPE) (2010)